THE OHIO STATE UNIVERSITY

OVRhyp, Scramjet Test Aircraft

Student Authors: J. Aslan, T. Bisard, S. Dallinga, K. Draper, G. Hufford, W. Peters, and J. Rogers

Supervisor: Dr. G. M. Gregorek
Assistant: R. L. Reuss
Department of Aeronautical & Astronautical Engineering

Universities Space Research Association
Houston, Texas 77058

Subcontract Dated November 17, 1989
Final Report

May 1990

OVRhyp, Scramjet Test Aircraft

Student Authors: J. Aslan, T. Bisard, S. Dallinga, K. Draper, G. Hufford, W. Peters, and J. Rogers

Supervisor: Dr. G. M. Gregorek
Assistant: R. L. Reuss
Department of Aeronautical & Astronautical Engineering

Universities Space Research Association
Houston, Texas 77058

Subcontract Dated November 17, 1989
Final Report
RF Project 767919/722941

May 1990

ABSTRACT

(Gary Hufford)

A preliminary design for an unmanned hypersonic research vehicle to test scramjet engines is presented. The aircraft will be launched from a carrier aircraft at an altitude of 40,000 feet at Mach 0.8. The vehicle will then accelerate to Mach 6 at an altitude of 100,000 feet. At this stage the prototype scramjet will be employed to accelerate the vehicle to Mach 10 and maintain Mach 10 flight for 2 minutes. The aircraft will then decelerate and safely land, presumably at NASA Dryden Flight Test Center.

TABLE OF CONTENTS

LIST OF FIGURES

INTRODUCTION
(Gary Hufford)

This report presents a preliminary design for a research vehicle to test scramjet engines. The goal of this vehicle is to test scramjet engines in a Mach 6 to Mach 10 speed range.

The purpose of this airplane is to use the vehicle to test scramjet engine technology. Since scramjets have not been flight tested, there reliability at present is questionable. Many flight tests will be necessary in the development of scramjet engines. A Mach 6 test must be successful before higher Mach number tests can be conducted since no other engine has an operating range above Mach 6. Thus, a vehicle design must be constructed that will allow many different Mach number tests with a high degree of efficiency. The goal of this design of the research vehicle is to minimize the size and weight of the vehicle while still allowing the scramjets to be tested in the Mach 6 to Mach 10 speed range. The vehicle is to be launched from a carrier aircraft at Mach 0.8 at 40,000 feet. By minimizing the size of the research vehicle, the size of the carrier aircraft can be minimized. A small vehicle (under 45000 pounds) may even have the capability to be launched from an existing airplane such as a B-52. Thus, a small vehicle may greatly reduce the cost of a scramjet engine flight test by reducing material costs and by possibly eliminating the need to build a new carrier aircraft.

The base design of the research vehicle is given in Figure 1. Assuming the engine data given for the turbofanramjet and the scramjet

is accurate, this vehicle has a maximum Mach number of 9.35. A two minute cruise can be conducted at any Mach number less than or equal to Mach 8.75. This design will allow initial scramjet tests to be conducted.

Once the scramjets have been proven effective at Mach 8.75, rocket attachments can be made to the base design of Figure 1.2. These attachments are shown in Figure 1.3. The purpose of the rocket attachments is to increase the thrust in the transonic flight regime. An increase in thrust will eliminate the thrust pinch normally associated with this flight regime. A large increase in acceleration will reduce the fuel used by the turbofanramjet during transonic flight and will allow more fuel to be used by the scramjets at higher Mach numbers.

The rocket attachments will increase the aerodynamic drag and the weight of the base design of the research vehicle. Thus, it is advantageous to eject the rockets after their fuel has been exhausted. Therefore, the drag and weight increases will be limited to the region where the rockets are in operation. Thus, the thrust gain will far outweigh the drag and weight penalty during the rockets region of operation. After the rocket fuel has been exhausted and the rockets ejected, the drag and weight of the vehicle will be the same as the base design of the research vehicle.

The maximum Mach number of the design with rocket attachment is 9.9. The maximum Mach number for a two minute cruise is 9.25. Thus, the upper speed range for a scramjet test is increased by Mach .5 for the same vehicle design. Mach 9.9 is the maximum value the scramjet may be tested for any period of time for this vehicle.

To obtain higher Mach number tests another scramjet engine must be added to the design (presently we have three scramjet engines in the design). However, our airplane is not large enough to place another scramjet engine on the top of the aircraft. Another engine would reduce lifting surface area to unacceptable levels. Therefore, the aircraft must be enlarged or redesigned to add another engine. This report focuses on the base design and base design with rocket attachments. Topics included in this report include the determination of the aircraft configuration, weight determination, cost analysis, aerodynamic analysis, stability analysis, propulsion system analysis, mission profile determination, inlet design, cooling considerations, sonic boom analysis and internal systems.

Chapter 1

CONFIGURATION
(Kevin Draper)

During our initial design phase, many different configurations were considered. Information on delta wing, wing body, and lifting body arrangements was studied. Initial drag estimates, in conjunction with the General Electric Turbofanramjet engine data, directed our design toward incorporating two full scale G.E. Turbofanramjet engines and one SCRAMJET engine. Since the SCRAMJET engine information hadn't been released at this point, it was assumed that the SCRAMJET engine would be no larger than the G.E. Turbofanramjet engines being used. Initially, a combination deltawing and lifting body configuration with a leading edge sweep of seventy-five degrees was the overall design objective.

As our design configuration was drawn to scale, a major problem was encountered -- the plane's fuselage would have to be very large just to hold the full scale engines. The engine configuration being considered contained all three engines, side by side, on the underside of the aircraft. When drawn to scale, the engines -- without any inlet or isentropic ramp -- would barely fit within the delta wing configuration. At this point, alternate propulsion systems and arrangements were considered. Solid and liquid rockets were examined as alternatives. After research, it was decided that they were much too heavy to be a feasible alternative. Further information concerning a rocket propulsion system is presented later on in this paper.

Next, it was discovered that the initial drag estimates had been

too high. Since the idea of using a single inlet and diverting the airflow to the desired engines was still one of our design objectives, we decided to keep the twin turbofanramjet layout. The main reason for keeping this layout was the fact that it permitted the engines to use a single air intake. With twin engines, a symmetric thrust could be achieved for the turbofanramjet phase of the flight as well as in the SCRAMJET flight regime. With these concepts, and the lower drag, it was decided to use two G.E. turbofanramjet engines scaled to sixty percent size. The scaled engines would fit within the configuration that we had been wanting to use.

When the turbofanramjet engines were scaled, so too was the allowed size for the SCRAMJET engine. This allowed the frontal cross section of the aircraft to be smaller. These two preliminary designs can be seen in figures A.1 and A.2. The planform changes that were made between these two versions increased both the internal volume and the planform area. The planform area was increased in an effort to improve the aerodynamic characteristics of the design. The volume increase was much needed due to the voluminous nature of liquid hydrogen fuel.

Figure A.3 contains the altered version that resulted once the data for the SCRAMJET engine became available. In this version, the frontal area of the aircraft was further reduced, lowering drag once more. The isentropic ramp was extended beyond the trailing edge of the wing to avoid increasing wing planform area. This prevented the aspect ratio from becoming smaller than two. Again, there was a serious problem with incorporating three engines, cooling system, airframe structure, control system, and the required storage for the

hydrogen fuel. As the design process progressed, the aircraft kept getting larger, even after the engines were scaled down.

Instead of continuing the "airplane growth" cycle that had taken over our design efforts, it was decided to alter our design and investigate new engine arrangements. The over-under engine arrangement that had been decided against in the beginning became more appealing. Initially, the over-under engine concept had been abandoned for two main reasons. First of all, this arrangement would require two separate inlets and would require separate mechanisms to seal off the various inlets during the different phases of the flight. The second reason that this arrangement was not pursued initially was the concern for stability and control. With the over-under arrangement, it would not have been possible to design the nose of the aircraft to assist in balancing the pitching moments from the engines. However, once this over-under arrangement was given more consideration, it appeared more practical than our previous configuration. The SCRAMJET engine could be mounted on the top of the aircraft and the top portion of the fuselage could then be angled to maximize the inlet for the SCRAMJET engine's Mach number range. Similarly, the bottom portion of the fuselage could be angled to obtain the desired shock angle for the lower mach number ranges under which the turbofanramjet engine would be in operation. In order to maximize the thrust performance of both engines, an isentropic ramp needed to be incorporated into the design. The isentropic ramp would contribute to balancing the pitching moments since the expanding exhaust would provide a downward force on the tail of the aircraft. This downward force would help counteract the nose

down pitching caused by having the engine mounted above the airplane's center of gravity. If the aircraft's pitching behavior needs further assistance, the engine could be tilted slightly to lower its moment arm with the center of gravity. The separate inlets will cause a significant amount of drag during the flight phases in which they are not in use. However, the decision to alter our engine configuration also allowed us to use one G.E. turbofanramjet at ninety percent size instead of the twin engine configuration. This allowed a reduction in the overall intake area. With these changes, the new design's frontal area was not altered significantly from the old configuration. The overall size of the aircraft remained essentially the same, but the internal volume of the aircraft was increased. The reduction in the number of engines freed up a considerable amount of space within the aircraft. Also, the wing was contoured into the fuselage making it more of a lifting body than had been previously planned. This allowed an elliptical aft fuselage which increased the aircraft's internal volume.

This new design initially incorporated four angled control surfaces which served the multiple role of a lifting surface as well as horizontal and vertical control surfaces. The lower angled surfaces were designed to extend low enough so that skids could be mounted on them for the landing of the aircraft. This version of the design is shown at the end of this section. The use of these surfaces as skids during landing would have required a very strong wingtip structure and would have increased the aircraft weight. In addition to this, the control surface tips for this arrangement would have extended outside of the three dimensional shock cone. For these reasons, the lower control surfaces

were removed and the wing was extended and contoured into the fuselage. Also the wing wasn't allowed to project outside of the shock cone since it would not have remained with the aircraft for long if this had been allowed to happen! With this design, the skids will have to be mounted in the lower surface of the fuselage. The upper control surfaces were also shortened to ensure that they would remain inside of the three dimensional shock cone.

Various schematics of our current design are shown in figures A.5, A.6, A.7, A.8, and A.9. Figure A.5 gives the overall design configuration along with our weight estimate. Figure A.6 shows the same information as figure A.5 but also shows the internal location of the engines in all three views. In figure A.7, the distinction made between the aircraft's fuselage and wing is shown. This distinction was made for the purposes of aerodynamic analysis and much of the information calculated based on aircraft geometry is also given in this figure. Figure A.8 contains a cross-section down the center of the aircraft in order to further illustrate the engine arrangement as well as the location of the forward landing gear. Figure A.9 contains information resulting from our final aerodynamic and propulsive analysis. The center of gravity location is also shown in this figure.

As the drag, propulsion, and fuel storage calculations were refined, it became evident that there still wasn't sufficient fuel storage. The initial response to this situation was to modify the aircraft fuselage to gain as much volume as possible without making the vehicle excessively large. Two larger versions, shown in figures 1.1 and 1.2, were considered. It became obvious that the design was heading

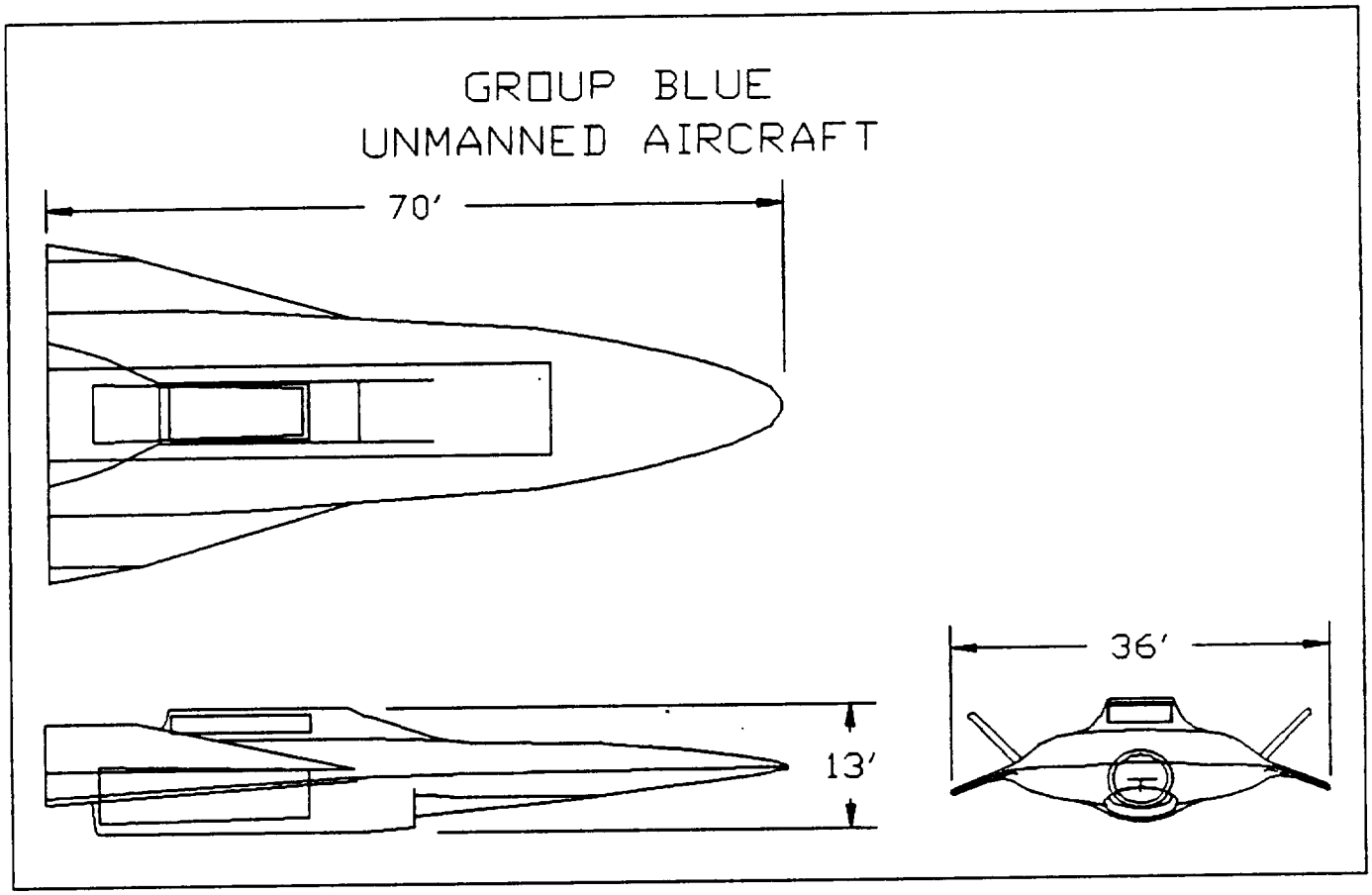

Figure 1.1

back into the same "growth" cycle that had been encountered with our earlier designs. Since one of the goals in the design was to keep the aircraft as small and light weight as possible, an alternate approach had to be found.

The design of the propulsion system and the approach used in determining the required fuel was altered. Instead of calculating the required fuel to fly certain trajectories and maintain test conditions, the available fuel volume was used as a constraint. Since fuel volume was critical and the SCRAMJET Mach 10 cruise range could not be met, it was decided to add solid rockets to the design. This design is also flexible and would facilitate preliminary testing of the SCRAMJET

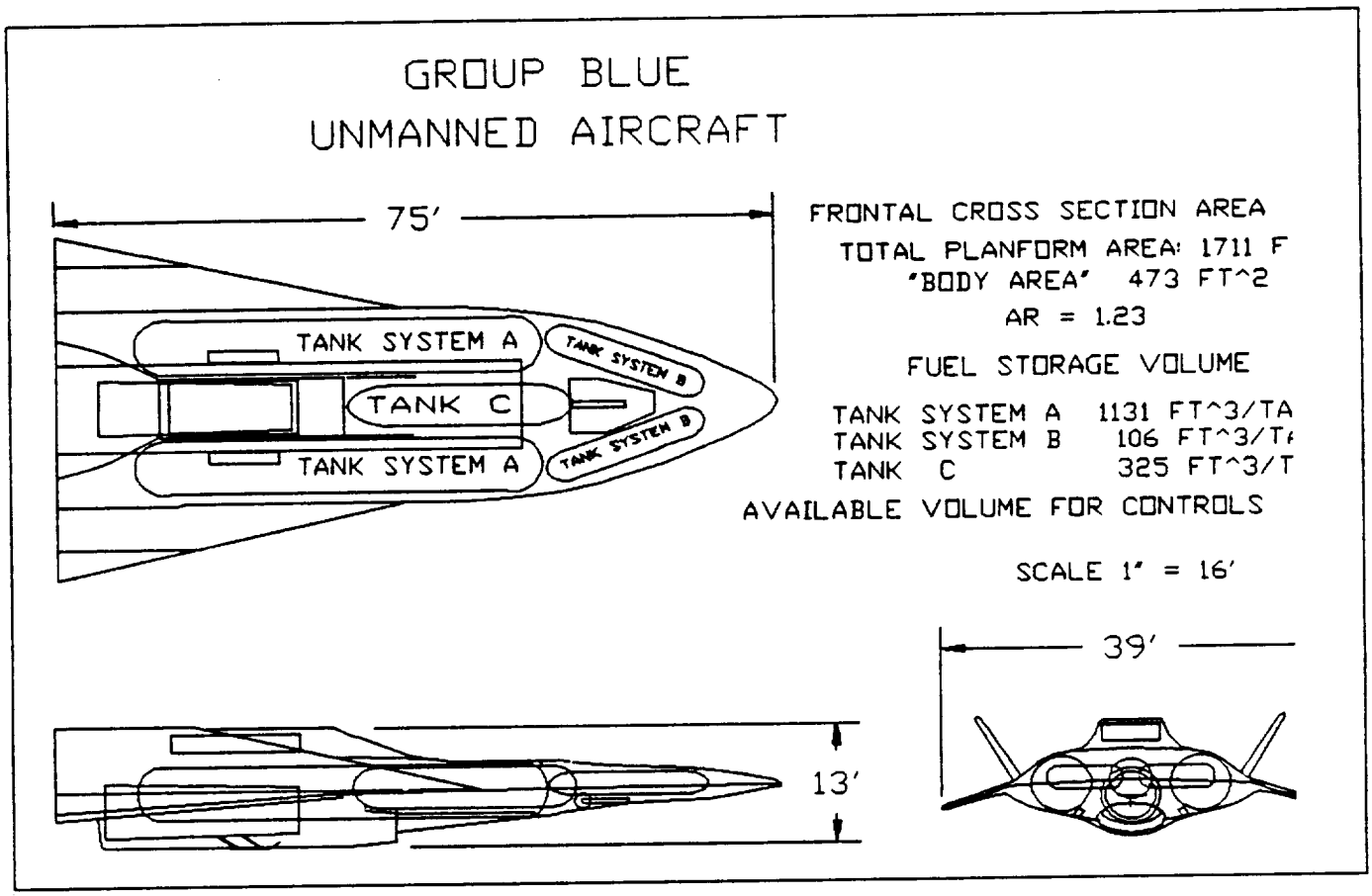

Figure 1.2

engines at lower Mach numbers since the fuel storage is sufficient to reach the low end of the testing regime without solid rockets. During later stages of development solid rockets can be added to achieve testing at higher speed ranges. The details of the propulsion system and analysis is given in the section on the propulsion system. The end result of this new approach was that the aircraft would be kept at a length of 60 feet and an available fuel volume of 1,500 cubic feet.

The current design configuration is given in figures 1.3 and the figures at the end of the section. Also shown is the aircraft version with the solid rockets, as well as various performance parameters for this configuration. The aircraft version without the solid rockets as

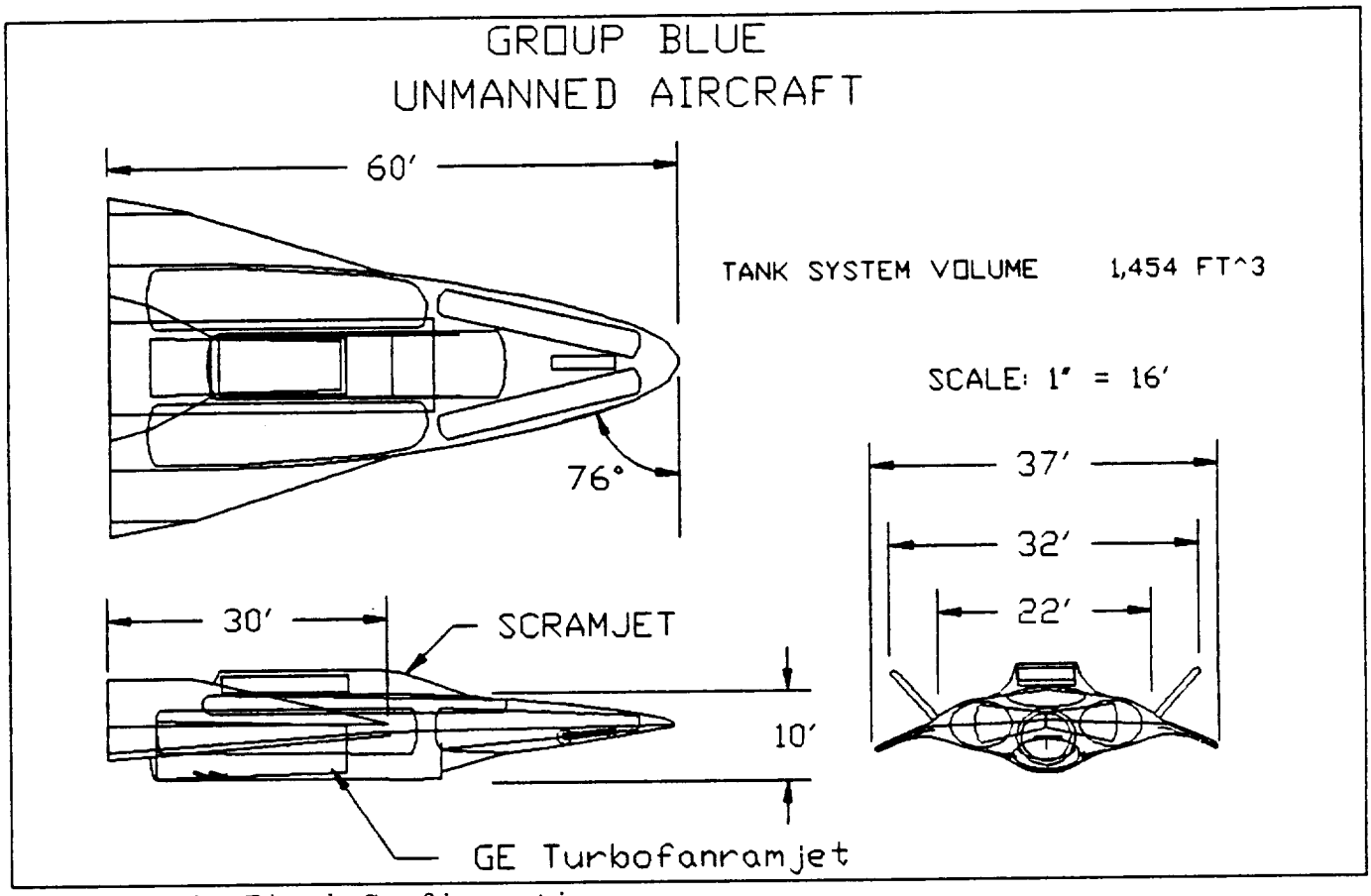

Figure 1.3: Final Configuration

well as the performance parameters for this version, and the fuel storage system and preliminary landing skids/wheel locations are given. The internal engine locations are also shown.

The current design still has volume limitations but it is a much more versatile design and adaptations can be made by altering the size of the solid rockets being used. The volume available with this design is fairly close to being a workable configuration. The limiting conflict at this stage is being able to accommodate both the control equipment as well as the extensive cooling system that is required by such a high speed aircraft.

BLUE CREW

Unmanned SCRAMJET Testing Vehicle

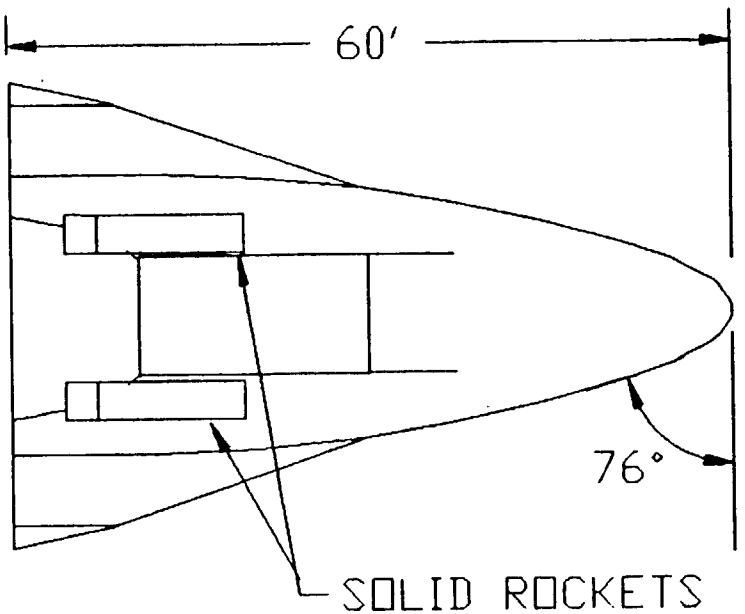

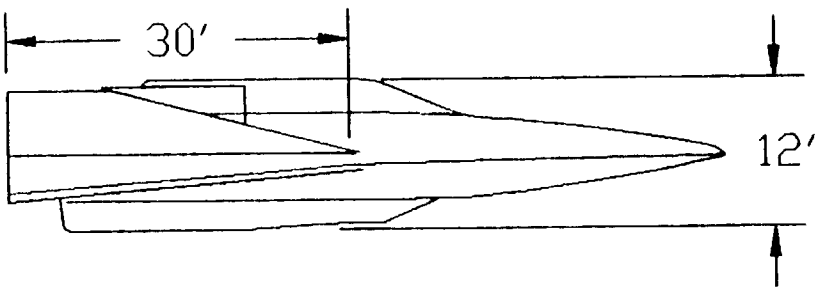

SOLID ROCKET ASSIST

Range = 1600 miles
Endurance = 32.6 minutes
Takeoff Weight = 44,000 lbs
Wing Loading = 54.19 lbs/ft^2
Landing Weight = 30,400 lbs
Wing Loading = 37.44 lbs/ft^2

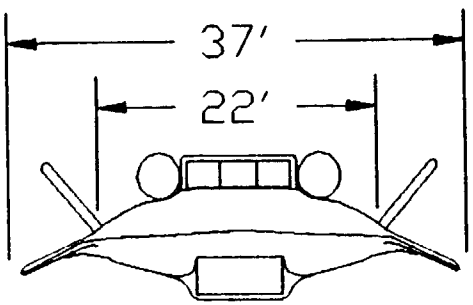

SCALE: 1" = 16'

BLUE CREW

Unmanned SCRAMJET Testing Vehicle

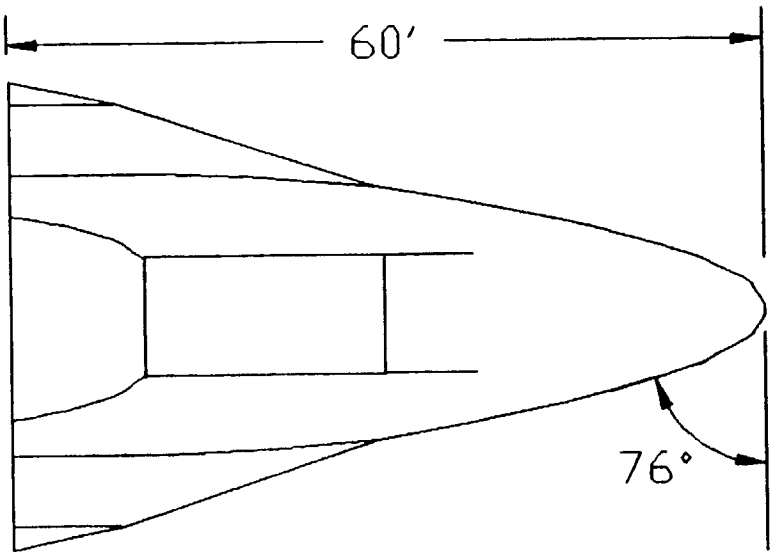

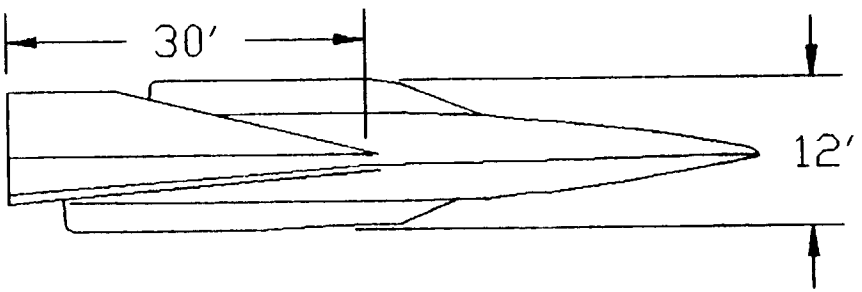

WITHOUT SOLID ROCKETS

Range = 1,500 miles
Endurance = 34.7 minutes
Takeoff Weight = 37,000 lbs
Wing Loading = 45.57 lbs/ft^2
Landing Weight = 29,900 lbs
Wing Loading = 36.82 lbs/ft^2
M max = 9.25

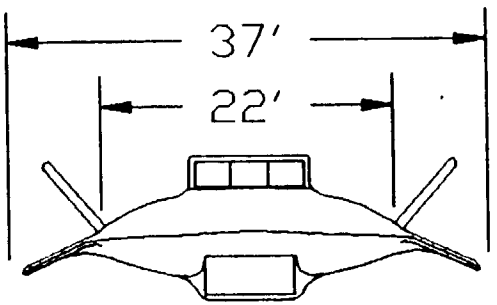

SCALE: 1" = 16'

BLUE CREW

Unmanned SCRAMJET Testing Vehicle

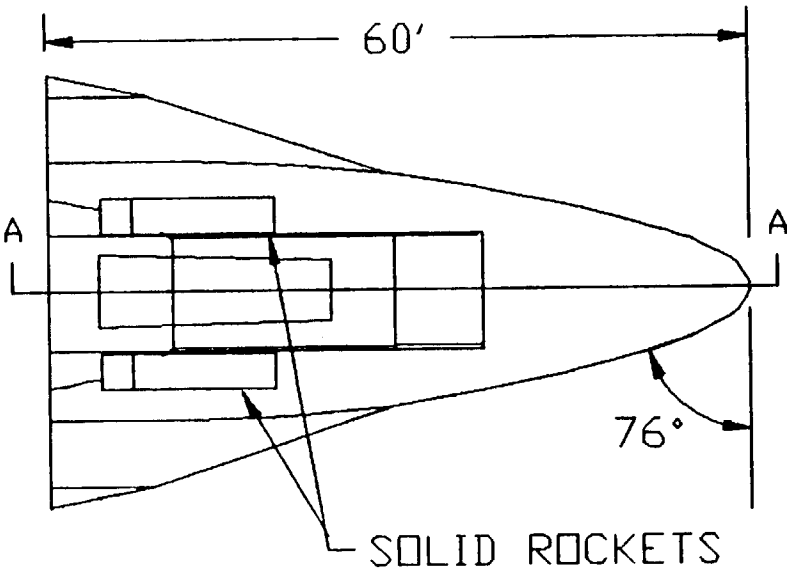

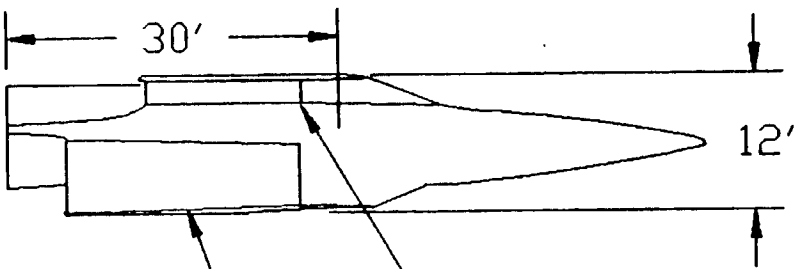

SECTION AA

PLANFORM DATA

AR = 1.69

Se = 812 FT^2

b = 37 FT

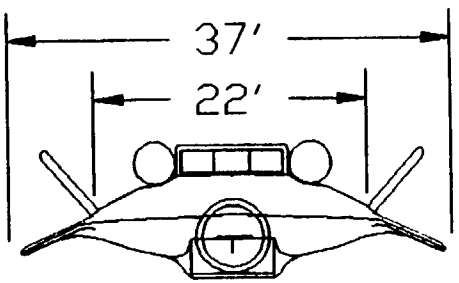

SCALE: 1" = 16'

Chapter 2

WEIGHTS ANALYSIS
(Scott Dallinga)

PURPOSE:

In the second design phase, the weight analysis tasks were divided into three areas of study. Component weights of eight major systems were calculated for each updated configuration(shown in table 8.1). Also, the position of each component in the aircraft was estimated to locate the center of gravity. Additionally, the center of gravity travel was calculated with fuel burn to verify the fuel tank configuration.

METHOD:

Calculation of most component weights were accomplished using a program based on WAATS, Weight Analysis for Advanced Transportation Systems, by C.R. Glatt. The original code is described in NASA Contractor Report CR-2420. The WAATS method uses statistical analysis of data from existing aircraft to calculate component weights of similar aircraft configurations. Correlating parameters are based on geometric characteristics and aircraft weight. Since the final weight is not known, an iterative process is used to calculate the aircraft gross weight. Power law relations are used to relate predominant physical characteristics affecting the weights of the components. A power law has an empirical constant multiplied by the relevant parameter value raised to an empirically defined exponent.

Table 8.1: Weights

WEIGHT STATEMENT	
Gross Takeoff Weight:	44,732
Empty Weight:	30,590
Gross Fuel Weight:	7,143
Useable Fuel Weight:	7,100
COMPONENT	**WEIGHT**
AERODYNAMIC	
Wing Structure	885
Vertical Stabilizers	1,560
STRUCTURE	
Main Body Structure	4,307
Secondary Structure	915
Thrust Structure	561
THERMAL PROTECTION	
Structural Insulation	1,050
Body Cover Panels	2,150
Active Cooling System	2,000
LAUNCH AND LANDING GEAR	
Launch Gear	112
Landing Gear	1,008
PROPULSION	
1 Turbofanramjet	5,400
3 SCRAMJET Modules	4,740
2 Solid Rocket Boosters	7,000
INLET SYSTEM	
Variable Ramps	731
Internal Ducts	592
CRYOGENIC FUEL SYSTEM	
Fuel Distribution System	679
Tank System A	672
Tank System B	410
Tank System C	500
CONTROLS AND AVIONICS	
Aerodynamic Controls	572
Electronics	1,919
Hydraulic System	340
Avionics	717

SYSTEMS:

The original WAATS program was modified to be used with the hypersonic research aircraft concept. There are eight major component areas used to obtain a weight buildup:

1. Aerodynamic surfaces
2. Body structure
3. Thermal protection systems
4. Launch and landing gear
5. Engine system
6. Inlet system
7. Cryogenic fuel system
8. Controls and avionics

AERODYNAMIC SURFACES:

Part of the problem in calculating the wing weight for the blue group's hypersonic vehicle is that there is no real distinction between the body and the wing. To properly apply the power law relations for wing weight, the wing area was defined as the outer thin region of the body where the thickness is less than seven and one-half inches. The bending moment at the wing root is the determining factor for wing weight. To properly apply the empirical relations, the wing span for structural considerations is two times the width of the body from the point where the thickness is 7.5 inches outboard to the edge. The coefficients used in the power law relation are for high-speed, high-temperature aircraft such as the X-15, F-108A, and the XB-70.

BODY STRUCTURE:

The three components which make up the body structure are the main structure, the secondary structure and the thrust structure. The engine compartment, avionics bay, and fuel tank area constitute the main body area of the plane. Secondary structures include the afterbody, which will be used as an expansion surface for the propulsion system. Landing gear doors are also included as secondary structures. The secondary structure weight is related to the size of these parts. The engines are supported by the thrust structure, whose weight is a function of the maximum thrust of the engines.

THERMAL PROTECTION SYSTEM:

A common way to keep the structural temperature within acceptable limits to use insulation with radiative cover panels installed to protect the insulation from flight conditions. Most likely, large portions of any Mach 10 aircraft will have to be actively cooled, perhaps in combination with the use of insulation and cover panels. At this point, due to the lack of detailed thermal analysis, an arbitrary value for the area covered by the TPS was selected. To be sure, the entire underbody of the vehicle will have to be protected from the high temperatures caused by air compression. The afterbody will need cooling to protect it from the hot gases ejected by the propulsion systems. Included with the thermal protection system is an allowance for the active cooling system. Two thousand pounds were allowed for this system.

LAUNCH AND LANDING SYSTEM:

In our case, landing gear weight is a function of landing weight or launch weight minus fuel weight. Launch and landing gear weights are related to similar vehicles which are air-launched.

PROPULSION SYSTEM:

The projected weights of the turbofanramjets and scramjets have been provided by General Electric. Engine mounts are sized according to maximum engine thrust. Two solid rocket boosters with a total weight of seven thousand pounds are included in the propulsion system weight. The boosters count towards the gross takeoff weight but are not included in the empty weight since they are ejected as they burn out.

INLET SYSTEM:

Average values were selected for the turbofanramjet inlet parameters since these parameters change as the aircraft accelerates through a range of Mach numbers and altitudes. An two dimensional inlet design was selected for the turbofanramjet engine. The scramjet inlet weight estimate was also based on a 2-D design with parameters similar to the turbofanramjet inlet.

CRYOGENIC FUEL SYSTEMS:

Included in the cryogenic fuel system are fuel tanks, fuel tank insulation and the fuel distribution system. Fuel tank weight is based on a three-tank system with a total volume of 1,500 cubic feet. The weight is a function of fuel tank volume. The insulation weight is a

function of fuel tank wetted area and fuel tank radiating temperature. The fuel tanks were shaped to fit in the available area of the plane. The fuel tank radiating temperature was estimated at 500 degrees F. since the structure is thermally protected, the fuel tank should not experience a value too much higher than this. An empirical correction factor was applied to the insulation weight since a flight duration of only 30 minutes is expected. A percentage of the useable fuel weight was allowed for liquid hydrogen boiloff.

CONTROLS AND AVIONICS:

Values for the weights of avionics, hydraulics, electrical, and aerodynamic orientation control systems were calculated based on empirical constants used in power law relations for similar aircraft. Aircraft size was the most important parameter involved in the empirical weight relations for these systems.

PROGRAM:

Power-law relations for components that were used in our design were taken from the WAATS program. For each weight estimate a data file containing relevant geometrical data as well as coefficients and exponents for power law relations was read into the derived weight analysis program. The data file contains the parameter values as well as a description of each variable and the variable's name used in the program to help future program users understand the methodology used.

CENTER OF GRAVITY TRAVEL CALCULATIONS:

To verify the fuel tank configuration of the aircraft, the center of gravity was determined with varying amounts of fuel in the tank system. Since a forward C.G. is desirable for stability considerations, the order of tank drainage was rear to front. The tanks were drained in the following order; A, C, then B. The rocket boosters were ejected after 200 lbs of fuel were burned. The rocket assisted phase of the flight experienced the farthest C.G. shift due to the high weight loss and aft position of the seven thousand pound boosters. C.G. shifts due to liquid hydrogen fuel burn were found fairly insignificant. Only about 19 percent of the total weight of the plane without the solid rocket boosters consists of liquid hydrogen.

Chapter 3

AERODYNAMICS

(John Aslan and Gary Hufford)

INTRODUCTION

In order to determine the preliminary aerodynamic performance of our vehicle, we developed three separate computer codes, one each for the subsonic, supersonic and hypersonic flight regimes. The use of the codes allow the user to change any geometrical aspect of the flight vehicle and quickly get the performance data for further study. Data from these codes can also be compiled and printed in graphical form. The codes were developed from various theories and will be described further.

There are a few common points in all three of the codes. First, the standard atmosphere tables are generated at 500 foot intervals. This is done by finding the temperature of each geometric height in the atmosphere. The gradient is either isothermal or it varies linearly with height. The altitudes at which changes occur can be found in any book where the standard atmosphere tables are presented. There are three separate regions of variation between 0 and 100000 feet, two vary linearly and one is isothermal. Once the temperatures are found, the ratio of a pressure at that specific altitude to a reference pressure at a reference altitude is found. This is calculated from an integrated form of the hydrostatic equation, depending only on temperature and geometric altitude. Then, the thermally perfect gas law is applied to calculate the density. These are generated in 3 separate parts in the

code corresponding to the three different regions of temperature gradients.

Next, the dynamic pressures at every altitude between 0 and 100000 feet in 500 foot increments and the Mach numbers between 0 and ten in 0.1 increments are found. The geometry of the vehicle is now read into the code. The user is prompted to enter a range of altitudes, Mach numbers and angles of attack. The user is then prompted to choose the maximum drag and lift and the minimum lift to cut out the data not pertinent to the particular aspect of the performance calculations. At the end of the program, various data such as lift coefficient, drag coefficient etc. are written to separate files for plotting purposes. Also, an overview including all data is written to a file for visual inspection of the relationship between all the data in that particular instance.

SUBSONIC

The subsonic theories used are compiled in "Fundamentals of Aircraft Design" by Leland M. Nicolai, 1975. Portions of the theory are presented in graphical form only, so the computer prompts the user for these data. Also, it should be mentioned that the aircraft was modeled as a delta wing configuration with thickness, but no camber. The resultant program is in appendix C.1.

For the lift calculations, linear two-dimensional theory corrected for wing sweep, compressibility and finite span were used. Wing-body interference effects are taken into account and are dependent on span, body diameter and Mach number. The lift interference factor is

determined from these and presented in graphical form in the reference. The user is prompted for the lift interference factor by the code. Since the aircraft design is of low aspect ratio, non-linear lift effects are also taken into account. This is done using non-linear theory, dependent on planform shape and aspect ratio, presented in graphical form in the reference. The computer prompts the user for this information. From this data, a lift-curve slope is found.

The flow over the entire wing was assumed to be turbulent, so the Prandtl approximation for the skin friction coefficient due to turbulence was used. The wing and body zero-lift drag coefficients are calculated separately. The Reynolds numbers were based on the mean aerodynamic chord and the body length respectively. The remainder of the drag is of that due to lift. For this preliminary design, the viscous and inviscid effects were combined into one parameter, dependent on the wing efficiency factor and aspect ratio. The computer prompts the user for the wing efficiency factor, which is presented in graphical form in the reference. The sum of the zero-lift drag coefficient and the drag coefficient due to lift give the total drag coefficient.

SUPERSONIC

The supersonic theories used are also compiled in "Fundamentals of Aircraft Design" by Leland M. Nicolai, 1975. Portions of the theory are also only presented in graphical form and must be entered by the user of the code. As previously indicated, the aircraft was modeled as a delta wing configuration with thickness, but no camber. This code is in appendix C.2.

The supersonic lift coefficient is based on supersonic linear theory, corrected for three-dimensional flow effects. Theoretical normal force coefficients dependent on aspect ratio, sweep and the supersonic similarity parameter are presented graphically in the reference. The user is prompted for these values by the computer, which is done at every Mach number. From this, a supersonic lift-curve slope is generated at every Mach number.

The drag coefficient is also modeled after supersonic linear theory. The wing leading edge was chosen to be more sharp than round, so the shock wave is assumed attached. Furthermore, the wing is also modeled as having a double-parabolic arc section. The computer next calculates whether the wing leading edge sees supersonic or subsonic flow, which depends on sweep. Once this is determined, the drag coefficient due to the shock wave is determined. The skin friction drag coefficient for the wing and body are then determined, in the same fashion described in the subsonic section.

Next, the drag coefficient due to lift is found. For this preliminary design, the viscous and inviscid effects are combined into one parameter, which is dependent on the lift-curve slope. The zero-lift drag coefficient and the drag coefficient due to lift are added together to give the total drag coefficient.

HYPERSONIC

The hypersonic code, listed in appendix C.3, was written from theory presented in "Hypersonic Aerodynamics" by R.Truitt, 1959. It is extracted from Newtonian flow as a two-dimensional, three-term series

for a double parabolic arc airfoil. Both lift and drag are dependent on the thickness ratio, hypersonic similarity parameter and normalized angle of attack. A chordwise and a normal force coefficient are generated. Lift and drag are found from these values. Also included in drag is skin friction drag calculated for the wing and body, as previously stated in the subsonic and supersonic sections. The values agree well with experiment for wings of finite aspect ratio at small angles of attack. This is because the region of three-dimensional flow occurs only over a small portion of the wing planform at hypersonic speeds ("Hypersonic Aerodynamics" p.63).

PROGRAM USE

For the final configuration shown in figure 3.1, the aircraft was modeled as a delta wing with a small body in the center for fuel. This area is shaded in figure 3.2. The areas and lengths input to the programs are given in figure A.9. Other input data included an average thickness to chord ratio of 3/30=0.1, a leading edge radius of .02% (which equal a 1/8 inch radius, which according to temperatures estimation will be sufficient), a sweep angle of 76 degrees and body width, and body cross-sectional area.

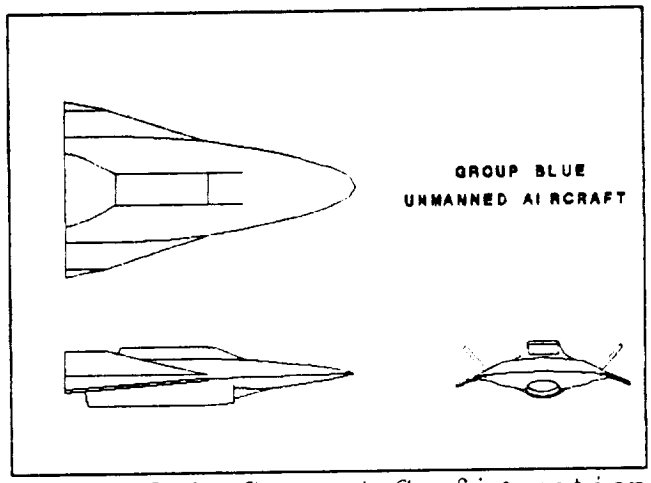

Figure 3.1: Current Configuration

Using this data in the programs, the pertinent aerodynamic was obtained. The non-dimensional representation of this data follows this

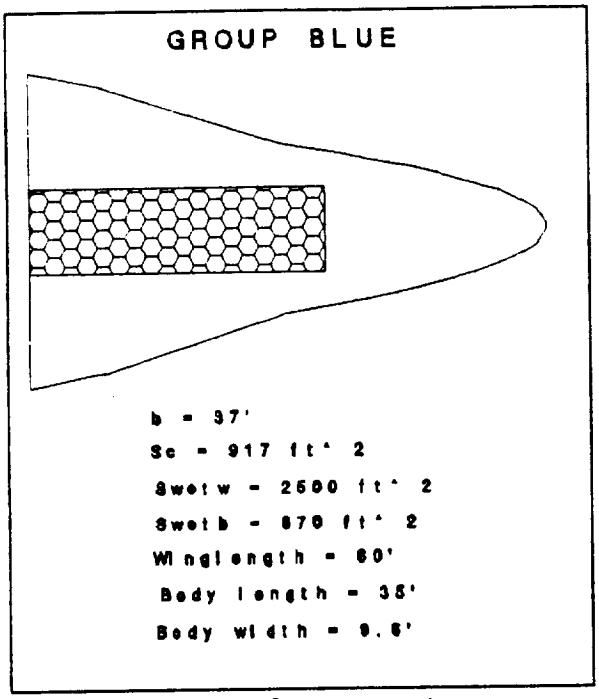

Figure 3.2:Reference Areas

section. This data was then used by the propulsion group along with the engine data to obtain a viable flight profile. The glide portion of the flight profile was determined by the aerodynamics group since no engines were used in this portion. A brief description of this calculation will be given.

Aerodynamic Results

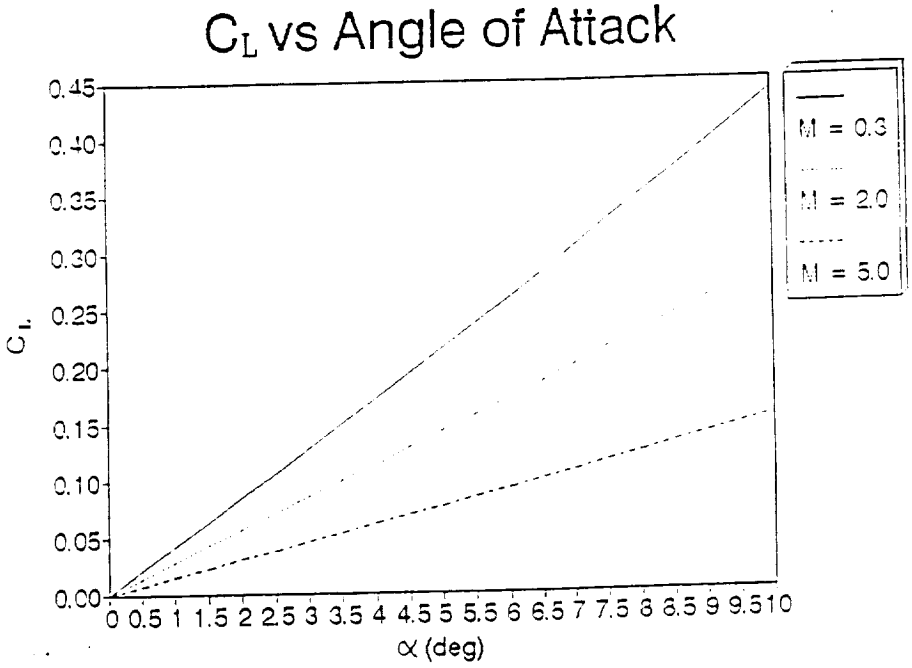

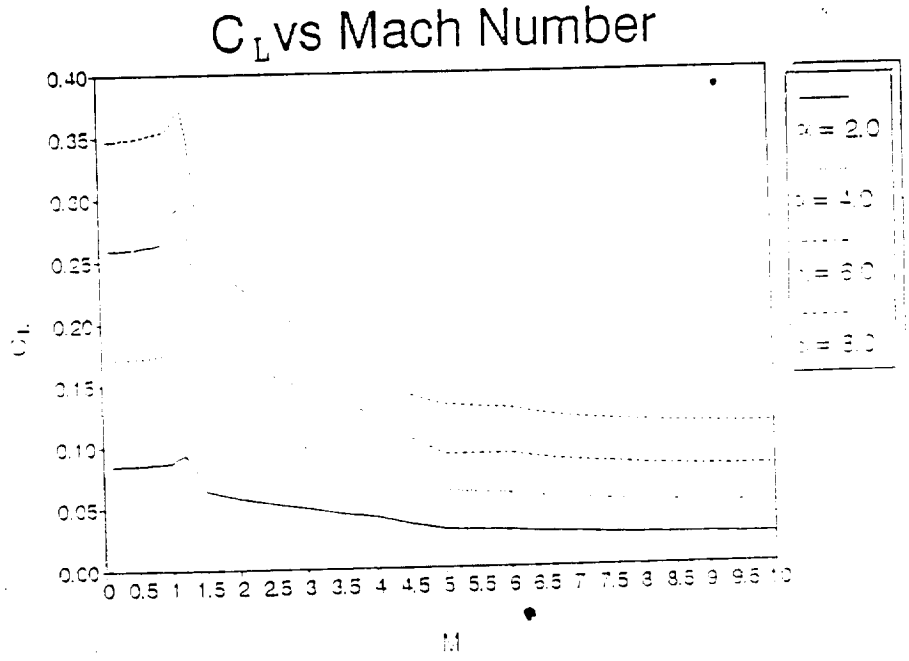

Drag Polar

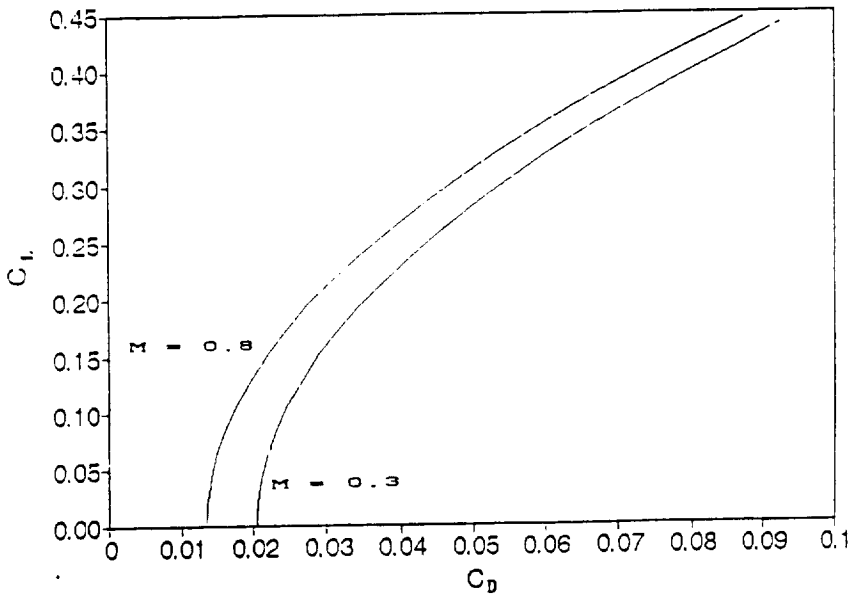

Drag Polar

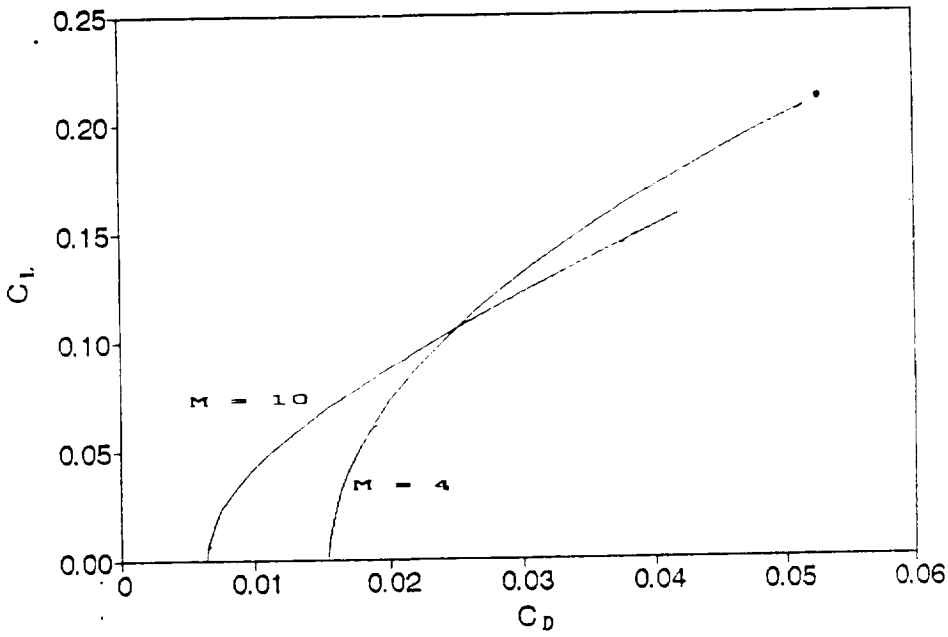

C_D vs Mach Number

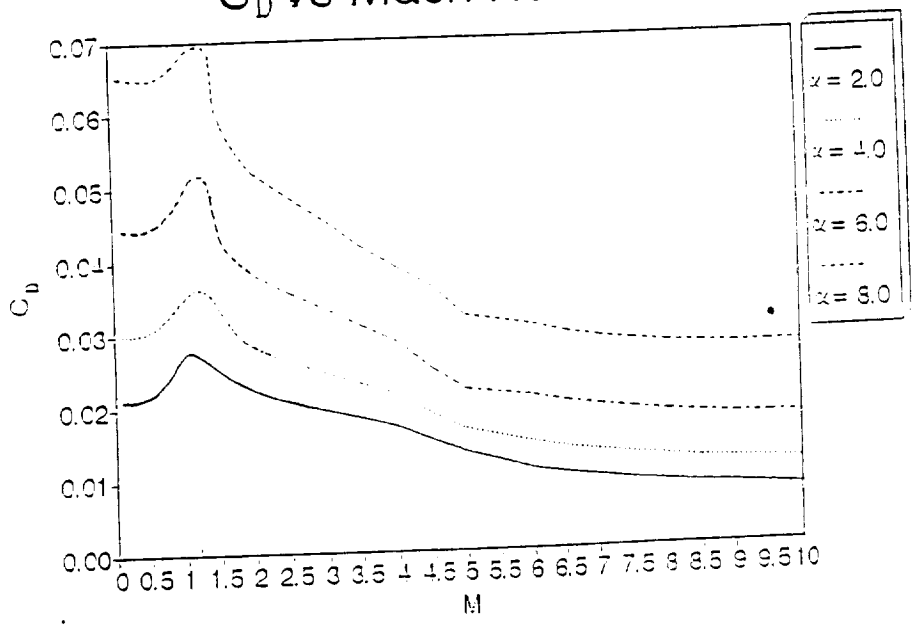

L/D vs Mach Number

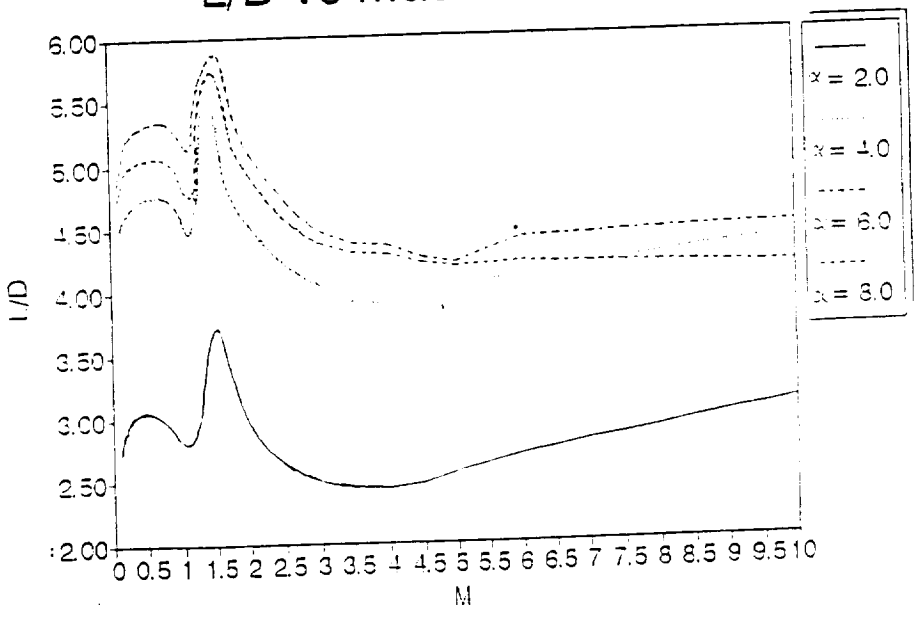

C_M vs. Angle of Attack

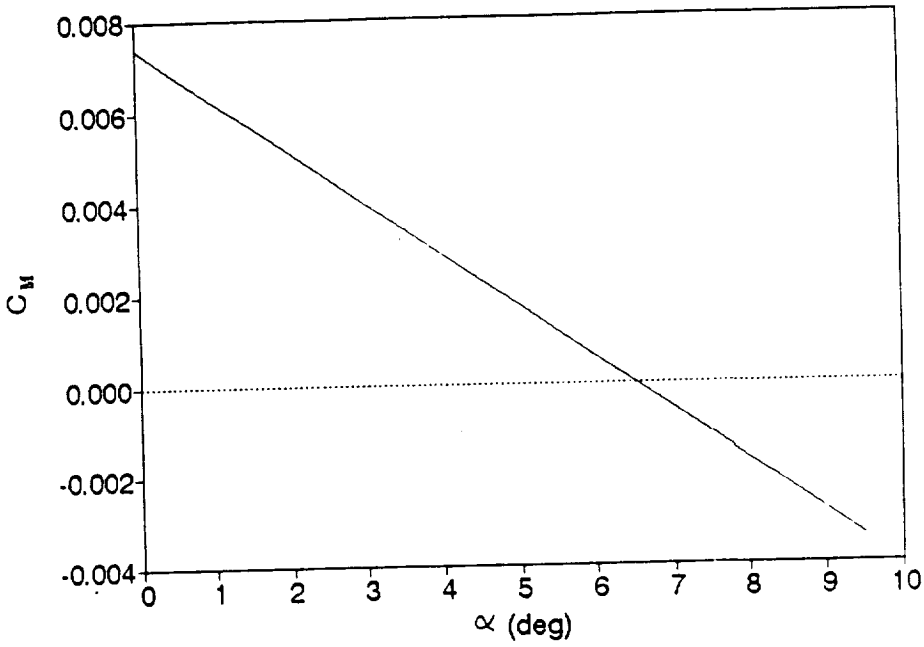

Static Margin Variation

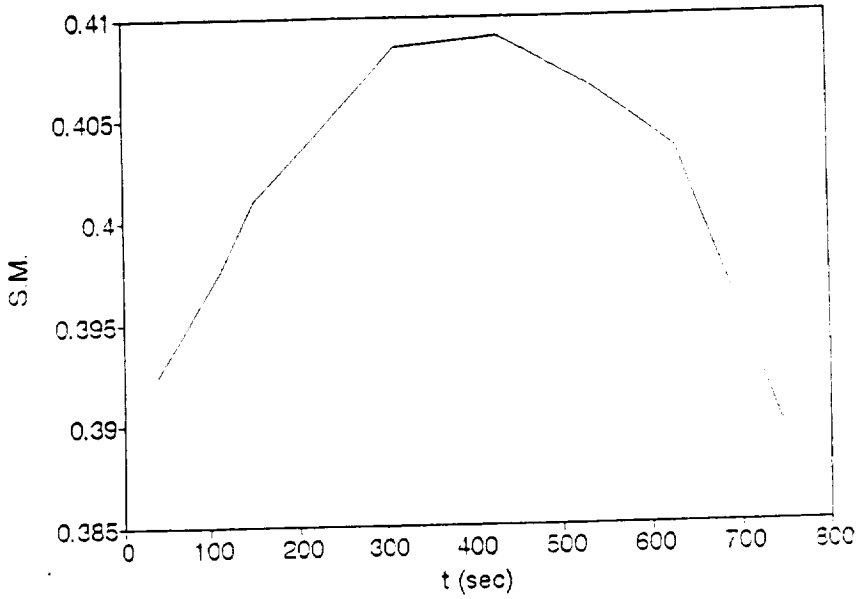

Chapter 4

LONGITUDINAL STABILITY

(John Aslan)

The longitudinal stability of the aircraft must be known throughout the entire flight to determine what type of, if any, stability augmentation system must be implemented. The reference used is "Fundamentals of Aircraft Design" by Leland M. Nicolai, 1975. The basic method of this reference is used in the analysis, with some new assumptions to tailor it to that of a wing-body design. The contribution of the wing-body and propulsion units to the moment about the center of gravity will be used to determine the static longitudinal stability.

The two sets of winglets at the rear of the aircraft were found to contribute about 2/3 of the lift of the aircraft, and the rest of the aircraft as 1/3 of the lift. This was determined by finding the lift-curve slopes of the individual parts by the same method that was used in determining the lift-curve slope of the entire aircraft (see Aerodynamics). The aerodynamic center of the entire aircraft was then assumed to be that of the winglets. The aerodynamic center of the entire aircraft and the rest of the aircraft were found to vary between 40% and 50% of their respective mean aerodynamic chords, depending on the flight mach number.

Now that the aerodynamic centers of the aircraft have been found, the center of gravity and its travel must be found. This was accomplished using a weight estimation program, which is described in this report. Next, a basic moment equation is written, taking into consider-

ation the thrust vectors and lift and drag at arbitrary angles of attack. The longitudinal distances are referenced to a fixed point on the aircraft, namely the leading edge of the winglets. To simplify the equations, the following assumptions were made:

1. small angle of attack
2. vertical contributions negligible, because they are relatively small distances compared to the horizontal distances
3. lift coefficient >> drag coefficient
4. the moments about the aerodynamic centers of the aircraft components are not contributing, because no suitable method for determining these was found.

From the final moment equation, the moment coefficient at zero angle of attack and the moment-curve slope are found by breaking down the single moment equation into a constant part and one that depends on angle of attack. Once these equations are known, the center of gravity and aerodynamic centers are determined for a specific time in the flight. The distances and forces are substituted into these equations, and the curve found.

During the turbofanramjet only phase of the flight, landing (plot at end of chapter) and acceleration from Mach 2 to Mach 5, the aircraft is statically stable. However, with the scramjets or rockets running, the nose-down moment is quite considerable, which makes the moment at zero angle of attack negative, with the slope still negative. In this

configuration, trimming is not possible. A stability augmentation system will be needed to accomplish this. Also, a plot at the end of the chapter shows the variation in static margin as the fuel is used in tank order A, C, then B. As can be seen, the static margin remains almost constant and is positive, which is a criterion for static longitudinal stability. Further analysis and wind tunnel testing are needed to get an accurate assessment of the situation.

Chapter 5

SONIC BOOM
(Terry Bisard)

Introduction

With the mission profile requiring high supersonic flight, the amount of sonic boom produced by the aircraft becomes very important. A sonic boom is produced when the plane travels at supersonic speed and forms shock waves. A large rise and fall in pressure results from the quick passage of the shock waves. These sonic booms passing over land can be strong enough to damage people's hearing and even shatter building windows. Due to this, the F.A.A. has stipulated that no aircraft may produce a sonic boom over 1 lb/ft^2 while traveling over United States airspace.

Method of Calculation

In designing our supersonic plane, flight path consideration must be given to the sonic boom it produces. The Morris prediction method was used to estimate the sonic boom signature produced by our aircraft. This method assumes a flying diamond shape and the change in pressure is given by:

$$dPl = .363*Kr*(Pa/Pg)^{.5}*Kl*(M^2-1)^{.375}/M*W^{.5}*Lw^{-.25}*Pa^{-.5}*H^{-.75}*Pg$$

Where: Kr,Kv - Shape factor constants

Pg,Pa - Pressure at altitude and sea level

M - Mach number

W - Weight of aircraft

Lw - Length of aircraft

H - Flight altitude

Results

By writing a computer program, the sonic boom signature can be found. Using this method, the sonic boom can be found for the flight profile at various altitudes and Mach numbers. As is seen in fig. 5.1, our sonic boom signature was very small and was above legal limits only for Mach numbers between 1.1 and 2.5. Even when our sonic boom was above the legal limit it did not fan out very far. The small sonic boom signature comes about from the aircraft's relatively low weight (~50,000 lb.) and a short total length of only 60 feet.

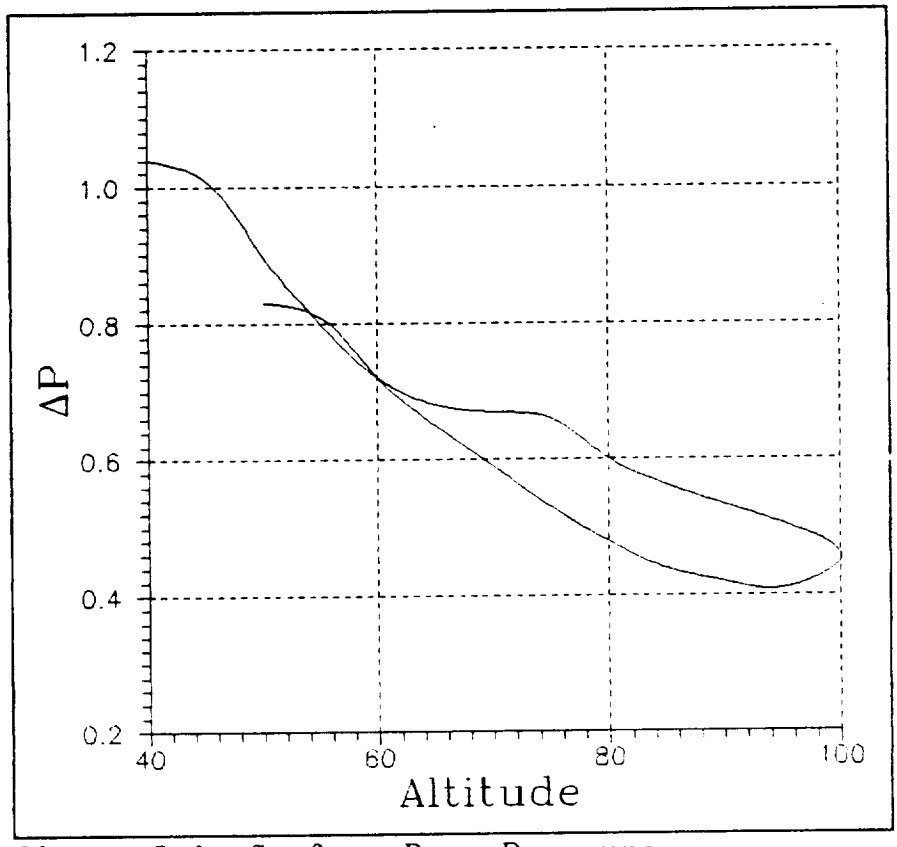

Figure 5.1: Surface Boom Pressure

Chapter 6

PROPULSION
(Warren Peters)

Introduction

The ultimate purpose of the propulsion system of this aircraft is to accelerate to the desired mach number and to test the scramjet engines. One of our personal goals was to keep the plane as small as possible, which means a compact power plant configuration and the minimum amount of fuel necessary to complete the mission.

Of the many types of propulsion systems available, we decided to use a combination of turbofan/ramjets, scramjets, and rocket engines. Liquid rocket engines were eliminated from consideration because of the large weight of the hardware necessary to use one, so the propellant of choice was a solid propellant. Calculations show that solid rockets are too heavy and bulky to use on our small aircraft if it is the only propulsive system available, as shown last quarter. However, if the solid rockets are used to augment a turbofan/ramjet, the results are quite acceptable. The turbofan/ramjet engine is capable of producing most of the thrust necessary to accelerate from launch to M = 6, provide a powered landing and is insurance in the case of a scramjet failure. The scramjets are necessary for the plane because testing them is the purpose of this analysis.

Last quarter we ended with a propulsive configuration of 2 scramjets and 1 turbofan/ramjet engine that was sized down to 90%. The total amount of fuel used in this configuration was 12,000 lbs, which was far too large for the size of the plane we wanted this quarter. The

total amount of fuel contained in this quarter's design was 7,100 lbs, and the power plant system was designed around this. An extra scramjet engine was added this quarter to bring a total of 3 scramjets. More scramjet engines were not used because the small size of our plane would not permit it. Two small external solid rockets were also added to the design that assist in the thrust pinch and low speed operations, and are ejected after they have burned out. The third and final change was that the turbofan/ramjet was upscaled by 2%, leaving the total dimensions at 92% of full size.

Rocket

The largest innovation in the powerplant package was the addition of 2 solid rocket engines that are used in the early stages of the flight. As mentioned earlier, solid rockets were dismissed for use as the only propulsion system from lanuch to M = 6 because of the severe weight penalty incurred. However, a small set of solid rockets used in conjunction with the turbofan/ramjet engine increases performance and decreases the hydrogen fuel weight. The following is a list of the major advantages of using the solid rockets.

Performance - The high thrust levels produced by a solid rocket engine increases the acceleration loads to values greater than 1g. This large acceleration decreases the time that the aircraft burns fuel from launch to M = 6. Since the turbofan/ramjet engine burns less hydrogen fuel for a smaller amount of time, the total amount of hydrogen fuel used decreases. The decrease in hydrogen is necessary because of it's low density and large volume requirements. Another problem is that the

calculated transonic drag values come very close to the levels of thrust available from the turbofan/ramjet at the thrust pinch. The innovative configuration of our aircraft makes it difficult to accurately describe the drag levels, but if rocket engines are used, the thrust levels are extensive. This increase in thrust is much more that the increase in drag, and the worry of the thrust pinch has been put to rest.

Size/Weight - The rockets used on our aircraft are quite compact compared to the airbreathing systems and fuel. The density of the solid fuel makes the rockets small enough that the drag is not an inhibiting factor. Since the rockets are attached to the exterior of the aircraft. drag is a consideration. Although the drag is by no means negligible. the increase in thrust is more than enough to compensate. Another attractive feature of placing the rockets on the exterior is that the plane can remain small since it does not need to use the volume on the interior of the aircraft. The weight of the casing and components necessary to contain a solid rocket are small when compared to either the weight of solid propellant or the hardware that would be utilized to run a liquid rocket engine.

Expendability - The result of placing the rockets on the exterior of the aircraft and using solid propellants is that the rockets may be ejected after they have burned out. The rockets will produce drag as they are being used and will add to the total mass of the aircraft. but may be ejected after their purpose has been fulfilled. The drag producing shells and extra weight of the hardware will be absent from the larger mach number flight.

Design

A particular solid rocket that would fit our specifications is not already in production, so a rocket was designed to fit our needs. The solid fuel that was used is the same fuel that is used in the first stage of the Minuteman Missile. The fuel specs were obtained in Rocket Propulsion Elements by George Sutton, see references. The following table is the list of the fuel specifications and the final design dimensions.

Fuel composition	16% Al, 70% NH4CIO4	Chamber Pressure	850 psia
	14% polymer binding	Burn time	29.8 s
Density	.0636 lb/inches cubed	Thrust (constant)	25000 lbs
Burning Rate	.349 in/s	Fuel Weight	3480 lbs
Specific Impulse	214 s	Web thickness	10.4 in
Outer Diameter	30 in	Elastomeric liner	.1 in
Length	12.33 ft	case weight	113 lbs
L/D	4.9		

Grain Configuration - Slotted Tube

Rocket Design Calculations

The calculations that were used can be seen in figure 6.2. These calculations were based on the process found in Rocket Propulsion Elements. The criteria set out from the aircraft is that one rocket must produce a constant 25000 lbs of thrust for 29.8 seconds. Also, the length must be less than 13 ft in order to fit in the correct place on the aircraft.

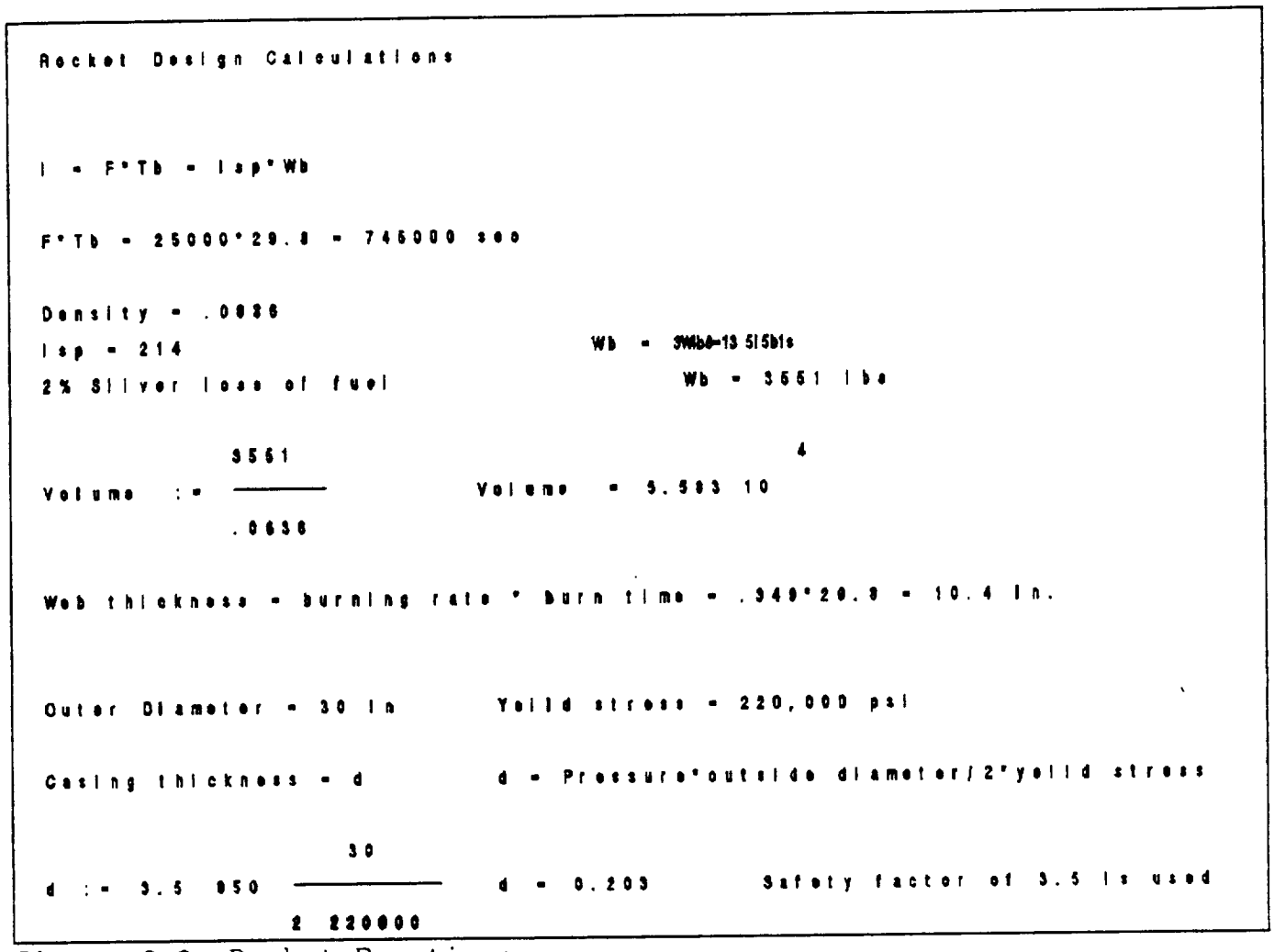

Figure 6.2: Rocket Equations

Rocket Spreadsheet Design

The equations as set forth in figure 6.2 have been entered into a spreadsheet program. See figure 6.3. I varied the parameters of total thrust and outer diameter, and the outputs were weight and length. Length/Diameter was also calculated so that the correct grain configuration could be determined. The final dimensions of the rocket have already been displayed in the table contained in the Rocket Design Section.

Rocket Design Program

Force (lbs)	Outside Diameter (in)	Burn Time (s)	Weight (lbs)	Volume (in)	Inside Diameter (in)	Length (in)	L/D
30000	50	49.68944	3387.916	54334.51	15.31677	53.33614	1.066723
30000	48	49.68944	3387.916	54334.51	13.31677	62.83041	1.308967
30000	46	49.68944	3387.916	54334.51	11.31677	75.76706	1.64711
30000	44	49.68944	3387.916	54334.51	9.31677	94.37102	2.144796
30000	42	49.68944	3387.916	54334.51	7.31677	123.3009	2.935737
30000	40	49.68944	3387.916	54334.51	5.31677	174.2269	4.355673
40000	44	37.26708	3387.916	54334.51	17.98758	54.93365	1.248492
40000	42	37.26708	3387.916	54334.51	15.98758	63.62317	1.514837
40000	40	37.26708	3387.916	54334.51	13.98758	74.9235	1.873087
40000	38	37.26708	3387.916	54334.51	11.98758	90.15515	2.372504
40000	36	37.26708	3387.916	54334.51	9.987578	111.6985	3.102736
40000	34	37.26708	3387.916	54334.51	7.987578	144.3212	4.24474
40000	32	37.26708	3387.916	54334.51	5.987578	199.1655	6.223921
50000	44	29.81366	3387.916	54334.51	23.19006	46.03018	1.046141
50000	42	29.81366	3387.916	54334.51	21.19006	51.97873	1.237589
50000	40	29.81366	3387.916	54334.51	19.19006	59.2837	1.482092
50000	38	29.81366	3387.916	54334.51	17.19006	68.43182	1.800837
50000	36	29.81366	3387.916	54334.51	15.19006	80.16824	2.226896
50000	34	29.81366	3387.916	54334.51	13.19006	95.69298	2.814499
50000	32	29.81366	3387.916	54334.51	11.19006	117.068	3.658374
50000	30	29.81366	3387.916	54334.51	9.190062	148.156	4.938532
50000	28	29.81366	3387.916	54334.51	7.190062	197.1266	7.040237
60000	40	24.84472	3387.916	54334.51	22.65839	53.24605	1.331151
60000	38	24.84472	3387.916	54334.51	20.65839	60.51152	1.592408
60000	36	24.84472	3387.916	54334.51	18.65839	69.5098	1.930828
60000	34	24.84472	3387.916	54334.51	16.65839	80.88795	2.379057
60000	32	24.84472	3387.916	54334.51	14.65839	95.65039	2.989075
60000	30	24.84472	3387.916	54334.51	12.65839	115.4423	3.848076
60000	28	24.84472	3387.916	54334.51	10.65839	143.1521	5.112576
60000	26	24.84472	3387.916	54334.51	8.658385	184.3505	7.090403
60000	24	24.84472	3387.916	54334.51	6.658385	251.3216	10.47173

Figure 6.3: Rocket Calculations

Turbofan/Ramjet (M=.8 to M=6, and landing)

For the acceleration from launch to M=6, 1 turbofan/ramjet engine sized to 92% of full scale was used. The reason for scaling the engine down was to integrate it correctly into our airframe configuration.

There were two main purposes in using a turbofan ramjet in our configuration. The first reason is that we wanted a powered landing. In the case that the calculated flight trajectory would not match the test conditions, power may be needed to maneuver the aircraft at or near the time of landing. Another prominent reason is that if the scramjets should fail at anytime during the test, the turbofan/ramjet would be able to provide enough power to get the aircraft to Edwards. There is enough fuel for the turbofan/ramjet to take the plane the entire distance from launch and still have excess fuel left over. As a final note, since no other propulsion system could be found that provided data for analysis, we has little choice but to use the turbofan/ramjet.

Data

Detailed analysis of the performance of the turbofan/ramjet engine was given to us by General Electric. The scaling relationships for the engine were also given to us by G.E. The data consisted of thrusts, fuel flow rates (FFR) and airflow rates at different altitudes, mach numbers and SFCs. The data was not readily analyzable until it was transformed into a more usable form. The data was somewhat sparse, so I developed a scheme to relate these points into a continuous curve that could be used to find thrusts and FFRs at any altitude and mach number.

The first step was to plot the thrust versus altitude on a graph using the few points given to us. A curve was then fit through these points to provide a continuous thrust/altitude relationship. This was plotted for 7 different mach numbers that would be encountered through

the operating region of the turbofan/ramjet operation (M=.8to6). See figure 6.4.

The next step was to repeat this process on another graph, but to use FFR instead of thrust in order to obtain a FFR vs thrust curve. Again, this was given at different mach numbers as shown in figure 6.5. Both the thrust and FFR calculations were given for the maximum attainable SFC at each point. This was chosen because analysis showed that the larger acceleration from this higher thrust overcame the increased FFR and gave the minimum amount of fuel burned.

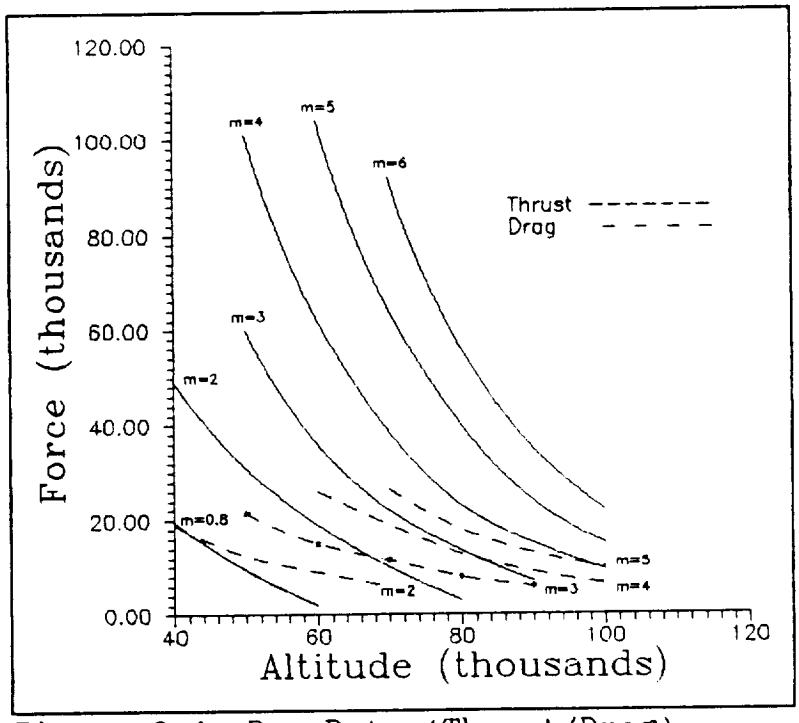

Figure 6.4: Raw Data (Thrust/Drag)

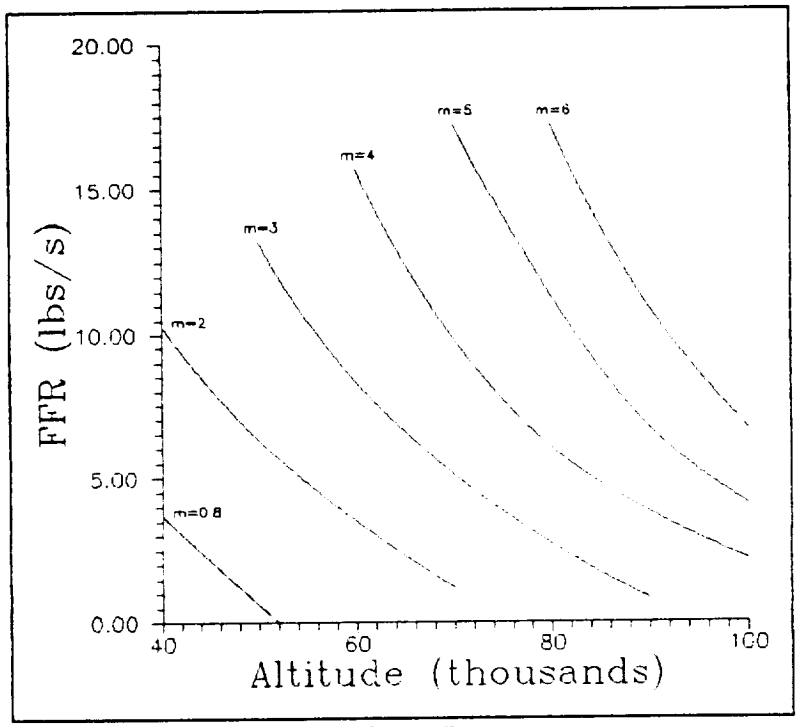

Figure 6.5: Fuel Flow Rate

The final step was to use the values from the aerodynamic program that gave drag at different altitudes and mach numbers. This set of data, drag versus Altitude at a given mach number, was overlaid onto

the thrust vs. alt graph because both of these forces are used in conjunction in the calculation of the flight profile. See figure 6.4.

Scramjet (M=6 to M=9.25)

The purpose of this vehicle is to test a scramjet engine at a high mach number after accelerating from M=6 at 100k ft. The total number of scramjets chosen was 3. The size of the scramjet could not be changed since no scaling relationships could be found. Instead of scaling the engine, multiple engines may be used as a single propulsive unit. We used 3 scramjet engines because this was the size limitation of our aircraft. Any more engines would have improved the fuel rates, but would have decreased the lifting surface and destroyed the aerodynamics of the upper lifting surface.

Using the scramjet data that was provided by GE for their engines, I again set up a set of curves that would be the relationships for a more continuous distribution of thrusts vs speeds. I mention speed only because the scramjets will operate only at 100k ft, thus, the altitude is not a variable. I used the GE curves of thrust vs fuel equivalence ratios (ER7) at different speeds and replotted it as thrust vs speed at a different ER7 values. See figure 6. This was preferable because it provided a thrust output for varying speeds, which are the parameters that the fuel program uses as inputs. Please note that drag was a given distribution over the M=6 to M=10 speed range due to constant altitude. The drag was not plotted on the thrust curve because of the simple nature of the trajectory.

The fuel flow rate vs speed was also plotted for the scramjet engines using the method mentioned for the thrust levels. See figure 6.7. For each ER7, there was a given thrust and FFR, so as can be seen, the ER7 is the unifying factor between the graphs.

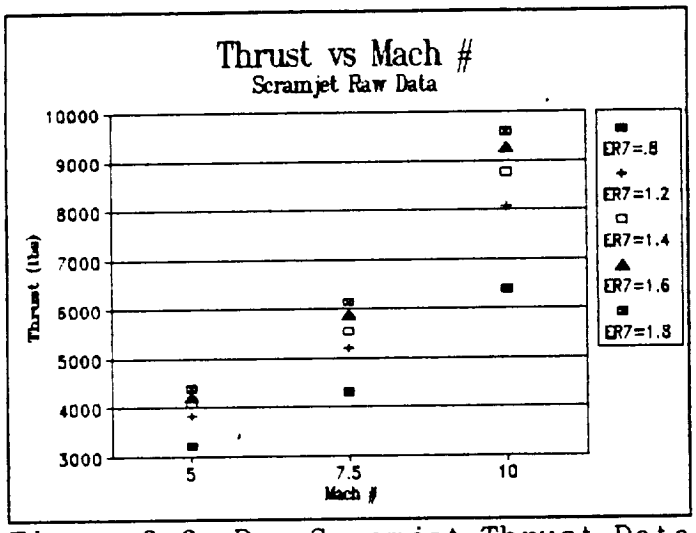

Figure 6.6: Raw Scramjet Thrust Data

Turbofan/Ramjet-Scramjet Fuel Program

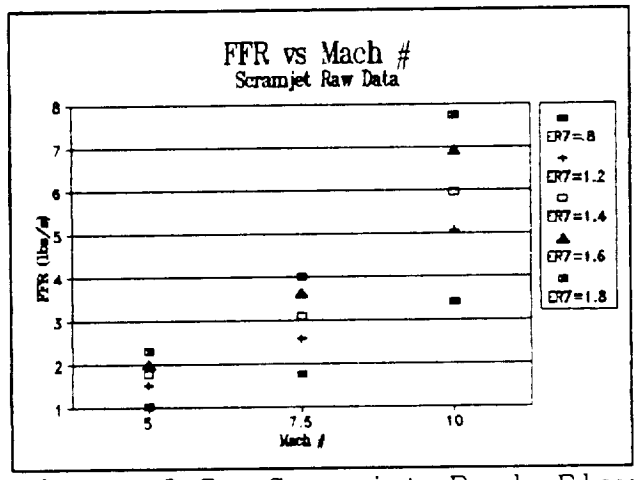

Figure 6.7: Scramjet Fuel Flow Rates

The purpose of this program was to take the thrust, drag and fuel flow rates and calculate the amount of fuel used, distance, accelerations etc.. This program was used for the turbofan/ramjet and scramjet acceleration plus the scramjet cruise time. The glide portion and subsonic cruise before landing are handled in the glide portion of this report. The program is based on Newtons Second Law and the relationship between FFR and time. The program was integrated into a spreadsheet so that the inputs could be easily changed and the results readily graphed. An example of a portion of the numerical spreadsheet listing is located in Figure 6.8. A few of the particulars are included and list as follows:

n Scaled 90% 1 Engine 44000

M1	Total Thrust	Total FFR lbs/s	Drag lbs	Acc ft/s	Time s	Fuel lbs	Weight lbs
0.9	66928	3.30096	19000	35.89	2.7027	8.9214	43591
1	74122.4	4.57056	21000	41.72	11.625	53.133	41338
1.5	82586.4	6.47496	23000	49.2	9.8583	63.832	39074
2	89780.8	8.2524	27000	53.2	9.1168	75.236	36799
2.5	46552	9.9452	21500	21.92	22.125	220.03	36579
3	49937.6	11.638	23900	22.92	21.16	246.26	36333
3.5	52900	13.9656	25500	24.28	19.972	278.93	36054
4	52900	14.812	25000	24.92	19.464	288.3	35765
4.5	48244.8	13.5424	23000	22.73	21.339	288.98	35476
5	51111.2	16.8948	18500	29.6	16.385	276.83	35200
5.5	37568.8	13.5092	11270	24.06	20.16	272.34	34927
					173.91	2072.8	

Scramjet Acceleration

M1	Drag lbs	ACC ft/s	Time s	Fuel lbs	Weight lbs
6	8500	5.26	190.11	1209.1	33990
7	9500	6.915	144.6	1214.7	32776
8	10400	8.94	111.86	1211.4	31564
9	11001	11.42	21.883	296.07	31268
			468.45	3931.3	

Scramjet Steady State

M	Drag lbs	ACC ft/s	Time s	Fuel lbs	Weight lbs
9.25	11300	0	120	720	30548

Fuel lbs
6724.05

Figure 6.8: Turbofan/Ramjet Spreadsheet

- The program is based on a changing mass as the fuel is continuously being burned.
- Using Newtons Second Law, the thrust, drag and mass are used to calculate accelerations, distances and times derived from the kinematic equations of motion.
- Uses changing FFRs and time in order to calculate the fuel usage

The need for this program and the versatility built into it will now be discussed. The beginning of our iteration loop for the turbofan/ramjet starts with the designation of a flight profile (M vs Alt). The thrusts and drags can now be obtained from the raw data curves in figure 6.4. Using the same flight profile, the fuel flow rates can be obtained from the graph in figure 6.5. The thrusts, drags and fuel flow rates can now be easily entered into the program. The outputs are distance, time, fuel and accelerations. Since the fuel weight is our major concern, we continued to pick various flight profiles until we optimized the fuel burned in this region. The difference between the best and worst flight profiles was approximately 4000 lbs, which is half of the entire fuel weight! The optimization of the profile was critical in the success of

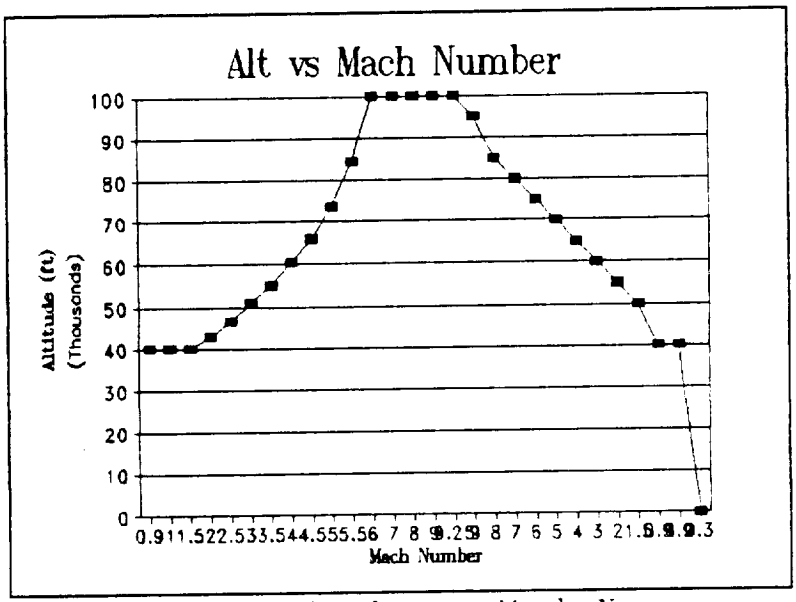

Figure 6.9: Altitude vs. Mach No.

our aircraft. The final result of this profile iteration is shown in figure 6.9.

The iteration loop for the scramjets was somewhat different. A flight profile was not the beginning of the iteration because we were at a constant altitude and the profile was trivial. The start of this iteration loop was the choice of a single ER7 or a combination of different ER7s over the speed range used to read thrusts and FFR from the graphs in Figure 6.6 and Figure 6.7. These values were fed into the scramjet portion of the program Again, the fuel weight burned was the prime consideration. The result of this optimization was that a constant ER7 of 1.2 was to be used for the entire speed range. This saved us another 2000 lbs of fuel over the case of a poorly optimized choice of ER7.

The scramjet cruise portion was included on the spreadsheet but could have been done by hand. The thrust was set equal to drag and the corresponding FFR was used for the 2 minute cruise.

Profile (Acceleration and Cruise)

All of the graphs that will be presented in this section are direct results from the fuel spreadsheet program. All of these cases were considered for both the configuration that included the rocket and that which was "rocketless".

Fuel Percentages

See figures 6.10 & 6.11. The comparison of the rocket and rocketless versions both show that over 50% of the fuel is used in the

scramjet acceleration. The turbofan/ramjet cruise is the other major portion of fuel. Note that adding the rockets decreases the amount of fuel needed in the turbofan/ramjet and lets the scramjets do more work and attain a higher mach number.

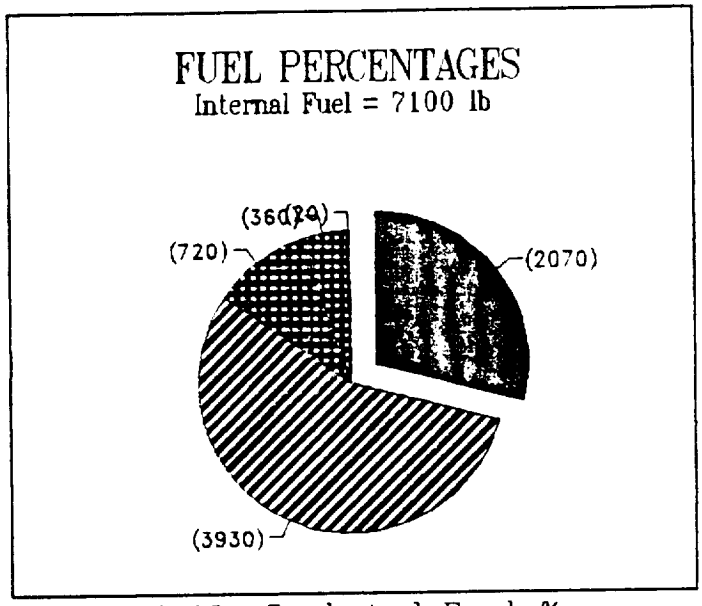

Figure 6.10: Rocketed Fuel %.

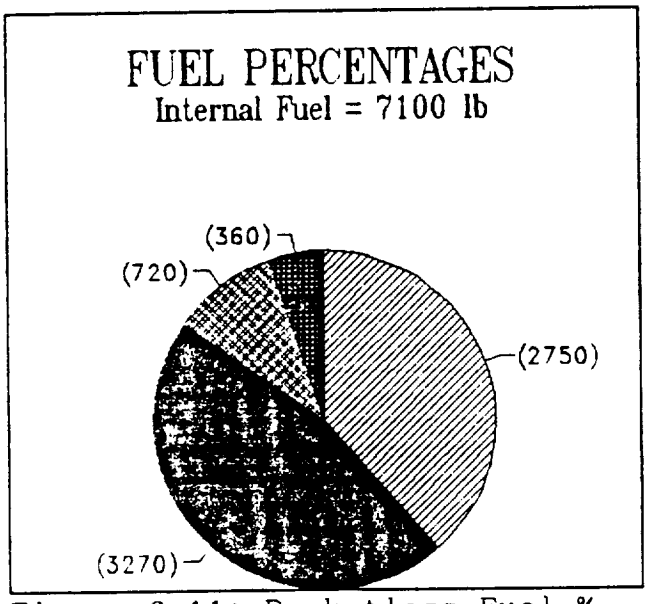

Figure 6.11: Rocketless Fuel %.

Force vs M

See figures 6.12 & 6.13. This graph plots the thrust and drag vs M for the entire acceleration stage. The primary design is to keep the thrust curve higher than the drag curve at all times. On the graph of the rocketless configuration in figure 6.13, you can see that at the transonic region the aircraft experiences a thrust pinch. This is due to the high drag because of transonic effects on aerodynamics. The rocket version in figure 6.12 shows our solution to this problem. The high thrust is considerable compared to the smaller increase in drag. The result is not only less fuel used, but there is no fear of not breaking the speed of sound.

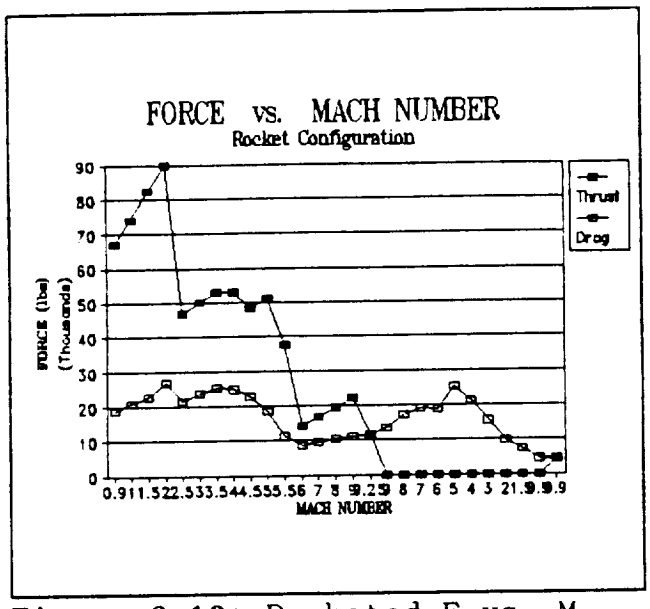

Figure 6.12: Rocketed F vs. M

Acc vs M

See figures 6.14 & 6.15. These graphs depict the data found in the spreadsheet program. The rocket accelerations are considerably higher in the earlier region as would be expected. The negative accelerations are due to the glide portion of our profile (deceleration). The slight discontinuity near M=5 to 6 is due to the fact that the scramjets were turned on a little early to aid in the acceleration at that point.

The rest of the figures (6.16 through 6.21) are plots of different variables through the profile and have been provided to give any additional information that you may have wanted to see.

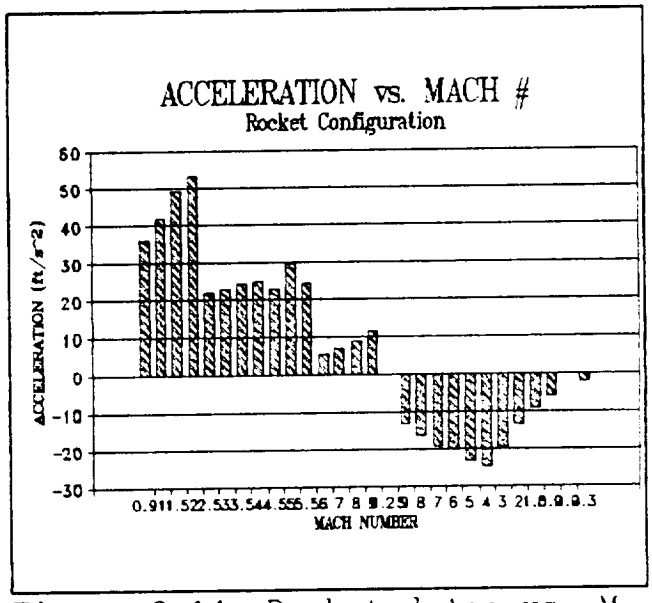

Figure 6.14: Rocketed Acc vs. M

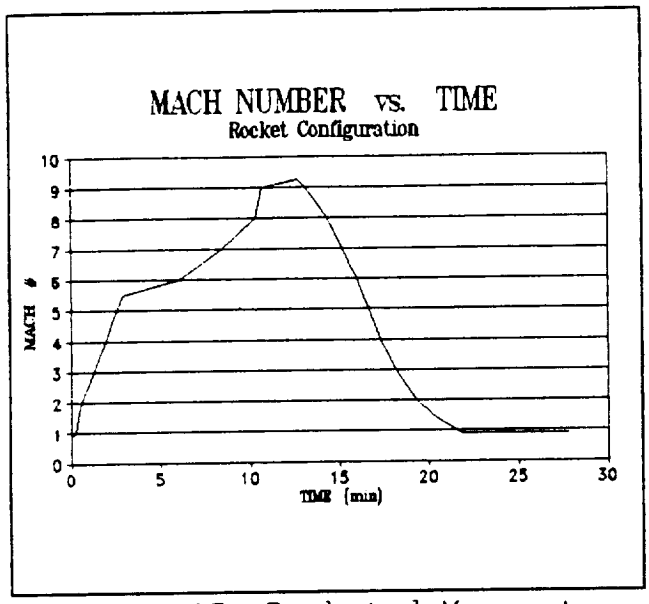

Figure 6.17: Rocketed M vs. t

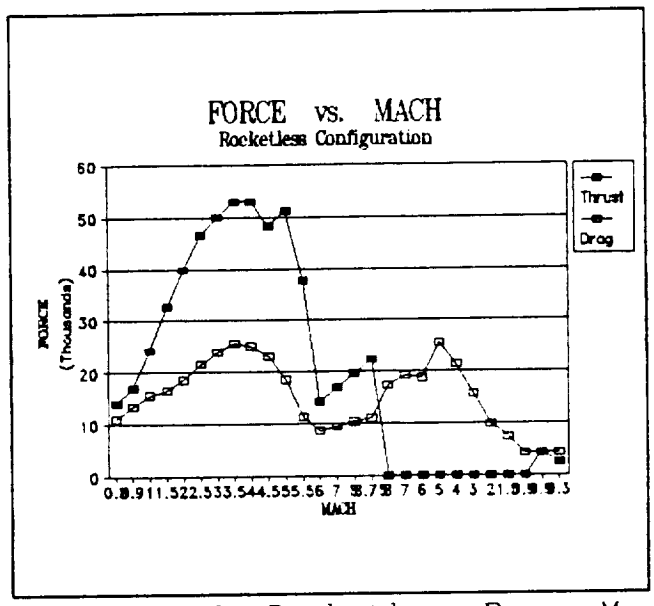

Figure 6.13: Rocketless F vs. M

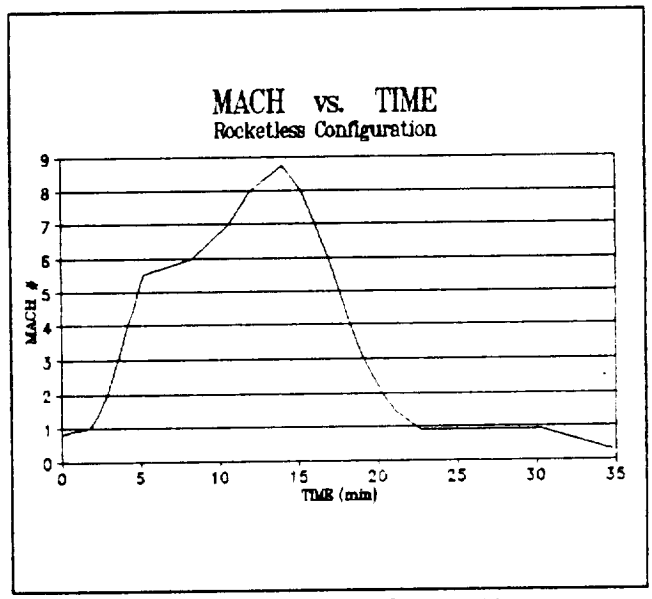

Figure 6.18: Rocketless M vs. t

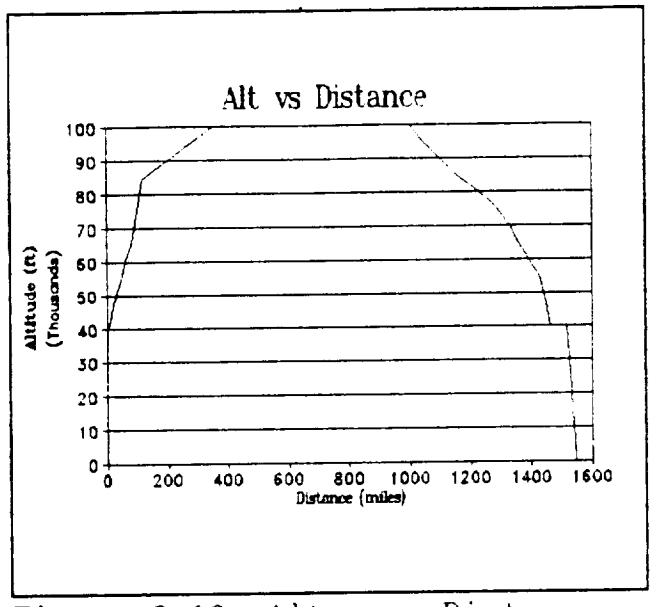

Figure 6.19: Alt. vs. Dist.

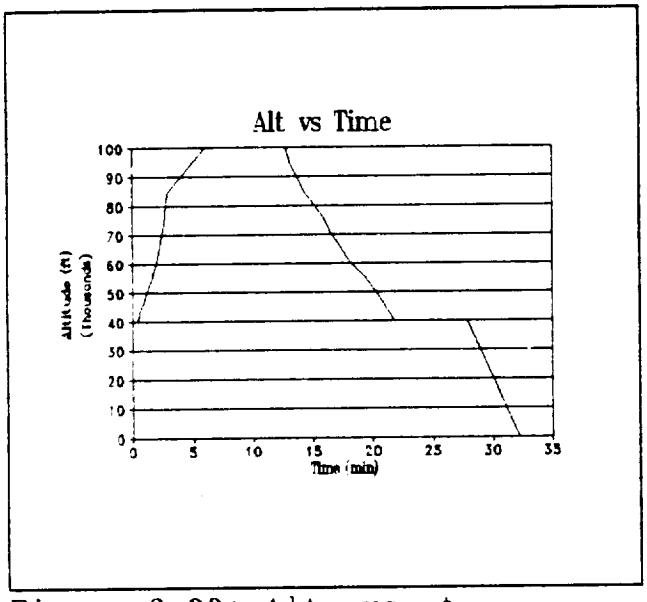

Figure 6.20: Alt. vs. t

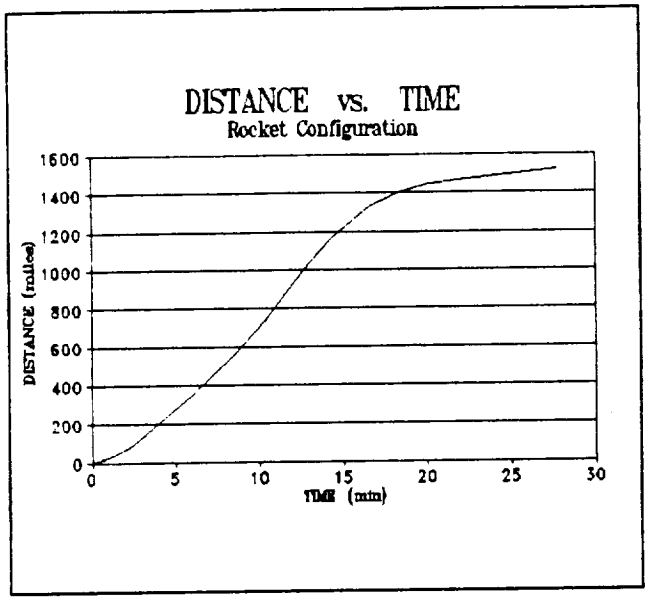

Figure 6.21: Dist. vs. t

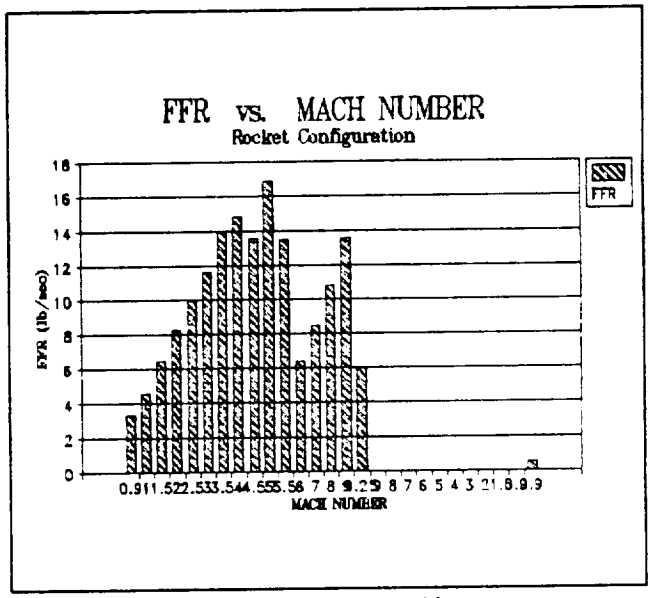

Figure 6.16: FFR vs. M

Chapter 7

GLIDE CALCULATION
(Gary Hufford)

The last portion of the mission profile is the glide and landing portion. After the two minute Mach 10 cruise has been completed, all engine systems are shut down. The airplane will then gradually decrease Mach number and altitude until Mach 0.9 at 40,000 feet is reached. This point will also be thirty miles off the California coast in preparation for landing at Edward's Air Force Base. This point was chosen such that the sonic boom created as the airplane reaches Mach 0.9 from Mach 10 will not affect the California coastline.

After this 75 mile cruise the airplane will begin its landing descent. This descent will be gradual from Mach 0.9 at 40,000 feet to Mach 0.3 at sea level. Thirty miles have been allowed for this descent. This last 30 miles will allow landing at Edwards Air Force base. The fuel needed for the Mach 0.9 cruise is 227 pounds. This was computed by setting thrust equal drag and finding the corresponding fuel flow rate. By computing the velocity, the time needed for a 75 mile cruise was calculated. The fuel was computed by multiplying time and fuel flow rate.

The fuel needed for the thirty mile descent to landing is 132 pounds. To compute this value the deceleration to travel thirty miles must first be computed. From the acceleration, time and thrust were computed. With the thrust level known the fuel flow rate is determined. Fuel needed is then computed by multiplying fuel flow rate and time.

The glide descent and fuel computation are given in tabular form in Chapter 6. The glide and landing profile were chosen arbitrarily to obtain approximately a 500 mile distance. This portion of the mission profile can be seen graphically in Chapter 8. The fuel computations are given in Chapter 6.

Chapter 8

FLIGHT PLAN

(Gary Hufford)

The flight plan is shown in Figure 8.1. The carrier aircraft will take-off from McChord Air Force Base in Washington and fly over the Pacific Ocean where the vehicle will be launched. The research vehicle will fly in a straight line through the Mach 10 cruise and descent until the aircraft reaches Mach .9 at 40,000 feet approximately 30 miles off the coast. At Mach 0.9 and 40,000 feet approximately thirty miles off the coast. At Mach 0.9 and 40,000 feet the subsonic cruise will begin to land at Edwards.

Four reasons exist for choosing this flight plan. First, we must fly over water for safety reasons. If something should go wrong, no lives will be endangered. Second, the length of the flight plan is the projected range of the vehicle for a successful test. At any point during the test, if the test is aborted sufficient fuel will be left to land at Edwards Air Force Base correctly utilizing the turbofanramjet. Third, we must fly close to land to be able to maintain ground based communications. At Mach 10 the vehicle will cover large distances and several ground based stations may be necessary to maintain constant communication. And fourth, the sonic boom problem becomes non-existent for this flight plan. By flying through Mach 1 at 40,000 feet, thirty miles off the coast, the sonic boom produced is well within tolerable limits.

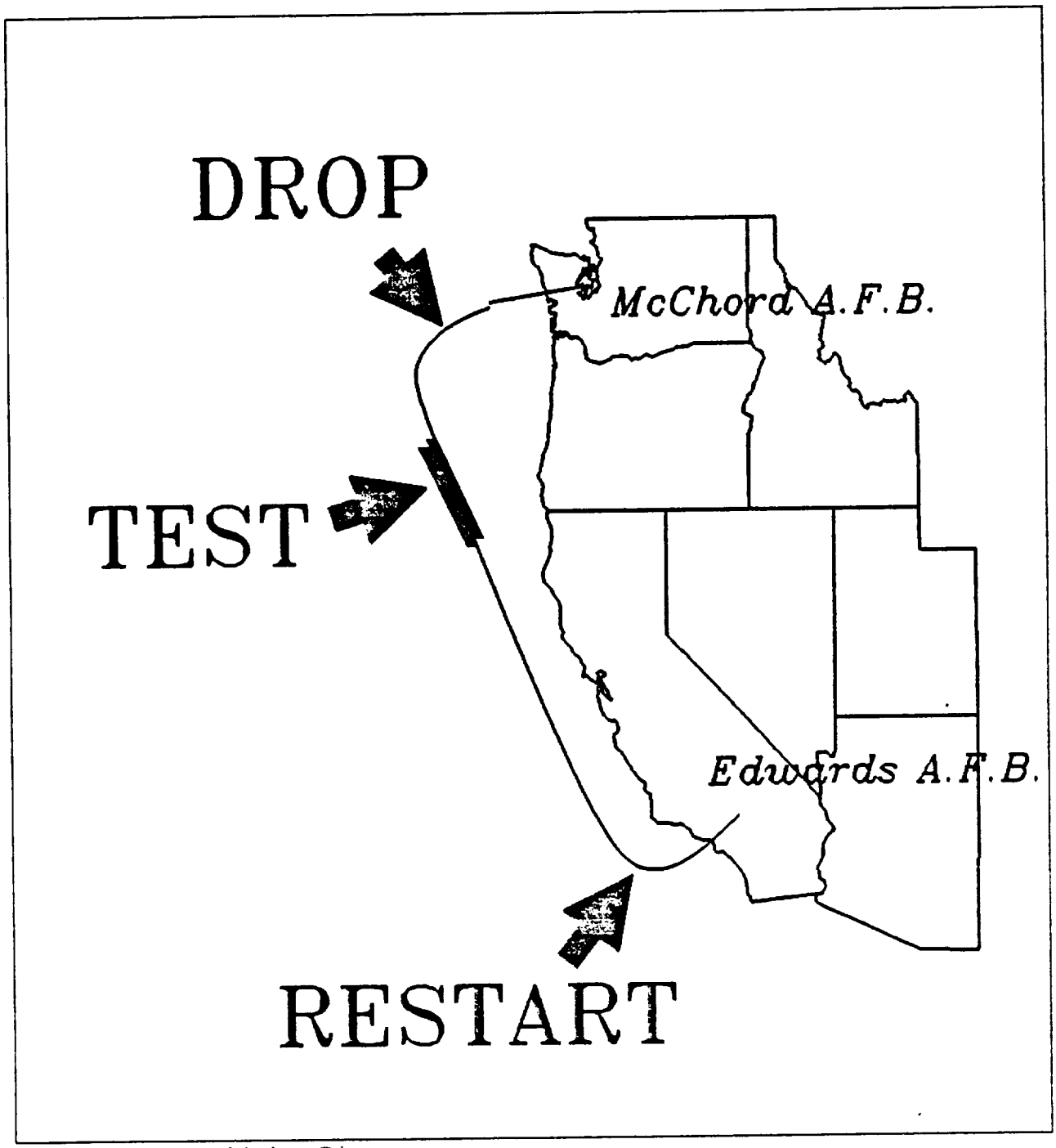

Figure 8.1: Flight Plan

Chapter 9

SCRAMJET INLET DESIGN

(Terry Bisard)

Introduction

The purpose of the inlet is to slow down the free-stream flow and to create a favorable pressure gradient and weight flow rate to enter into the combustion chamber. Designing a supersonic inlet is a very complicated task. In actuality an inlet is of a three-dimensional design, but to make caculations simpler, our inlet assumes a two dimensional wedge shaped design. Using oblique shock theory and the method of characteistics, the flowfield inside the inlet can be analyzed.

For our supersonic research vehicle, we decided to put our SCRAMjets on the top surface of the aircraft and the turbofanramjet on the bottom of the aircraft. This allows two separate inlet systems to be designed to make the two different engine systems to operate more efficiently. Also, because the supersoic inlet only has to vary from Mach six to ten, the total inlet geometry is less complex. Inlet Geometry

The compression angle is the angle at which the inlet converges. Values for the compression angle vary between six and eight degrees. A few drawbacks to high compression angles are high total pressure losses, and early shock induced boundary layer separation. The only problem with a low angle is increased inlet length. As the compression angle increases the flow gradients become steeper. This occurs because the

of these conditions must be met while keeping the inlet length less than 18 feet.

Flowfield Analyzation

In analyzing the inlet, one must consider the series of reflected shocks that develop. Because of these shocks, the flow is slowed down and there is a tremendous loss of total pressure. Instead of lengthy, complex hand calculations, a computer program was developed to calculate the flowfield parameters at certain stations along the inlet. Oblique shock analysis can be used because our SCRAMjet inlet assumes a two-dimensional wedge shape design.

To maintain organization, the main program consists of many program subroutines. The OBLIQUE subroutine calculates flow conditions behind an oblique shock wave and the GEOM subroutine pinpoints the position in the inlet that these conditions occur. The program should be run for several different cases to find the best inlet design configuration.

Boundary Layer Interaction

In analyzing any body in a hypersonic flow, the viscous boundary layer must be taken into consideration. This is especially important in inlet design, because turbulent flow entering a conbustion chamber could disrupt an efficient thrust process. For a SCRAMjet inlet, the boundary layer is very large and is on the order of 20% or more of the entire flow entering the combustor.

To insure that only a small boundary layer interacts with the flow going inot the conbustor, a boundary layer reduction system needs to be

Chapter 10

TURBOFAN/RAMJET INLET

(Jim Rogers)

Unlike the Scramjet Inlet which operates only in a narrow mach number region, the turbofan/ramjet inlet must operate from subsonic speeds from about mach 0.4 during landing up to a blistering mach 6.0. The accomplishment of such a design is not a trivial task. The requirements of the system change drastically throughout the operational region.

Through each region, the inlet must provide the appropriate mass flow required by the engine at the correct conditions. Along with this, the air flow must be of good quality. That is to say, it should have approximately the same conditions across the compressor. If inequalities exist, the results could be disastrous.

DESIGN

The first concept desired for this aircraft was a conical inlet. This was mainly for aesthetics, but never-the-less it was the first. It soon became apparent that a conical inlet would not suit our purposes. In order to accomplish the mission throughout the profile, the inlet would have been far too complex to be feasible. The next logical step was to design a two-dimensional inlet.

By studying the required ramp angles to provide a suitable pressure recovery at mach 6, a few tendencies were noted. One of these was that if the ramps generally increased as the mach number decreased through the channel, the pressure loss wouldn't be quite as bad. At this point

as much as 2 inches at the inlet. Due to the unknown nature of the boundary layer in the hypersonic region, a 4 inch initial bleed diverter is implemented just prior to the inlet. If the boundary layer becomes too much of a problem in this area, surface cooling will be applied in order to shrink it. This doesn't eliminate the boundary effects. The boundary layer must be stripped throughout the inlet. The external ramp section will be made of perforated metal sheets which can provide just the right amount of mass flow to strip the boundary layer as it attempts to grow through this section. To account for all boundary layer mass losses and possible auxiliary system losses, the actual capture area is increased by 20%, to 6 ft^2.

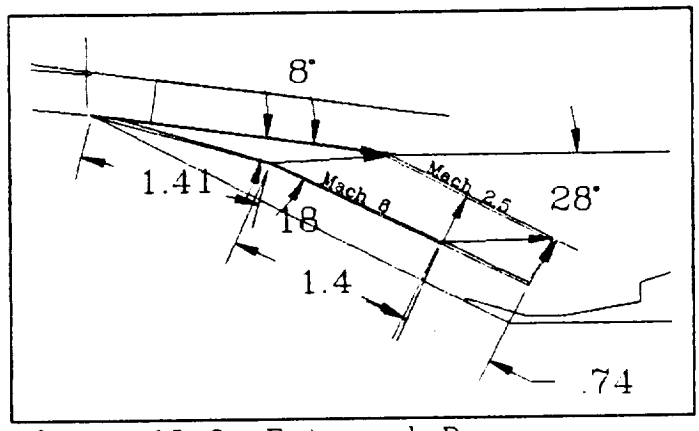

Figure 10.2: External Ramps

smooth increase in area at all mach numbers. The 2-D section of the inlet is shown in figure 10.4.

At the end of the 2-D section of the inlet, another system of boundary layer diverters is located. At this point a rectangular to circular divergent section will gate the flow into the compressor. This section is one solid piece, except for two 4 ft^2 door sections on either side which provide the necessary mass flow rate at the subsonic speeds. The engine will be in a starvation period through some of the faster

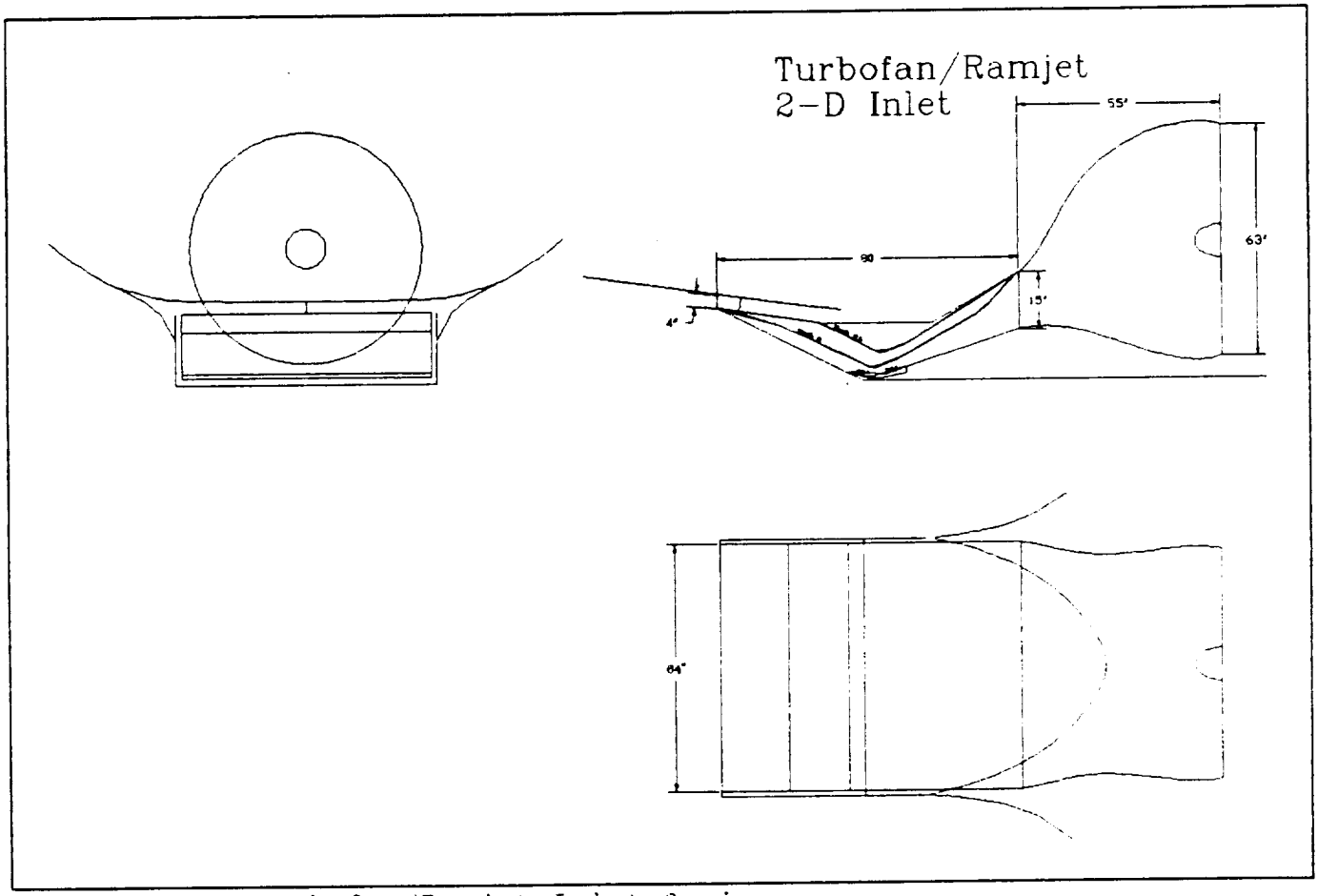

Figure 10.5: Turbofan/Ramjet Inlet 3-view

subsonic speeds. This is acceptable due to the rocket assist on ascent and the quick descent, where this is thought not to be critical.

The test of efficiency for an inlet seems to be the level of pressure recovery available. Figure 10.6 shows the pressure recovery throughout the flight profile.

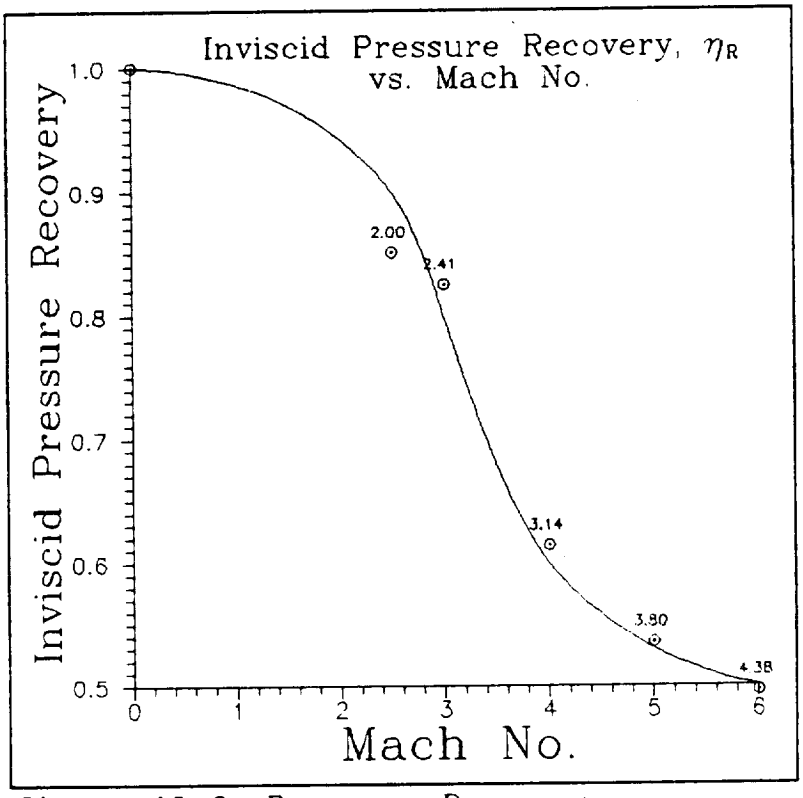

Figure 10.6: Pressure Recovery

Chapter 11

COOLING
(Jim Rogers)

Introduction

As a body moves at low supersonic speeds, the heating of the body is not a very important consideration. As the speed increases, the heating of the body increases. At hypersonic speeds, as those encountered by the vehicle under study, the heating becomes a primary concern. For example, the recovery temperature at Mach 10 is greater than 4000°R. There are very few materials which are solid at these temperatures, and none (as of yet) that can be used reliably for an aircraft's structure.

Even if these materials were available, the vehicles internal temperature would be far too great for the electronics, fuel system, and hydraulic system. If the vehicle were to be manned, a further constraint on the internal heat would be present. The pilot would also not be able to exit the aircraft until after a lengthy cool-down period. This design, being unmanned, will not be concerned with post-landing problems at this time.

Cooling Methods

As a result of the previous discussion, this aircraft will need to have some sort of cooling system. There are two basic types of cooling, active and passive. Passive cooling attempts to design the structure in such a way so as to provide a highly conductive path to shunt the heating away from the "hot spots" to the cooler areas where the heat may be radiated away. This type of system cannot provide the cooling rate

required near the forward surfaces, therefore, although some passive cooling may be found to be useful, the subject will not be discussed further here.

Since passive cooling is not adequate, an active cooling system needs to be considered. By using some secondary fluid, the heating can be diverted into this fluid and carried away. There are three basic types: transpiration, direct convection, and indirect convection. Figures 11.1 thru 11.3 display schematics of each of these systems.

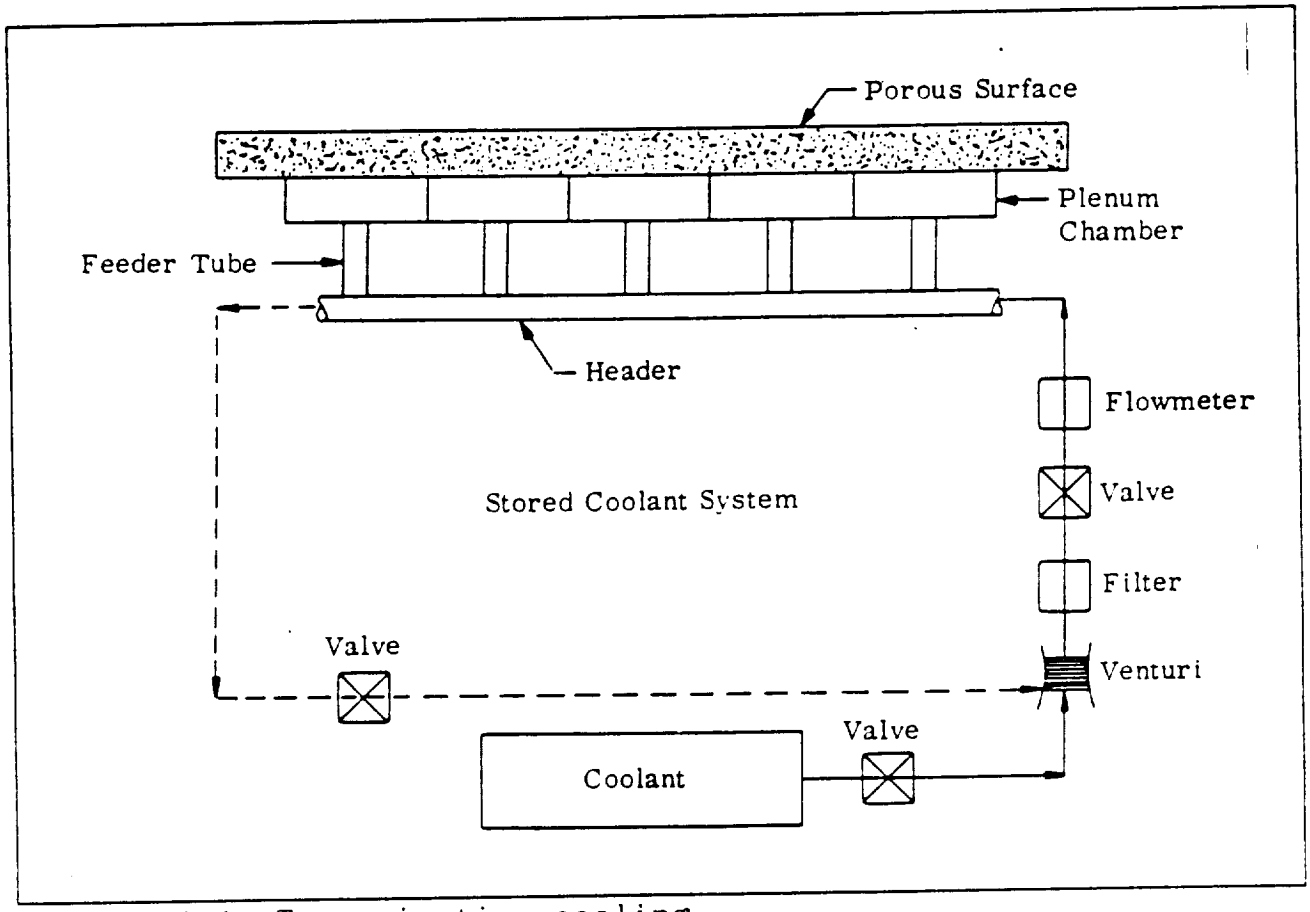

Figure 11.1: Transpiration cooling

Transpiration cooling, illustrated in figure 11.1, uses a porous surface material with which a fluid is forced to seep out to the boundary layer. This provides a layer of fluid in between the hot boundary layer and the cooler aircraft surface. The heat is still transferred from the boundary layer, but the surface into which it is going is being continuously replaced. This mass transfer into the boundary layer causes the boundary layer to increase in size while decreasing the surface friction. This system appears very good aerodynamically, but does require the aircraft to carry the fluid which increases overall weight. This fluid could be water (actually some water mixture such as water-glycol), hydrogen or just air.

Air is appealing because it does not need to be carried in the aircraft. The air would be "scooped up" as the aircraft is flying. This method may naturally provide the necessary pressure to drive the system. The primary problem with this method is the capture area required to provide the necessary mass flow rate. If the mass flow can be provided, the air can be passed through a heat exchanger to cool and then passed through the porous surface providing the cooling. The heat exchanger cools the air by heating the hydrogen fuel on its way through the fuel system.

A variation on this theme is to use water or hydrogen to provide the fluid cooling layer. The advantages of these methods is that the fluid does not need to be cooled before used and the lack of the large capture area reduces drag. The disadvantage is the additional weight of these fuels. Although hydrogen may be lighter, the increase in volume and the safety issues preclude its use. Another problem is the

streaking which may occur, possibly leaving the surface dangerously exposed to the extreme conditions it wasn't designed to withstand.

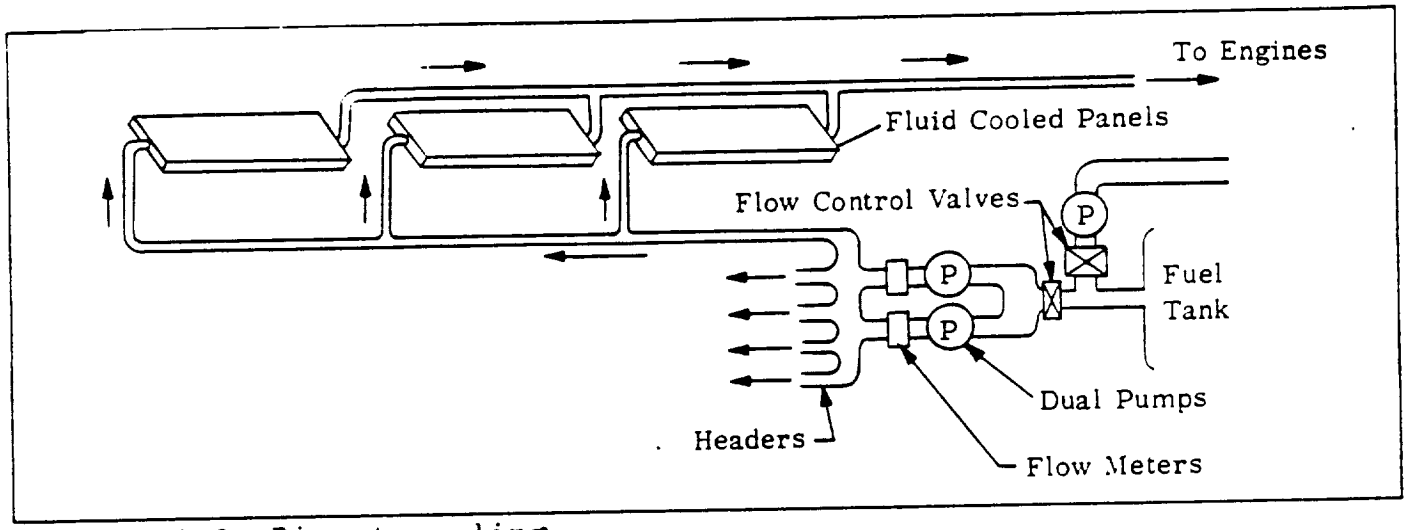

Figure 11.2: Direct cooling

Figure 11.2 illustrates the direct convection method. This method directs the hydrogen fuel around the aircraft cooling the surfaces by transferring the heat to the fuel. This method is an effective cooling technique but does have its problems. The dangers of an aircraft literally lined with a dangerously explosive substance needs no elaboration. Another problem is hydrogen's tendency to react with titanium. Because the structure, at this point of the development, will be made of a titanium-aluminum alloy, this method looks unattractive.

A variation on this method is called spray cooling. A pressurized coolant is sprayed through a nozzle causing the liquid droplets to vaporize as the hit the hot surface. The resultant vapor is routed to another portion to be cooled and then pumped back for repeated use. This method can use a water heat sink, or where the heating is extreme, a metal such as lithium can be used. Lithium's melting point is about 360°F, and has a heat flux capacity of at least 1200 BTU/ft^2-sec.

Lithium's heat capacity is also ten times that of water. The drawback is that the lithium system operates at a temperature of 1700°F as opposed to 200°F for the water system. Indirect cooling may provide an alternative.

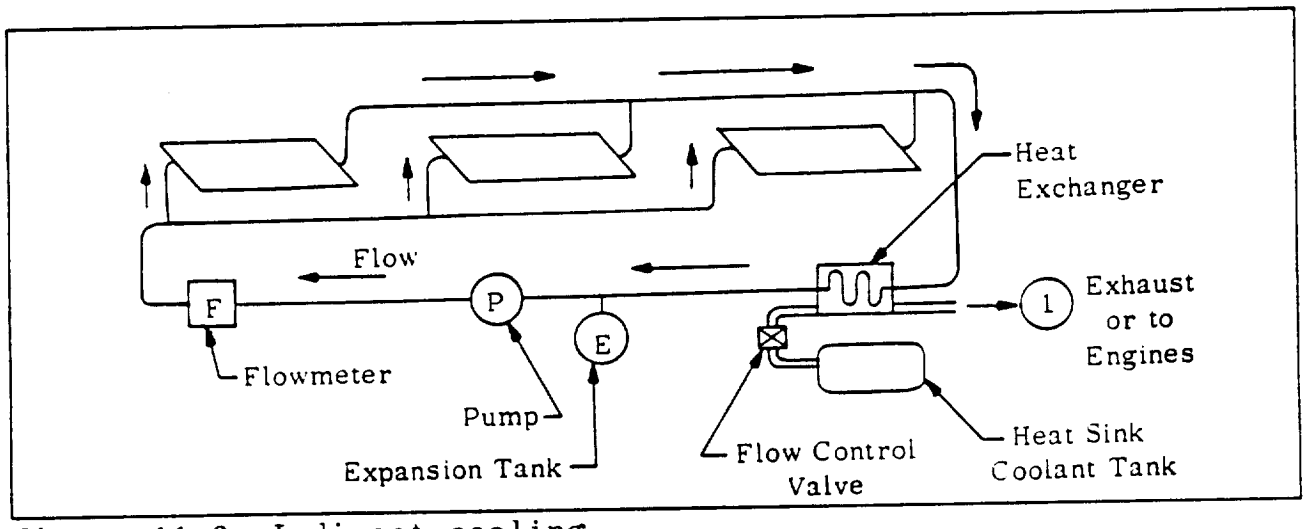

Figure 11.3: Indirect cooling

Figure 11.3 shows the indirect method. This method uses a secondary fluid such as a water-glycol mixture or even some gaseous substance which is pumped through the aircraft. The cooling fluid is cooled through a heat exchanger which transfers the heat to the fuel. This method has the advantages of localizing the hydrogen to a smaller area of the aircraft. It also relieves the material problems due to the reaction with hydrogen.

Configuration

The basic system types presented above have been considered for various areas of the aircraft. The most critical area is, naturally, where the temperature would be the highest, i.e. the leading edge. The enormous heat transfer rates occurring in the immediate area around the

leading edge narrow the possibilities of systems capable of keeping it cool.

The only type which cannot be used is transpiration. The high pressures at the leading edge and stagnation area preclude its use. While using some cooling system which ultimately uses the fuel to cool the aircraft appears attractive at this point, the fuel has a limited heat capacity which will quickly run low if used to cool the leading edge. Therefore the choice for leading edge cooling is a lithium spray cooling system which is relatively light(about 400lbs.) and self-contained. This system will provide cooling for 6" from the leading edge. Other systems are used elsewhere.

The rest of the forward surfaces will need cooling, although not nearly as much as the leading edge. A transpiration system is desired here, but at this point it is unknown the effects it may have on the inlets and how it may be bled off before them. If transpiration is not possible, a direct convection system will be used to cool the forward surfaces. As the fluid is heated, it is transferred to the rear of the aircraft where it can be used for transpiration cooling on the exhaust expansion surfaces. If this "free" transpiration coolant is not available (i.e. transpiration is used on the forward surfaces), a metal-matrix surface will be used on the exhaust surfaces.

Another critical area of heating is the propulsion area, including inlets. The large temperatures involved require an active cooling system. At this point a direct convection system looks appealing. A system of cooling plates will provide the necessary cooling via the hydrogen fuel as it is pumped to the engines.

The avionics bay, containing the communication and control electronics may need cooling to keep it below 100°F which may be required by these devices. If the fuel tank placement doesn't provide the necessary cooling, an indirect convection system will be used. This system will use a water-glycol mixture to cool the avionics bay. A heat exchanger will be used with the fuel to utilize more of hydrogens heat capacity.

The only areas not mentioned so far are the control surfaces. These surfaces can be exposed to extreme temperatures close to that of the forward surfaces. A metal-matrix material will be used on all control surfaces.

A hypersonic aircraft will prove to be a flying cooling system as discussed above. The economical use of these technologies may well prove to be the decisive factor in the feasibility of a hypersonic aircraft.

Chapter 12

SUPPORT SYSTEMS
(Jim Rogers)

Control

The control of a vehicle which flies at ten times the speed of sound has some interesting problems. At these speeds the temperature of the aircraft can adversely effect the control systems. To alleviate some of this problem, a fly-by-light system will be used. The system will be controlled by a dual-redundant, fault-tolerant, centralized system located in the avionics bay. By using this centralized, integrated opto-electronic system, the cooling of many areas may be eased.

At this point, the effects of these temperatures on the hydraulic system is unknown. The hydraulic system is required to actuate the control surfaces, inlets/exits, and landing gear. This system, not infallible, requires a backup system. Under consideration is a duplicate system or a backup electrical system.

The initial propulsion device will provide electrical power to the aircraft via generators. When the scramjet is being tested, the generators will not be producing any power. The primary propulsion system will not be started until the aircraft has reduced its speed considerably in order to conserve fuel. Possibilities for this system range from a hydrazene power generator to a secondary turbine using a ram input flow, although there may be a possibility of using the ramjet turbine by diverting some of the airflow through it. The length of time an auxiliary power system will be operating will be anywhere from 4-12

minutes, depending on the final deceleration decided upon for the flight plan.

Communication

An unmanned aircraft can either have a programmed flight plan or it can be radio-controlled. This aircraft will have both. An aircraft flying at hypersonic speeds will require a nearly real-time interface with minimum delay between command and reaction. This requires the telemetry data to be received often and quickly in order to maintain a tight control on it.

This requirement of quick communication requires a large bandwidth at high frequencies. As an arbitrary choice due to the uplink/downlink duality of the frequency range and the low signal absorbsion by the atmosphere, a X-band frequency will be used. Communicating with this aircraft will also require a number of stations.

The aircraft will fly over 1000 miles in about 15 minutes. A proposed flight plan would have the aircraft launched from the carrier plane flying out of McChord A.F.B. outside of Seattle, Wa. The path then runs parallel to the west coast and will land at Edwards A.F.B. east of Los Angeles, Ca. A system of uplink/downlink stations distributed along the coast will provide uninterrupted communication to/from the aircraft.

The critical stages of the flight, as with any other, is the beginning and the end. The carrier/test plane combination will perform as an integrated system from takeoff through separation. This should provide a higher level of safety during this phase. During landing, a

video camera is currently being considered to provide the controller a better feeling of the aircraft as it lands.

This will all be for naught if something goes wrong in the communication chain, even a momentary lapse. By having a programmed flight plan in memory prior to separation, the test can be conducted without external control. To land, a backup chase plane will be able to control the test plane via different channels allowing the "backseat" to land it if all else fails. This method was developed for the HiMAT research aircraft and seems reasonable.

The control and communication subsystems will become a very integrated, interlocked system. Figure 12.1 illustrates this system as it is currently envisioned. An interesting item is what type of antenna can be used at such high temperatures.

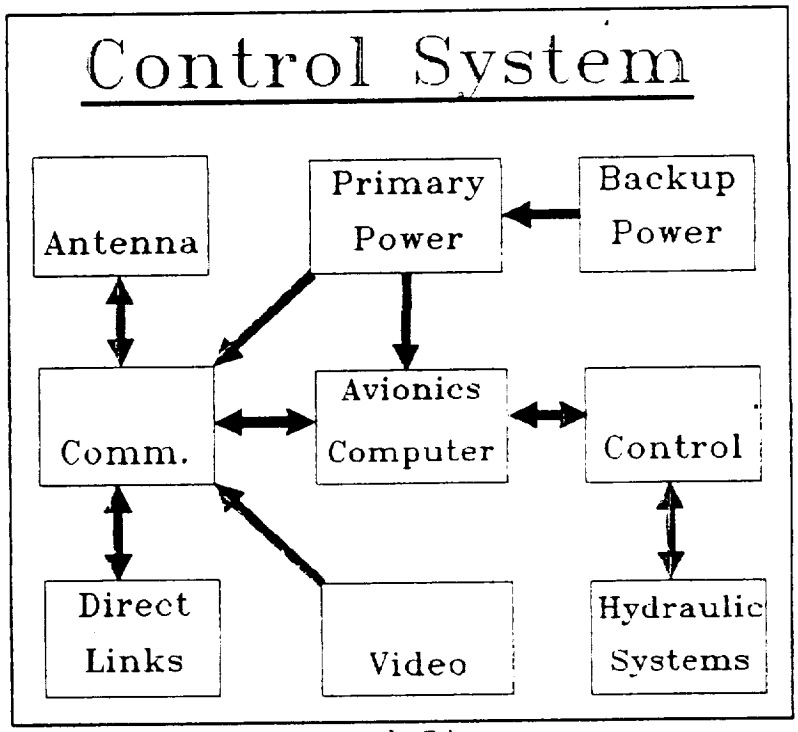

Figure 12.1: Control Diagram

Chapter 13

COST ANALYSIS

(Gary Hufford)

The total cost of the research vehicle has been estimated to be 3.7077 billion dollars. This figure was based upon statistical methods presented in Chapter 24 of "Fundamentals of Aircraft Design" by Leland Nicolai. This statistical method was based upon the top speed of the aircraft, the ampere weight of the aircraft, and the number of aircraft produced.

The following numbers were used in the cost analysis computation. The ampere weight was estimated to be 15000 pounds. This weight is the empty weight minus weight due to engines, landing gear, avionics and cooling system. The top speed used was 5943 knots. This is the speed at Mach 10 and 100,000 feet. The number produced is one.

A breakdown of the cost in eight different areas is given in Figure 1. The major areas of cost is in the number of engineering hours required and the developmental support of the vehicle. These are expected to be the major costs of a research vehicle of this type. The carrier aircraft was not figured into the costs of the research vehicle. The cost of the carrier aircraft is important and we have not overlooked designing the aircraft to minimize the cost of the carrier aircraft. Our small design will

Engineering Hours	1,880,000,000
Developement Support	1,175,000,000
Flight Test Operations	30,500,000
Tooling	403,800,000
Manufacturing Labor	93,930,000
Quality Control	122,000,000
Material and Equipment	1,030,000
Engine Costs	1,440,000
Total Cost for 1 Aircraft = 3.7077 Billion	

Figure 13.1: Cost Analysis

help minimize the cost of the carrier aircraft, possibly even eliminating the need for a new design if our design can possibly be launched from under the wing of a B-52.

CONCLUSION
(Gary Hufford)

We have shown that the vehicle described in this report can test scramjet engines up to a maximum Mach number of 9.9 at a cost approximately 3.7 billion dollars.

We feel that this design has three major advantages. First, it is a very small design. A small design is significantly cheaper when the carrier aircraft is figured into the cost analysis. A small design also minimizes the sonic boom problem present with a supersonic aircraft. Second, the aircraft can be used in an efficient manner to test scramjet engines at low Mach numbers (6 to 8) as well as higher Mach numbers (9 to 10). The low Mach number tests can be conducted with the base design and the high Mach number tests can simply add the rocket attachments to attain higher Mach numbers. The aircraft is not designed for a specific Mach number, rather it is a general design for a hypersonic airplane. Therefore, it does not require a specific Mach number for optimization. The aircraft is versatile in the selection of Mach numbers that the scramjets can be tested. Third, the aircraft has a separate engine system (turbofanramjet) that can be used if the scramjet tests fail. The turbofanramjet uses the same fuel as the scramjets. Thus, if the scramjet fails, the fuel meant for the scramjet can be diverted to the turbofanramjet to land the vehicle safely.

REFERENCES

1) Nicolai, L.M. Fundamentals of AIRCRAFT DESIGN. METS, Inc, San Jose, CA, 1975

2) Anderson, J.D.Jr. Modern Compressible Flow. McGraw Hill, New York, 1982

3) Anderson J.D.Jr. and Corda S. Viscous Optimized Hypersonic Waveriders Designed from Axisymmetric Flow Fields. AIAA-88-0369 26th Aerospace Sciences Meeting, 1988

4) Long, L.N. The Off-Design Performance of Hypersonic Waveriders. AGARD Conference Proceedings, 1987

5) Vaglio-Laurin, R. Turbulent Heat Transfer on Blunt-Nosed Bodies in Two-Dimensional Hypersonic Flow. JAS, Vol. 27, No. 1, Jan. 1960

6) Hanawalt, A.J., Blessing A.H. and Schmidt C.M. Thermal Analysis of Stagnation Regions with emphasis on Heat-Sustaining Nose Shapes at Hypersonic Speeds. JAS, Vol. 26, No. 5, May 1959

7) Ellison, J.C. Experimental Stagnation-Point Velocity Gradients and Heat Transfer Coefficients for a Family of Blunt Bodies at Mach 8 and Angles of Attack. NASA TN D-5121,1969

8) Dunavant, J.C. Heat Transfer to a Delta-Wing Half-Cone Combination at Mach Numbers of 7 and 10. NASA TN D-2199, 1964

9) Savage, R.T. High Temperature Performance of Flexible Thermal Protection Materials. AIAA-84-1770 19th Thermophysics Conference, 1984

10) Jackson, L.R., Davis, J.G. and Wichorek, G.R. Structural Concepts for Hydrogen-Fueled Hypersonic Airplanes. NASA TN D-3162, 1966

11) Blair, J.D. and Carlin, C.M. Integrated Control System Concept for High-Speed Aircraft. AIAA-83-2564 Aircraft Design, Systems and Technology Meeting, 1983

12) McConarty, W.A. and Anthony, F.M. Design and Evaluation of Active Cooling Systems for Mach 6 Cruise Vehicle Wings. NASA CR-1916, 1971

13) Helenbrook, R.G. and Anthony, F.M. Design of a Convective Cooling System for a Mach 6 Hypersonic Transport Airframe. NASA CR-1918, 1971

14) Kreith, F. and Bohn M.S. Principles of Heat Transfer. Harper & Row, New York, NY, 1986

15) Kempel R.W. and Earls M.R. Flight Control Systems Development and Flight Test Experience with the HiMAT Research Vehicles. NASA TP-2822, 1988

16) Goldsmith, E.L. and Seddon, J. Intake Aerodynamics. AIAA Education Series, 1975.

17) Henry, John R., Mackley, Ernest A., and Torrence, Marvin G. Investigation of the Compression Field and the Flow Distribution in the Throat of a Two-Dimensional, Internal Compression, Mach Number 6.9 Inlet. NASA TM X-605, 1961.

18) Simmons, J.M. and Weidner, E.H. Design of Scramjet Inlets with Rectangular Capture Cross-Section and Circular Throat. NASA TM 87752, 1986.

19) Small, William J., Weidner, John P., and Johnston, P.J. Scramjet Nozzle Design and Analysis as Applied to a Highly Integrated Hypersonic Research Airplane. NASA TN D-8334, 1976.

20) Trexler, Carl A. and Souders, Sue W. Design and Performance of A Local Mach Number of 6 of an Inlet for an Integrated Scramjet Concept. NASA TN D-7944, 1975.

21) Goldsmith, E. L. and Seddon, J. Intake Aerodynamics, AIAA Education Series, 1975.

22) Simmons, J. M. and Weidner, E. H. Design of Scramjet Inlets with Rectangular Capture Cross-Section and Circular Throat. NASA TM 87752, 1986.

23) Trexler, Carl A. and Souders, Sue W. Design and Performance of a Local Mach Number of Six of an Inlet for an Integrated Scramjet Concept. NASA TN D-7944, 1975.

APPENDICES

Appendix A

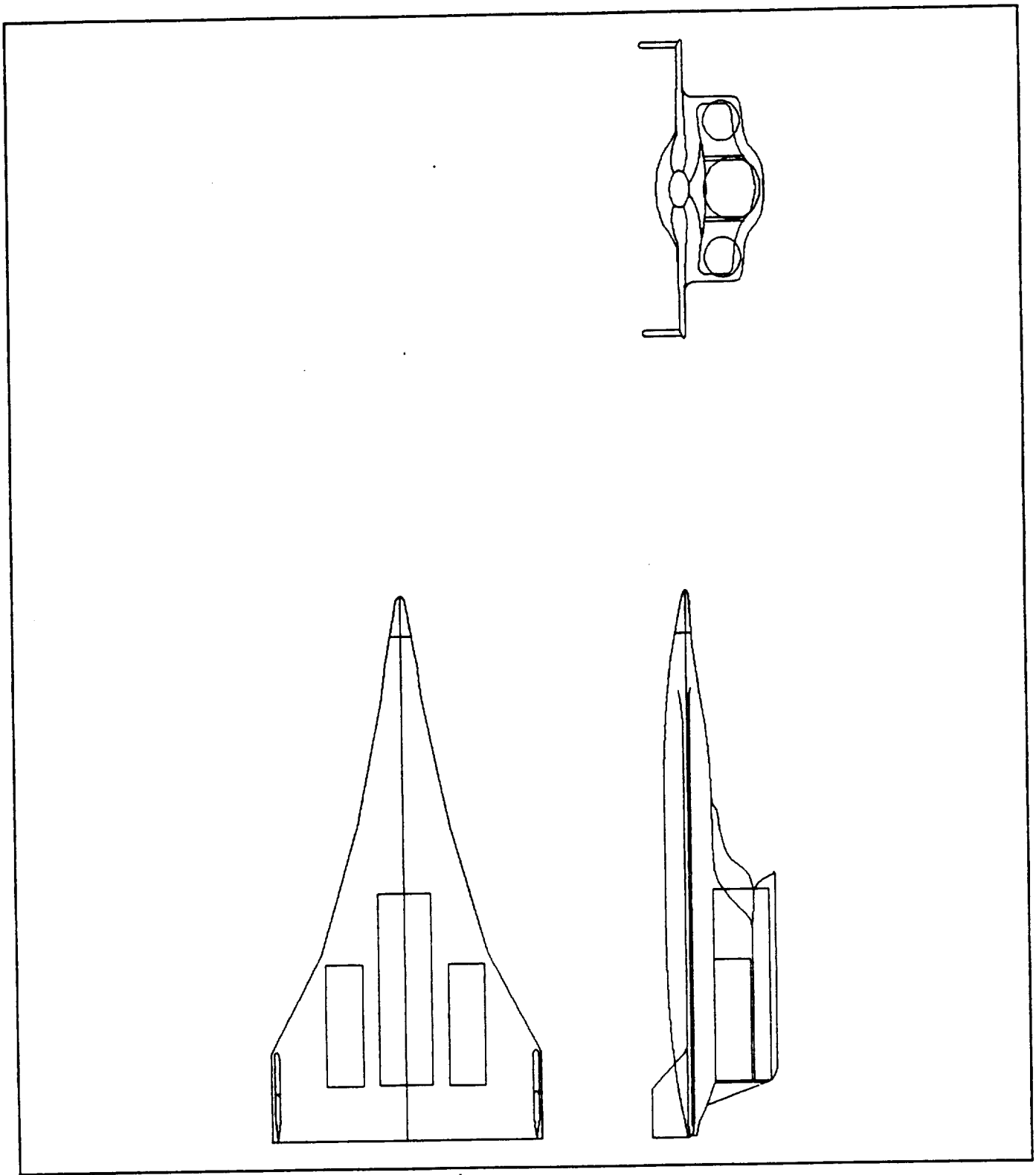

Figure A.1: Initial configuration

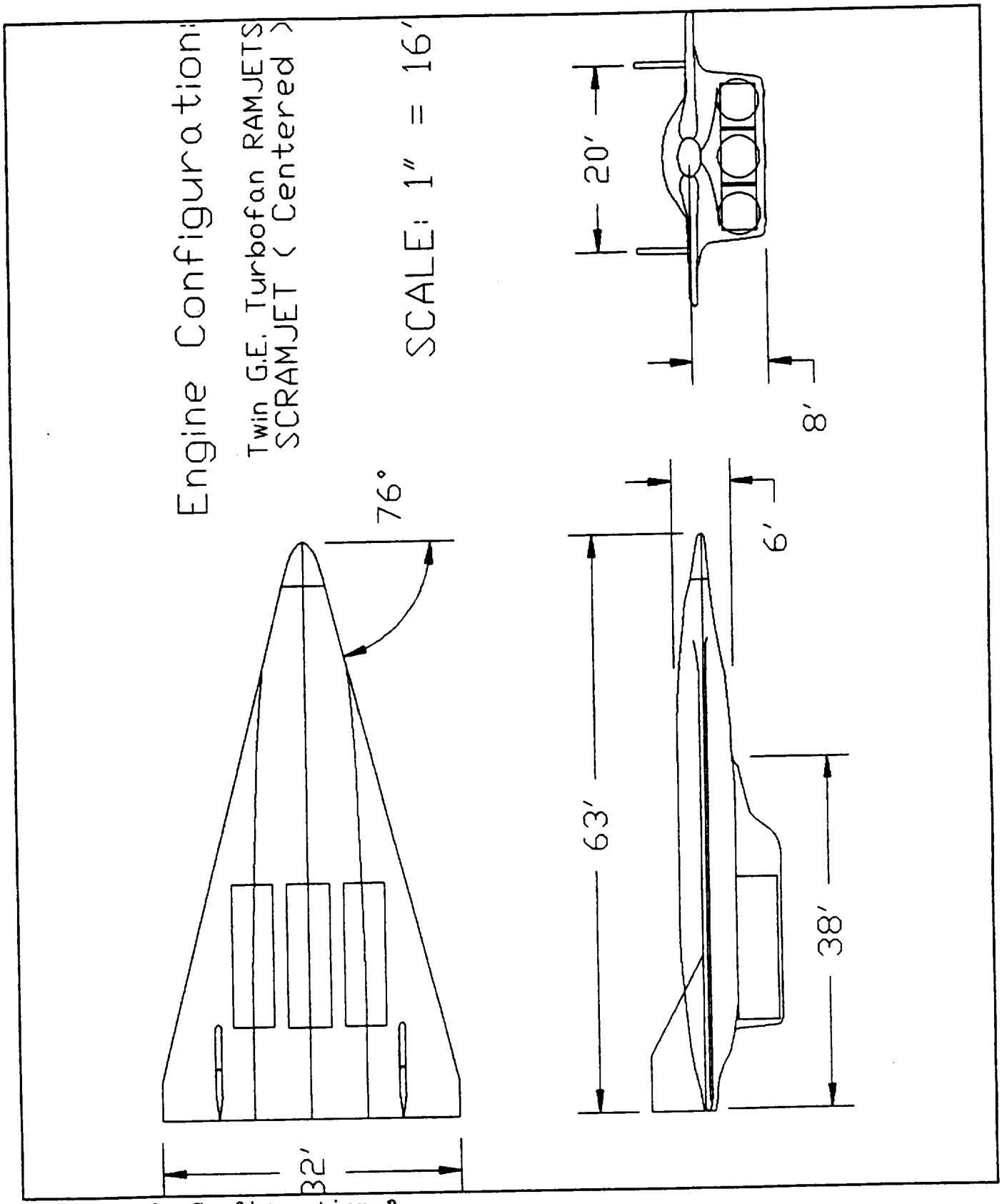

Figure A.2: Configuration 2

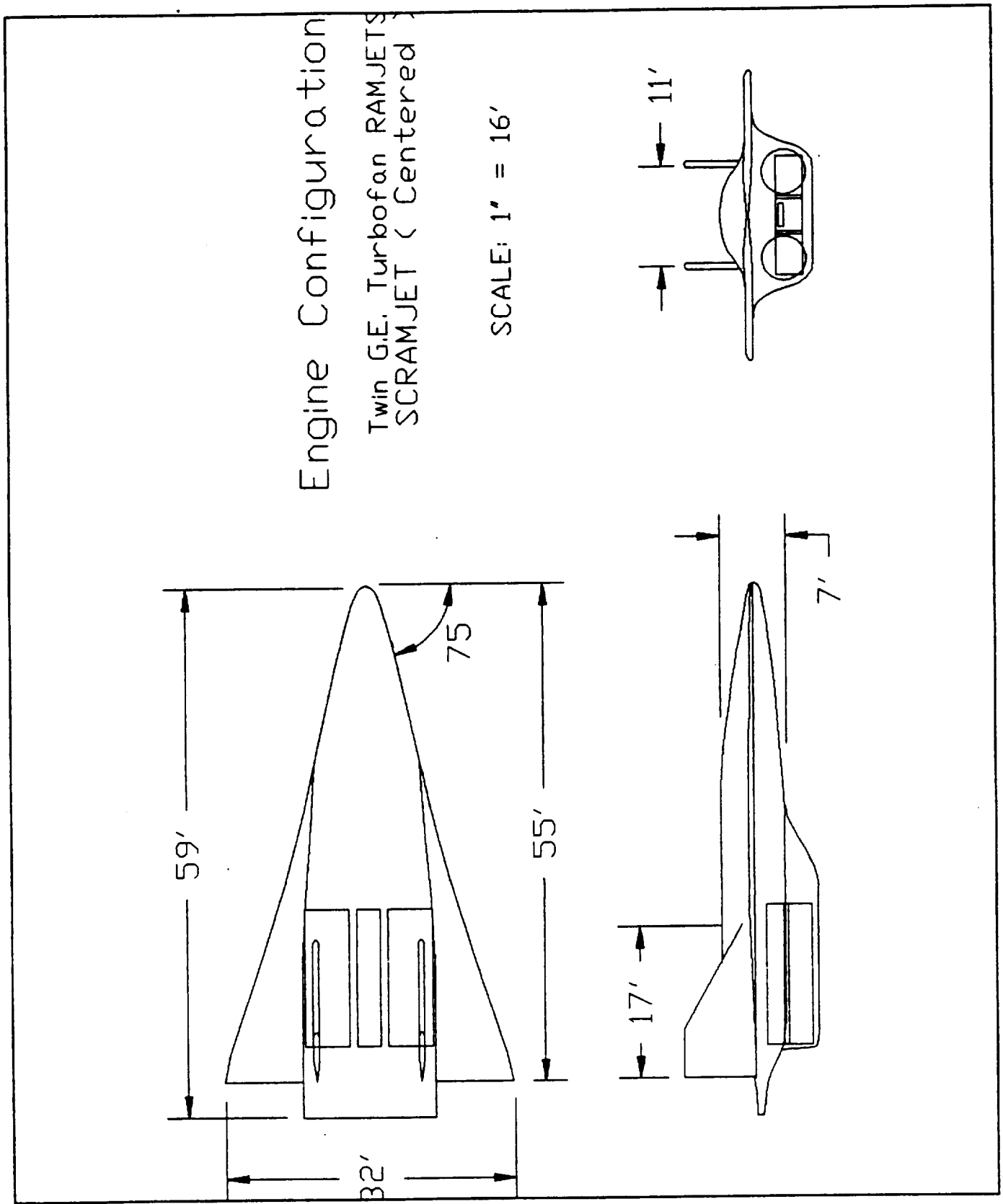

Figure A.3: Configuration 3

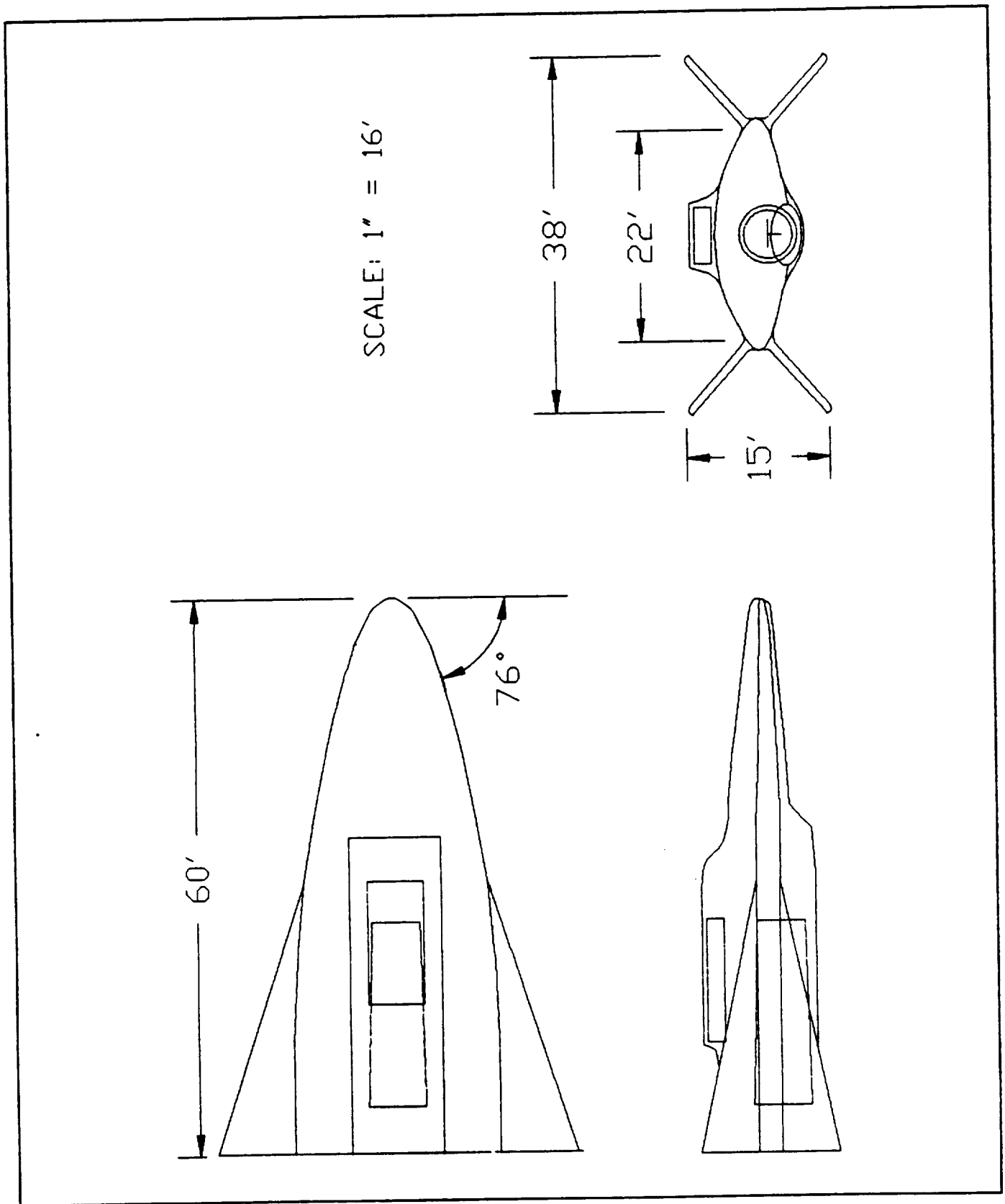

Figure A.4: Configuration 4

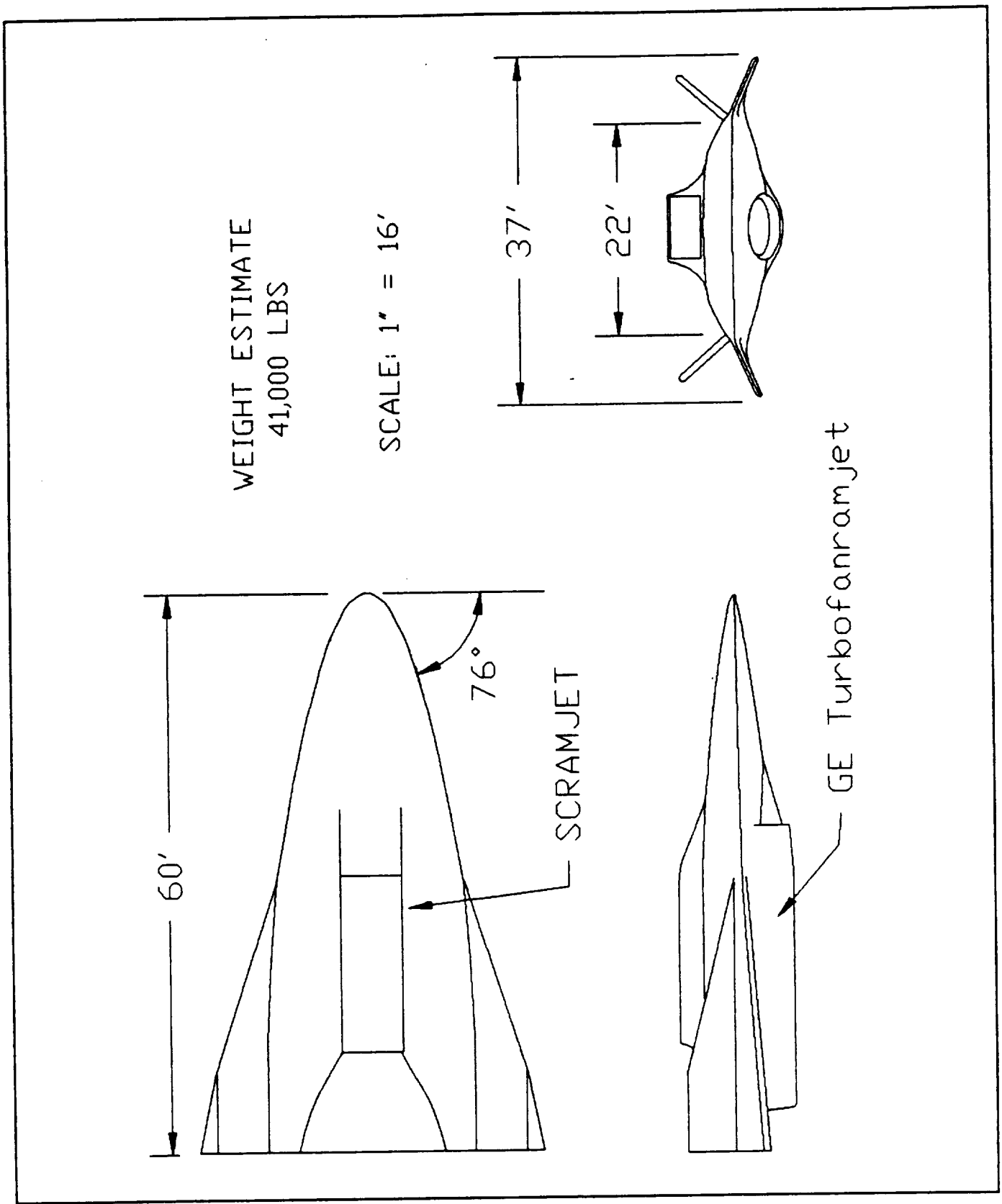

Figure A.5: Configuration 5

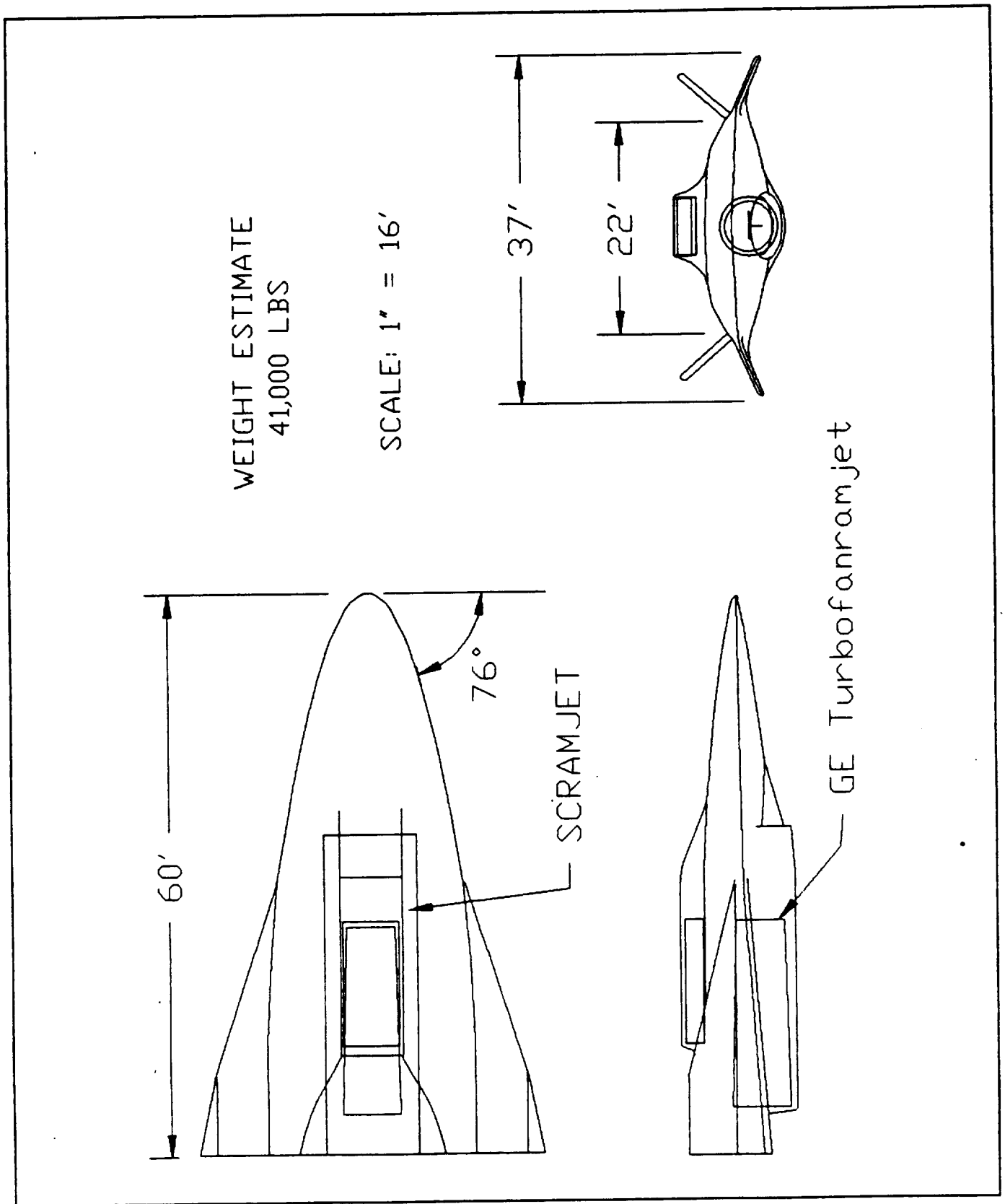

Figure A.6: Engine location

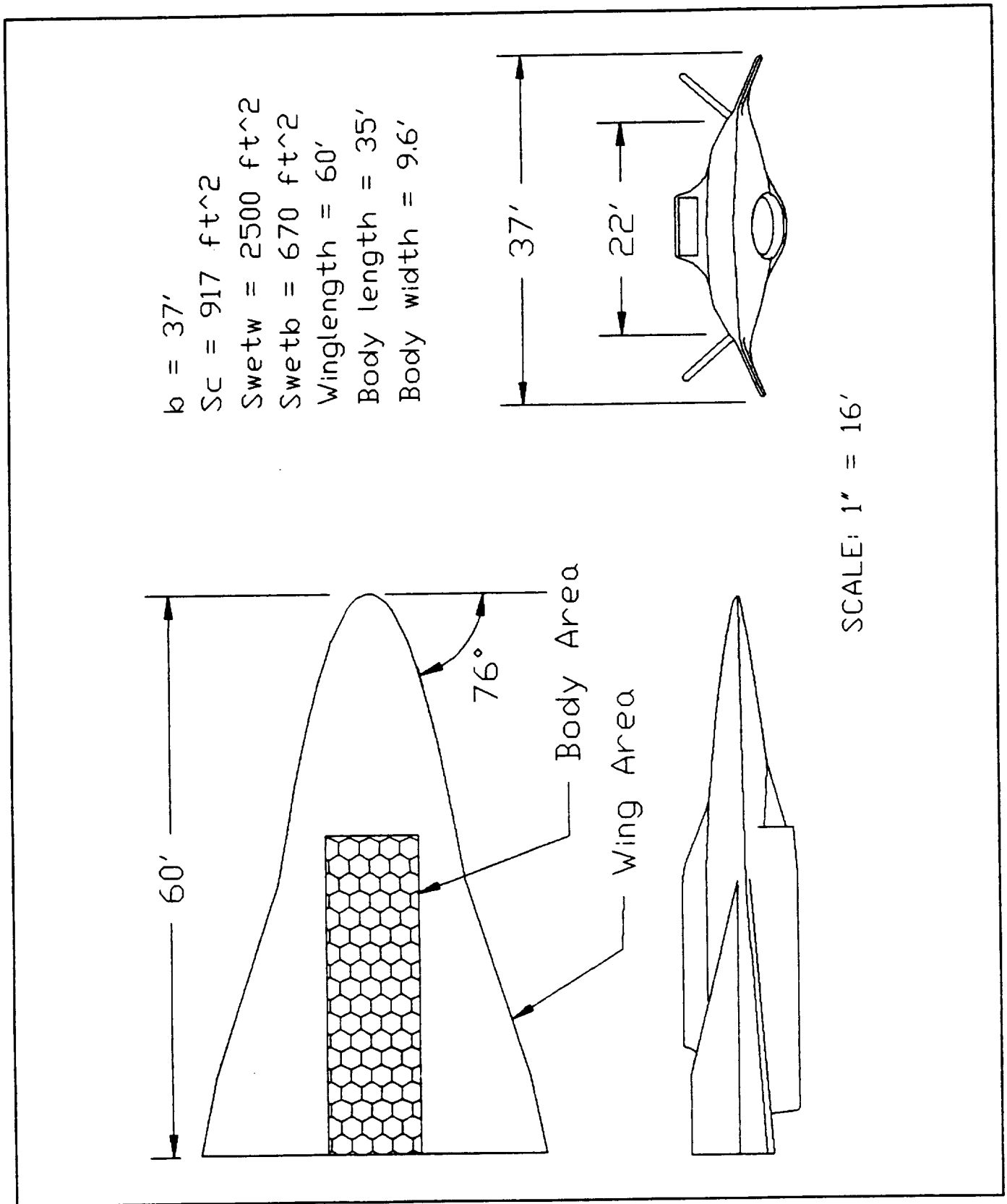

Figure A.7: Reference values

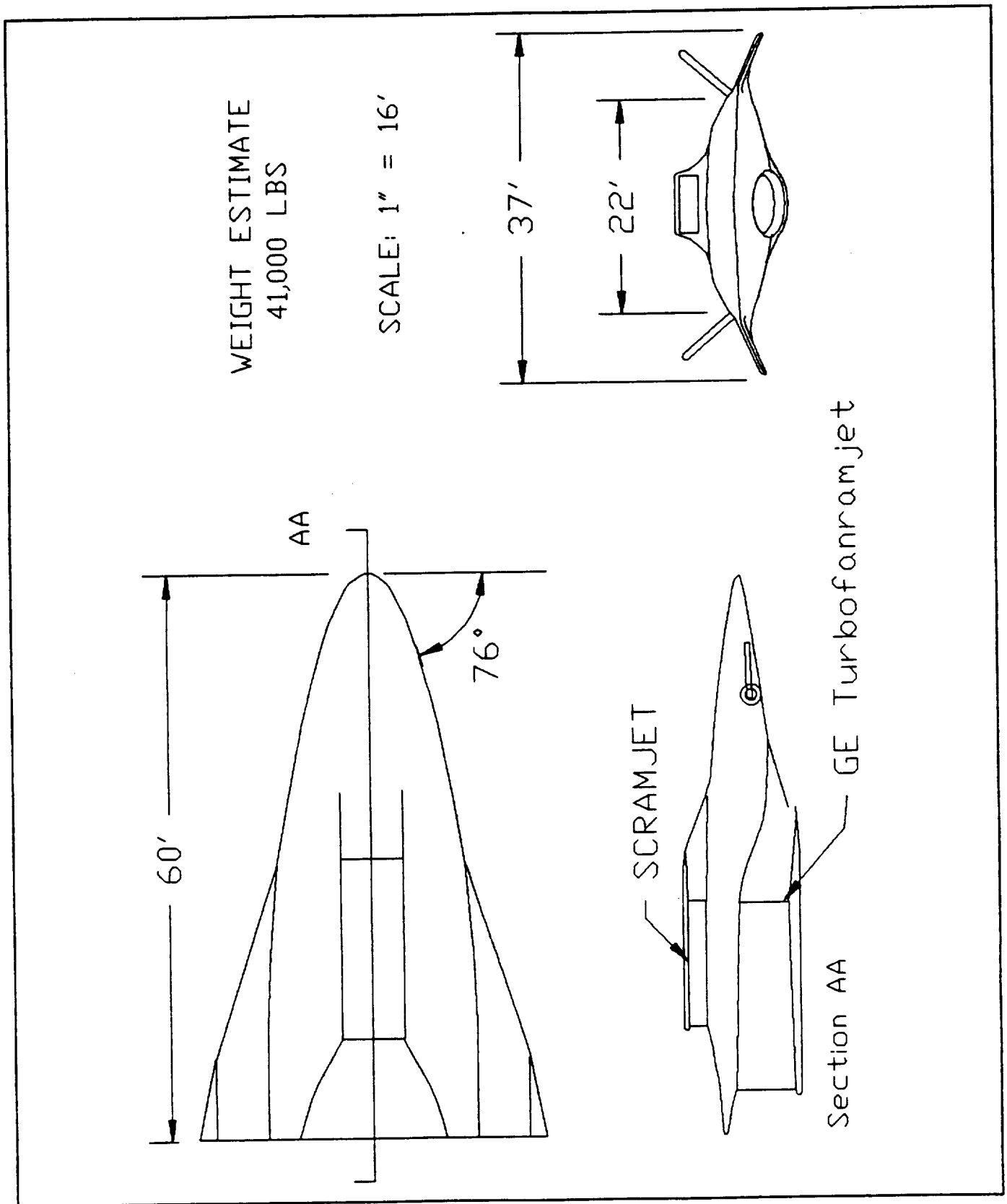

Figure A.8: Cut-away view

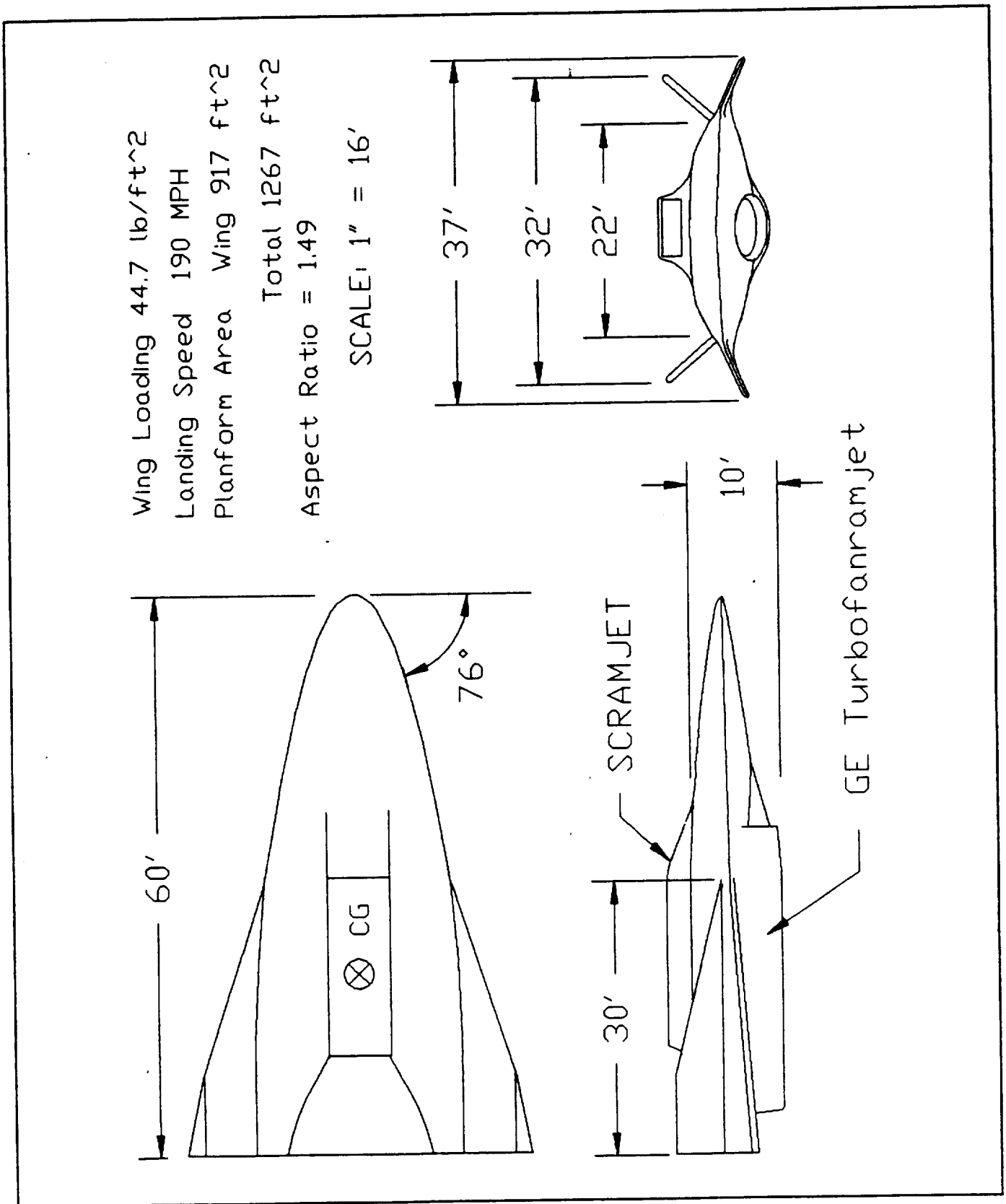

Figure A.9: Final configuration

Appendix B
Weights Analysis Program

4ØØØØ.ØØØØØ	ESTIMATED GROSS WEIGHT	EGW
29Ø5.Ø	DELTA WING WT COEF	WINGC
3.Ø	ULTIMATE LOAD FACTOR	ULF
16.Ø	STRUC. SPAN (ACROSS MID CHORD)	SPAN
2Ø5.Ø	WING PLANFORM AREA	SWING
Ø.65	WING ROOT THICKNESS	ROOT
Ø.621	DELTA WING WT EXP	WINGE
3.9	VERT TAIL WT COEF	VTC
4ØØ.Ø	PLANFORM AREA	SVERT
1.ØØ	WT EXPONENT	VTE
1ØØØ.Ø	BODY WETTED AREA	SWET
6Ø.Ø	BODY LENGTH	LBOD
15ØØ.Ø	MAX. DYNAMIC PRESSURE (Qmax)	QMAX
5.87	BODY HEIGHT	HBOD
1.Ø	BODY WT. EXP.	BODE
1.275	BODY TEMP WT MOD FACT (5ØØ F)	BTMOD
33ØØØ.Ø	MAX TURBOFANRAMJET NET THRUST	TTURBO
5ØØØ.Ø	MAX SCRAMJET NET THRUST	TSCRAM
Ø.ØØ625	THRUST STRUCT. WT COEFF	TSC
69.Ø	WT INTERCEPT	TSI
Ø.4	SECONDARY BODY WT COEF	SBODC
2ØØØ.Ø	THERM PROTECTION SURFACE AREA	STPS
Ø.7	BODY INSUL. UNIT WEIGHT COEF	BINSC
1.4	BODY COVER PANELS UNIT WT COEF	BCOVC
Ø.ØØ25	LAUNCH GEAR WT. COEFF	LGC
Ø.ØØ916	AIR LAUNCHED LNDG GEAR WT COEF	LNDGC
1.124	WT EXP	LNDGE
54ØØ.Ø	INDIVIDUAL TURBORAMJET WEIGHT	TURBO
158Ø.Ø	INDIVIDUAL SCRAMJET WEIGHT	SCRAM
1.Ø	# OF TURBORAMJETS	XTURBO
3.Ø	# OF SCRAMJETS	XSCRAM
Ø.ØØ4	ENGINE MOUNT WT. COEFF.	ENGMTC
Ø.53	LH2 INTEGRAL TANK WT COEF	TANKC
1932.Ø	FLIGHT TIME (SEC)	TFLIGHT
4ØØ.Ø	FUEL TANK RADIATING TEMP (F)	TRAD
4.345	DUCT (INTERNAL) WT INTERCEPT	DII
4.Ø	LIP TO ENGINE FACE LENGTH (FT)	LINLET
2.Ø	NUMBER OF INLETS	XINLET
5.8	INLET CAPTURE AREA (FT^2)	SCAPT
118.Ø	INLET PRESSURE (PSIA)	PINLET
9.Ø	DESIGN MACH NUMBER	DMACH
117.35	INLET RAMP WT COEF	RAMPC
8.Ø	RAMP LENGTH (FT)	LRAMP
Ø.294	INLET RAMP WT EXP.	RAMPE
35.Ø	INLET SPIKE WT COEF	SPIKEC
Ø.323	AERO ORIENT. CONTROL WT COEF	CONTC
Ø.9Ø3	EXP	CONTE
37.Ø	PLANE GEOMETRIC SPAN (FT)	GSPAN

```
          1.167    ELECTRIC. SYS WT COEF.                ELECC
          4.64     HYDRAULIC SYS WT COEF.                HYDRC
         3Ø.Ø      AVIONICS SYS WT COEF                  AVIONC
          Ø.361                EXP.                     AVIONE
          Ø.Ø18    TRAPPED FUEL WT. COEF                 TRFUC
          Ø.ØØ6    INFLIGHT FUEL LOSS COEF               FLOSSC
        71ØØ.Ø     WEIGHT OF USEABLE FUEL                WUFUEL
        2ØØØ.Ø     ACTIVE COOLING WT. ALLOWANCE          ACOOL
       5           NUMBER OF FUEL TANKS                  NTANKS
   3.1       2.45       368.Ø      TANKA(I), TANKB(I), VTANK(I)
   3.1       2.45       368.Ø
   1.3       1.47       17Ø.Ø      TANKA= FUEL TANK MAJOR DIA
   1.3       1.47       17Ø.Ø      TANKB=            MINOR DIA
   4.Ø8      Ø.98       456.Ø      VTANK= FUEL TANK VOLUME
CAPACITY
        7ØØØ.Ø     ROCKET BOOSTER WEIGHT                 ROCKETS
```

```
      PROGRAM WEIGHT
*
*     This program is based on the Weights Analysis of Advanced
*     Transportation Systems (WAATS) written by C.R. Glatt.  NASA
*     Report CR-2420.
*
*     The program takes formatted input from a data file that has a
*     description of each variable following the
*     numerical value.  This allows input files to be edited easily
*    on a word processor by changing the appropriate numeric values.
*
      REAL LBODY,LGC,LNDGC,LNDGE,LRAMP,LINLET
*
*************** data input
*
      OPEN( UNIT=1, FILE='WEIGHT.DAT',STATUS='OLD' )
      READ(1,1)       EGW
      READ(1,1)       WINGC
      READ(1,1)       ULF
      READ(1,1)       SSPAN
      READ(1,1)       SWING
      READ(1,1)       ROOT
      READ(1,1)       WINGE
      READ(1,1)       VTC
      READ(1,1)       SVERT
      READ(1,1)       VTE
      READ(1,1)       SWET
      READ(1,1)       LBODY
      READ(1,1)       QMAX
      READ(1,1)       HBODY
      READ(1,1)       BODE
      READ(1,1)       BTMOD
      READ(1,1)       TTURBO
      READ(1,1)       TSCRAM
      READ(1,1)       TSC
      READ(1,1)       TSI
      READ(1,1)       SBODC
      READ(1,1)       STPS
      READ(1,1)       BINSC
      READ(1,1)       BCOVC
      READ(1,1)       LGC
      READ(1,1)       LNDGC
      READ(1,1)       LNDGE
      READ(1,1)       TURBO
      READ(1,1)       SCRAM
      READ(1,1)       XTURBO
      READ(1,1)       XSCRAM
      READ(1,1)       ENGMTC
      READ(1,1)       TANKC
      READ(1,1)       TFLIGHT
```

```
      READ(1,1)       TRAD
      READ(1,1)       FTSWET
      READ(1,1)       DII
      READ(1,1)       LINLET
      READ(1,1)       XINLET
      READ(1,1)       SCAPT
      READ(1,1)       PINLET
      READ(1,1)       DMACH
      READ(1,1)       RAMPC
      READ(1,1)       LRAMP
      READ(1,1)       RAMPE
      READ(1,1)       SPIKEC
      READ(1,1)       CONTC
      READ(1,1)       CONTE
      READ(1,1)       GSPAN
      READ(1,1)       ELECC
      READ(1,1)       HYDRC
      READ(1,1)       AVIONC
      READ(1,1)       AVIONE
      READ(1,1)       TRFUC
      READ(1,1)       FLOSS
      READ(1,1)       WUFUEL
      READ(1,1)       ACOOL
      CLOSE(UNIT=1)
*
1     FORMAT(F12.5)
*
*               GENERAL CALCULATIONS
      WTO= EGW
*  Max total thrust
      TTOT= XTURBO*TTURBO + XSCRAM*TSCRAM
*  Temperature correction factor
      TEMPFCT= Ø.2Ø3 * DMACH + Ø.4
*  Gross fuel at takeoff
      GRFUEL= WUFUEL+ FLOSS*WUFUEL
*  Fuel tank volume to hold gross fuel  (LH2)
      VTANK= GRFUEL/4.389
*  Landing weight
1Ø    WLAND= WTO - GRFUEL
*
*************** weight calculations
*
*               weight of aerodynamic surfaces
*
      WWING= WINGC*( WTO*ULF*SSPAN*SWING/ROOT)**WINGE*1.ØE-6
      WVERT= VTC*SVERT**VTE
      WAERO= WWING + WVERT
*
*               weight of body structure
*
      A= Ø.341 * BTMOD
      B= (LBODY*ULF/HBODY)**Ø.15 * QMAX**Ø.16 * SWET**1.Ø5
```

```
      WBASIC= A*B**BODE
      WTHRST= TSC * TTOT + TSI
      WSECST= SBODC * SWET
      WSTRUCT= WBASIC + WTHRST + WSECST
*
*             thermal protection
*
      WINSUL= BINSC * STPS
      WCOVER= BCOVC * STPS
      WTPS= WINSUL + WCOVER + ACOOL
*
*             launch and landing gear
*
      WLAUNCH= LGC * WTO
      WLG= LNDGC * WLAND**LNDGE
      WGEAR= WLAUNCH + WLG
*
*             engine system weight
*
      WTURBO= XTURBO * TURBO
      WSCRAM= XSCRAM * SCRAM
      WENGMT= ENGMTC * TTOT
      WENGINES= WTURBO + WSCRAM + WENGMT
*
*             inlet system weight
*
     B=1.733*(LINLET*XINLET)**.5*(SCAPT/XINLET)**.3334*PINLET**.6667
      WIDUCT= DII * B
      WRAMP= RAMPC*(LRAMP*XINLET*(SCAPT/XINLET)**.5*TEMPFCT)**RAMPE
      WSPIKE= SPIKEC * XTURBO
      WINLET= WIDUCT + WRAMP + WSPIKE
*
*             fuel system
*
      WFUNCT= TANKC * VTANK
              TCORR= Ø.7 + TFLIGHT*8.ØE-5
              A= TCORR*(Ø.ØØØ7 * TRAD + Ø.24)
      WINSFT= A * FTSWET
              A= Ø.ØØ651 - 2.995E-8 * TTOT
              B= .1 + .175 * LBODY
      WFUSYS= A*TTOT + B*LBODY
      WCRYO= WFUNCT + WINSFT + WFUSYS
*
*             controls and avionics
*
              A= WTO**Ø.6667*(LBODY + GSPAN)**Ø.25
      WORIENT= CONTC * A**CONTE
      WELECT= ELECC * (SQRT(WTO) * LBODY**Ø.25)
              C= (LBODY+SSPAN)**Ø.5 * 1.25
      WHYDR=HYDRC*((SWING+SVERT)*QMAX/1ØØØ)**.334 + C
      WAVON= AVIONC*WTO**AVIONE
      WCONT= WORIENT + WELECT + WHYDR + WAVON
```

```
*
*               final summation
*
      WNEW= WAERO+WSTRUCT+WTPS+WGEAR+WENGINES+WINLET+WCRYO+WCONT
     &+GRFUEL
*
*               iteration loop
*
         ERR= ABS(WTO-WNEW)
         IF( ERR .LT. Ø.Ø1 ) GOTO 2Ø
         WTO= WTO*(WNEW/WTO)**1.1
         GOTO 1Ø
*
*               print output
*
2Ø       OPEN(UNIT= 2, FILE='WEIGHT.OUT', STATUS='NEW' )
         WRITE(2,*) '                    FINAL WEIGHT ESTIMATES'
         WRITE(2,*) 'Gross takeoff weight                ',WTO
         WRITE(2,*) 'Empty weight                        ',WLAND
         WRITE(2,*) 'Gross fuel weight                   ',GRFUEL
         WRITE(2,*) 'Useable fuel weight                 ',WUFUEL
         WRITE(2,*)
         WRITE(2,*) '    Aerodynamic Surfaces            ',WAERO
         WRITE(2,*) 'Wing structure                      ',WWING
         WRITE(2,*) 'Vertical stabilizer                 ',WVERT
         WRITE(2,*)
         WRITE(2,*) '    Body Structure                  ',WSTRUCT
         WRITE(2,*) 'Main body                           ',WBASIC
         WRITE(2,*) 'Secondary body structure            ',WSECST
         WRITE(2,*) 'Thrust structure                    ',WTHRST
         WRITE(2,*)
         WRITE(2,*) '    Environmental Protection        ',WTPS
         WRITE(2,*) 'Structure insulation                ',WINSUL
         WRITE(2,*) 'Body cover panels                   ',WCOVER
         WRITE(2,*) 'Active cooling allowance            ',ACOOL
         WRITE(2,*)
         WRITE(2,*) '    Launch & Landing Gear           ',WGEAR
         WRITE(2,*) 'Launch gear                         ',WLAUNCH
         WRITE(2,*) 'Landing gear                        ',WLG
         WRITE(2,*)
         WRITE(2,*) '    Engine System                   ',WENGINES
         WRITE(2,*) 'Turbofanramjet                      ',WTURBO
         WRITE(2,*) 'Scramjet                            ',WSCRAM
         WRITE(2,*) 'Engine mounts                       ',WENGMT
         WRITE(2,*)
         WRITE(2,*) '    Inlet System                    ',WINLET
         WRITE(2,*) 'Internal ducts                      ',WIDUCT
         WRITE(2,*) 'Variable ramps                      ',WRAMP
         WRITE(2,*) 'Spike                               ',WSPIKE
         WRITE(2,*)
         WRITE(2,*) '    Cryogenic Fuel System           ',WCRYO
         WRITE(2,*) 'Integral fuel tank                  ',WFUNCT
```

```
WRITE(2,*) 'Fuel tank insulation                    ',WINSFT
WRITE(2,*) 'Fuel distribution system                ',WFUSYS
WRITE(2,*)
WRITE(2,*) '    Control and avionics system         ',WCONT
WRITE(2,*) 'Aerodynamic orientation controls        ',WORIENT
WRITE(2,*) 'Electrical system                       ',WELECT
WRITE(2,*) 'Hydraulic system                        ',WHYDR
WRITE(2,*) 'Avionics                                ',WAVON
CLOSE( UNIT= 2 )
STOP
END
```

Appendix C.1
Subsonic program

```
      IMPLICIT REAL (A-Z)
      DIMENSION T(2Ø5), RHO(2Ø5), P(2Ø5), Q(2Ø5,1Ø5)

      INTEGER I,J,MSUB,ALTSUB,SELE

      OPEN(1,FILE='A515.DAT',STATUS='NEW')
      OPEN(4,FILE='GEOM1.DAT',STATUS='OLD')
      OPEN(12,FILE='NICOL.DAT',STATUS='OLD')
      OPEN(2,FILE='CL.DAT',STATUS='NEW')
      OPEN(3,FILE='CD.DAT',STATUS='NEW')
      OPEN(7,FILE='MACH.DAT',STATUS='NEW')
      OPEN(8,FILE='ALT.DAT',STATUS='NEW')
      OPEN(9,FILE='LD.DAT',STATUS='NEW')
      OPEN(1Ø,FILE='DRAG.DAT',STATUS='NEW')
      OPEN(11,FILE='LIFT.DAT',STATUS='NEW')
      OPEN(13,FILE='ALPHA.DAT',STATUS='NEW')

      R = 1716.
      GØ = 32.2
      PI = 3.14157
      GAM = 1.4

C*****************************
C   Atmosphere from Ø -> 36ØØØ ft
C*****************************

      DO 6 I=1,73
        P1 = 2116.2
        T1 = 518.69
        A = -.ØØ356624
        H = 5ØØ*(I-1)
        T(I) = T1+A*H
        P(I) = P1*EXP(-GØ/(R*T(I))*H)
        RHO(I) = P(I)/(T(I)*R)
  6   CONTINUE

C*******************************
C   Atmosphere from 365ØØ -> 82ØØØ ft
C*******************************

      DO 7 I=74,165
        T1 = 389.99
        P1 = 464.86
        H1 = 365ØØ
        H = 5ØØ*(I-1)
        T(I) = T1
```

```
        P(I) = P1*EXP(-GØ/(R*T1)*(H-H1))
        RHO(I) = P(I)/(T1*R)
   7  CONTINUE

C*********************************
C   Atmosphere from 825ØØ -> 1ØØØØØ ft
C*********************************

      DO 1Ø I=166,2Ø1
        H1 = 825ØØ
        P1 = 55.837
        T1 = 39Ø.24
        A = .ØØ1646
        H = 5ØØ*(I-1)
        T(I) = (H-H1)*A+T1
        P(I) = P1*EXP(-((GØ/(R*T(I)))*(H-H1)))
        RHO(I) = P(I)/(T(I)*R)
  1Ø  CONTINUE

C*****************************************
C  Dynamic pressures at various altitudes and mach numbers
C  Q(alt,M)
C*****************************************

      DO 15 ALTSUB=1,2Ø1
        DO 2Ø MSUB=1,1Ø1
          M = Ø.1*(MSUB-1)
          Q(ALTSUB,MSUB) = P(ALTSUB)*(GAM/2)*M*M
  2Ø    CONTINUE
  15  CONTINUE

C*****************************************
C    Airflow Data
C*****************************************

 1ØØØ WRITE(6,*) ('  Starting Mach number (.1 min):')
      READ(5,*) SM
      WRITE(6,*) ('  Ending Mach number (.9 max):')
      READ(5,*) EM
      WRITE(6,*) ('  Step size (.1 multiples):')
      READ(5,*) STM

      WRITE(6,*) ('  Starting altitude (Ø ft min):')
      READ(5,*) SALT
      WRITE(6,*) ('  Ending altitude (1ØØØØØ ft max):')
      READ(5,*) EALT
      WRITE(6,*) ('  Step size (5ØØ ft multiples):')
      READ(5,*) STALT

      WRITE(6,*) ('  Starting angle of attack:')
      READ(5,*) SALP
      WRITE(6,*) ('  Ending angle of attack:')
```

```
      READ(5,*) EALP
      WRITE(6,*) ('  Step size:')
      READ(5,*) STALP

      WRITE(6,*) ('  Max drag:')
      READ(5,*) MAXD

      WRITE(6,*) ('  Max lift:')
      READ(5,*) MAXL

      WRITE(6,*) ('  Min lift:')
      READ(5,*) MINL


C*****************************************
C     Geometry Data
C*****************************************

      WRITE(6,*) ('  Span (ft):')
      READ(4,*) SPAN
      WRITE(6,*) ('  Wing ref. area SE (ft^2):')
      READ(4,*) SE
      WRITE(6,*)('   Wetted wing area (ft^2):')
      READ(4,*)SWETW
      WRITE(6,*) ('  Wetted body area (ft^2):')
      READ(4,*) SWETB
      WRITE(6,*) ('  Max wing length (ft):')
      READ(4,*) WL
      WRITE(6,*) ('  Max body length (ft):')
      READ(4,*) BL
      WRITE(6,*) ('  Sweep angle (deg):')
      READ(4,*) SWP
      WRITE(6,*) ('  Max wing thickness to chord:')
      READ(4,*) TC
      WRITE(6,*) ('  Leading edge radius (% chord):')
      READ(4,*) RLE
      WRITE(6,*) ('  Body cross-section area (ft^2):')
      READ(4,*)  SB
      WRITE(6,*) ('  Body width (ft):')
      READ(4,*)  BD

      SWPR = SWP*(PI/180)
      AR = (SPAN*SPAN)/SE

C*********************
C   Subsonic Inputs
C   If changing airflow properties only,
C   the proceeding variables do not need to be changed.
C*********************

      DBD = BD/SPAN
      CSWP = COS(SWPR)
```

```
      WRITE(6,1ØØ) DBD
 1ØØ  FORMAT(1X,'  Get F for d/b = ',F7.5,' from FIG. 11.3:')
      READ(12,*) F
      WRITE(6,1Ø2) AR
 1Ø2  FORMAT(1X,'  Get C1 for AR = ',F12.5,' from FIG. 2.6:')
      READ(12,*) C1
      WRITE(6,1Ø6) AR
 1Ø6  FORMAT(1X,' Get e' for AR = ',F12.5,'  from FIG. 11.5:')
      READ(12,*) EPR
      WRITE(6,1Ø8) RLE
 1Ø8  FORMAT(1X,' Get K'' for RLE = ',F12.5,'  from FIG. 11.6:')
      READ(12,*) KDPR

      DO 55 MACH=SM,EM,STM
         DO 5Ø ALT=SALT,EALT,STALT
            DO 6Ø ALPHAD=SALP,EALP,STALP
               ALPHA = ALPHAD*(PI/18Ø)
               ALTSUB = ALT/5ØØ+1
               MSUB = MACH/.1+1
               MAC = .5*WL
               MU = .317E-1Ø*(T(ALTSUB)**1.5*(734.7/(T(ALTSUB)+216)))
               B = SQRT(1-MACH**2)

C*********************************
C   Subsonic Lift
C*********************************

      CLAW1 = 1+(TAN(SWPR))**2/(B*B)
      CLAW2 = SQRT(4+AR*AR*B*B*CLAW1)
      CLAW = (2*PI*AR)/(2+CLAW2)
      CLAWB = F*CLAW
      CL = CLAWB*ALPHA+C1*ALPHA**2

C*********************************
C  Subsonic Drag
C  CDØw
C*********************************
      IF (MACH.LT.Ø.25) THEN
        RR=.74Ø7*CSWP+.43Ø72
      ENDIF
      IF ((MACH.GT.Ø.25).AND.(MACH.LT.Ø.6)) THEN
         RR=.74Ø7*CSWP+.2Ø86*MACH+.37857
      ENDIF
      IF ((MACH.GT.Ø.6).AND.(MACH.LT.Ø.8)) THEN
         RR=.74Ø7*CSWP+.635*MACH+.12272
      ENDIF
      IF ((MACH.GT.Ø.8).AND.(MACH.LT.1)) THEN
         RR=.74Ø7*CSWP+1.18*MACH-.31328
      ENDIF

      REW = (RHO(ALTSUB)*MAC*MACH*SQRT(GAM*R*T(ALTSUB)))/MU
```

```
      CFP = .455/(LOG1Ø(REW))**2.58
      CDØW = CFP*(1+1.2*TC+1ØØ*TC**4)*RR*(SWETW/SE)

C*****************************
C  CDØB
C*****************************

      DE = SQRT(SB/.7854)
      REB = (RHO(ALTSUB)*BL*MACH*SQRT(GAM*R*T(ALTSUB)))/MU
      CF = .455/(LOG1Ø(REB))**2.58
      CDFB = CF*(1+6Ø/(BL/DE)**3+.ØØ25*(BL/DE))*(SWETB/SE)
      CDØB = CDFB
      CDØ = CDØW+CDØB


C*****************************
C    K'
C*****************************

      E = EPR*(1-(BD/SPAN)**2)
      KPR = 1/(PI*AR*E)

C*****************************
C    K''
C*****************************

      K = KPR+KDPR
      CD = CDØ+K*CL**2

      DRAG = CD*Q(ALTSUB, MSUB)*SE
      LIFT = CL*Q(ALTSUB, MSUB)*SE
      LD = CL/CD

      IF ((LIFT.GT.MINL).AND.(LIFT.LT.MAXL).AND.
     *(DRAG.LT.MAXD)) THEN

         WRITE(1,11Ø) MACH, ALT, ALPHAD
  11Ø    FORMAT(1X,' MACH: ',F7.3,'  ALT: ',F12.4,'  ALPHA: ',F7.3)
         WRITE(1,112) LIFT, DRAG
  112    FORMAT(1X,' LIFT: ',F14.7,'  DRAG: ',F14.7)
         WRITE(1,114) CL, CD
  114    FORMAT(1X,' CL: ',F8.5,'    CD: ',F8.5)
         WRITE(1,116) Q(ALTSUB,MSUB), LD
  116    FORMAT(1X,' DYNAMIC PRESSURE= ',F12.5,' L/D: ',F7.4)
         WRITE(1,*) ('      ')
         WRITE(2,*) CL
         WRITE(3,*) CD
         WRITE(7,*) MACH
         WRITE(8,*) ALT
         WRITE(9,*) LD
         WRITE(1Ø,*) DRAG
         WRITE(11,*) LIFT
```

```
        WRITE(13,*) ALPHAD
      ENDIF

  6Ø      CONTINUE
  5Ø    CONTINUE
  55 CONTINUE

1ØØ8  WRITE(6,*) ('   Enter Selection:')
      WRITE(6,*) ('         1.  Change geometry only')
      WRITE(6,*) ('         2.  Change airflow properties only')
      IF (SELE.EQ.1) THEN
        GOTO 1ØØØ
      ENDIF

      STOP
      END
```

Appendix C.2
Supersonic program

```
      IMPLICIT REAL (A-Z)
      DIMENSION T(2Ø5), RHO(2Ø5), P(2Ø5), Q(2Ø5,1Ø5)

      INTEGER I,J,MSUB,ALTSUB,FLAG,SELE

      CHARACTER*8 FCL, FCD, FCLD, FM, FALT

      OPEN(1,FILE='A515.DAT',STATUS='NEW')
      OPEN(4,FILE='GEOM1.DAT',STATUS='OLD')
      OPEN(2,FILE='CL.DAT',STATUS='NEW')
      OPEN(3,FILE='CD.DAT',STATUS='NEW')
      OPEN(7,FILE='MACH.DAT',STATUS='NEW')
      OPEN(8,FILE='ALT.DAT',STATUS='NEW')
      OPEN(9,FILE='LD.DAT',STATUS='NEW')
      OPEN(1Ø,FILE='DRAG.DAT',STATUS='NEW')
      OPEN(11,FILE='LIFT.DAT',STATUS='NEW')
      OPEN(12,FILE='ALPHA.DAT',STATUS='NEW')

      R = 1716.
      GØ = 32.2
      PI = 3.14157
      GAM = 1.4

C*****************************
C   Atmosphere from Ø -> 36ØØØ ft
C*****************************

      DO 6 I=1,73
        P1 = 2116.2
        T1 = 518.69
        A = -.ØØ356624
        H = 5ØØ*(I-1)
        T(I) = T1+A*H
        P(I) = P1*EXP(-GØ/(R*T(I))*H)
        RHO(I) = P(I)/(T(I)*R)
  6   CONTINUE

C*******************************
C   Atmosphere from 365ØØ -> 82ØØØ ft
C*******************************

      DO 7 I=74,165
        T1 = 389.99
        P1 = 464.86
        H1 = 365ØØ
        H = 5ØØ*(I-1)
```

```
        T(I) = T1
        P(I) = P1*EXP(-GØ/(R*T1)*(H-H1))
        RHO(I) = P(I)/(T1*R)
   7  CONTINUE

C*********************************
C   Atmosphere from 82500 -> 100000 ft
C*********************************

      DO 1Ø I=166,2Ø1
        H1 = 82500
        P1 = 55.837
        T1 = 390.24
        A = .ØØ1646
        H = 5ØØ*(I-1)
        T(I) = (H-H1)*A+T1
        P(I) = P1*EXP(-((GØ/(R*T(I)))*(H-H1)))
        RHO(I) = P(I)/(T(I)*R)
  1Ø  CONTINUE


C*****************************************
C  Dynamic pressures at various altitudes and mach numbers
C  Q(alt,M)
C*****************************************

      DO 15 ALTSUB=1,2Ø1
        DO 2Ø MSUB=1,1Ø1
          M = Ø.1*(MSUB-1)
          Q(ALTSUB,MSUB) = P(ALTSUB)*(GAM/2)*M*M
  2Ø    CONTINUE
  15  CONTINUE

C*****************************************
C    Airflow Data
C*****************************************

 1ØØØ WRITE(6,*) ('  Starting Mach number (1.3 min):')
      READ(5,*) SM
      WRITE(6,*) ('  Ending Mach number (5 max):')
      READ(5,*) EM
      WRITE(6,*) ('  Step size (.1 min):')
      READ(5,*) STM

      WRITE(6,*) ('  Starting altitude (Ø ft min):')
      READ(5,*) SALT
      WRITE(6,*) ('  Ending altitude (100000 ft max):')
      READ(5,*) EALT
      WRITE(6,*) ('  Step size (500 ft min):')
      READ(5,*) STALT

      WRITE(6,*) ('  Starting angle of attack:')
```

```
      READ(5,*) SALP
      WRITE(6,*) ('  Ending angle of attack:')
      READ(5,*) EALP
      WRITE(6,*) ('  Step size:')
      READ(5,*) STALP

      WRITE(6,*) ('  Max drag:')
      READ(5,*) MAXD

      WRITE(6,*) ('  Max lift:')
      READ(5,*) MAXL

      WRITE(6,*) ('  Min lift:')
      READ(5,*) MINL

C*****************************************
C     Geometry Data
C*****************************************

      WRITE(6,*) ('  Span (ft):')
      READ(4,*) SPAN
      WRITE(6,*)  ('  Wing ref. area SE (ft^2):')
      READ(4,*) SE
      WRITE(6,*)('  Wetted wing area (ft^2) ')
      READ(4,*) SWETW
      WRITE(6,*)  ('  Wetted body area (ft^2):')
      READ(4,*) SWETB
      WRITE(6,*) ('  Max wing length (ft):')
      READ(4,*) WL
      WRITE(6,*) ('  Body length (ft):')
      READ(4,*) BL
      WRITE(6,*) ('  Sweep angle (deg):')
      READ(4,*) SWP
      WRITE(6,*) ('  Max wing thickness (% chord):')
      READ(4,*) TC
      WRITE(6,*) ('  Leading edge radius (% chord):')
      READ(4,*) RLE
      WRITE(6,*) ('  Body cross-section area (ft^2):')
      READ(4,*)  SB
      WRITE(6,*) ('  Body width (ft):')
      READ(4,*) BD

C*****************************************************************
C*                          Supersonic                           *
C*****************************************************************

      DO 55 MACH=SM,EM,STM
         SWPR = SWP*(PI/180)
         B = SQRT(MACH**2-1)
         AR = (SPAN*SPAN)/SE
         MAC = .5*WL
         ATS = AR*TAN(SWPR)
```

```
      TSW = TAN(SWPR)/B
      SWET = SWETB+SWETW

         IF (TSW.LE.1) THEN
            WRITE(6,2Ø8) ATS, TSW
2Ø8         FORMAT(1X,'  When AR Tan(le sweep) =',F12.5,' and
     * tan(le)/B=',F12.7,' get Cna from FIG. 11.2:')
         ELSEIF (TSW.GT.1) THEN
            TSW = 1/TSW
            WRITE(6,21Ø) ATS, TSW
21Ø         FORMAT(1X,'  When AR Tan(le sweep) =',F12.5,' and
     *  B/TAN(LE)=',F12.7,' get Cna from FIG. 11.2:')
         ENDIF
       READ(5,*) BCLA

       DO 5Ø ALT=SALT,EALT,STALT
          DO 6Ø ALPHAD=SALP,EALP,STALP
             ALTSUB = ALT/5ØØ+1
             MSUB = MACH/.1+1
             ALPHA = ALPHAD*(PI/18Ø)
             MU = .317E-1Ø*(T(ALTSUB)**1.5*(734.7/(T(ALTSUB)+216)))
             CLAWB = BCLA/B
             CL = CLAWB*ALPHA

C*******************************
C    SUPERSONIC DRAG
C    CDØ OF THE WING (SUPERSONIC)
C    SHARP NOSED SECTIONS     IE.  LEADING EDGE RADIUS
C                                  LESS THAN .1% T/C
C*******************************

             IF (BCS.GE.1) THEN
                CDW = (16/3)/B*TC**2
             ELSEIF (BCS.LT.1) THEN
                CDW = (16/3)*(1/TAN(SWPR))*TC**2
             ENDIF

             REB = (RHO(ALTSUB)*BL*MACH*SQRT(GAM*R*T(ALTSUB)))/MU
             CF = .455/(LOG1Ø(REB))**2.58
             CFCCFI = 1/(1+.144*MACH**2)**.65
             CDFB = CFCCFI*CF*SWETB/SE
             REW = (RHO(ALTSUB)*WL*MACH*SQRT(GAM*R*T(ALTSUB)))/MU
             CDFW = CFCCFI*CF*SWETW/SE
             CDØ = CDFB+CDFW+CDW

C***********************************************
C  DRAG DUE TO LIFT; SUPERSONIC
C***********************************************

             K = 1/CLAWB
             CD = CDØ + K*CL**2
```

```
            DRAG = CD*Q(ALTSUB, MSUB)*SE
            LIFT = CL*Q(ALTSUB, MSUB)*SE
            LD = CL/CD

            IF ((LIFT.GT.MINL).AND.(LIFT.LT.MAXL).AND.
     *(DRAG.LT.MAXD)) THEN
               WRITE(1,*) ('          ')
               WRITE(1,11Ø) MACH, ALT, ALPHAD
11Ø            FORMAT(1X,' MACH: ',F7.3,'  ALT: ',F12.4,
     *'  ALPHA: ',F7.3)
               WRITE(1,112) LIFT, DRAG
112            FORMAT(1X,' LIFT: ',F14.7,'  DRAG: ',F14.7)
               WRITE(1,114) CL, CD
114            FORMAT(1X,' CL: ',F8.5,'    CD: ',F8.5)
               WRITE(1,116) Q(ALTSUB,MSUB), LD
116            FORMAT(1X,' Q= ',F 12.6,'  L/D= ',F1Ø.6)

               WRITE(2,*) CL
               WRITE(3,*) CD
              WRITE(7,*) MACH
               WRITE(8,*) ALT
               WRITE(9,*) LD
               WRITE(1Ø,*) DRAG
               WRITE(11,*) LIFT
               WRITE(12,*) ALPHAD
             ENDIF
            FLAG=1

6Ø        CONTINUE
5Ø      CONTINUE
55    CONTINUE

      WRITE(6,*) ('   Enter Selection:')
      WRITE(6,*) ('         1.  Change airflow')
      WRITE(6,*) ('         2.  Quit')
      READ(5,*) SELE
      IF (SELE.EQ.1) THEN
        GOTO 1ØØØ
      ENDIF

      STOP
      END
```

Appendix C.3
Hypersonic program

```
      IMPLICIT REAL (A-Z)
      DIMENSION T(2Ø5), RHO(2Ø5), P(2Ø5), Q(2Ø5,1Ø5)

      INTEGER I,J,MSUB,ALTSUB,SELE,GUIDON
      CHARACTER*8 QUEST

      OPEN(1,FILE='A515.DAT',STATUS='NEW')
      OPEN(4,FILE='GEOM1.DAT',STATUS='OLD')
      OPEN(2,FILE='CL.DAT',STATUS='NEW')
      OPEN(3,FILE='CD.DAT',STATUS='NEW')
      OPEN(7,FILE='MACH.DAT',STATUS='NEW')
      OPEN(8,FILE='ALT.DAT',STATUS='NEW')
      OPEN(9,FILE='LD.DAT',STATUS='NEW')
      OPEN(1Ø,FILE='DRAG.DAT',STATUS='NEW')
      OPEN(11,FILE='LIFT.DAT',STATUS='NEW')
      OPEN(12,FILE='ALPHA.DAT',STATUS='NEW')

      R = 1716.
      GØ = 32.2
      PI = 3.14157
      GAM = 1.4

C*****************************
C   Atmosphere from Ø -> 36ØØØ ft
C*****************************

      DO 6 I=1,73
        P1 = 2116.2
        T1 = 518.69
        A = -.ØØ356624
        H = 5ØØ*(I-1)
        T(I) = T1+A*H
        P(I) = P1*EXP(-GØ/(R*T(I))*H)
        RHO(I) = P(I)/(T(I)*R)
  6   CONTINUE

C*******************************
C   Atmosphere from 365ØØ -> 82ØØØ ft
C*******************************

      DO 7 I=74,165
        T1 = 389.99
        P1 = 464.86
        H1 = 365ØØ
        H = 5ØØ*(I-1)
        T(I) = T1
        P(I) = P1*EXP(-GØ/(R*T1)*(H-H1))
```

```
        RHO(I) = P(I)/(T1*R)
    7  CONTINUE

C*********************************
C   Atmosphere from 825ØØ -> 1ØØØØØ ft
C*********************************

      DO 1Ø I=166,2Ø1
        H1 = 825ØØ
        P1 = 55.837
        T1 = 39Ø.24
        A = .ØØ1646
        H = 5ØØ*(I-1)
        T(I) = (H-H1)*A+T1
        P(I) = P1*EXP(-((GØ/(R*T(I)))*(H-H1)))
        RHO(I) = P(I)/(T(I)*R)
   1Ø  CONTINUE

C*****************************************
C  Dynamic pressures at various altitudes and mach numbers
C  Q(alt,M)
C*****************************************

      DO 15 ALTSUB=1,2Ø1
        DO 2Ø MSUB=1,1Ø1
          M = Ø.1*(MSUB-1)
          Q(ALTSUB,MSUB) = P(ALTSUB)*(GAM/2)*M*M
   2Ø    CONTINUE
   15  CONTINUE

      WRITE(6,*) ('  Span (ft):')
      READ(4,*) SPAN
      WRITE(6,*)  ('  Wing ref. area SE (ft^2):')
      READ(4,*) SE
      WRITE(6,*)('  Wetted wing area (ft^2) ')
      READ(4,*) SWETW
      WRITE(6,*)  ('  Wetted body area (ft^2):')
      READ(4,*) SWETB
      WRITE(6,*) ('  Max wing length (ft):')
      READ(4,*) WL
      WRITE(6,*) ('  Body length (ft):')
      READ(4,*) BL
      WRITE(6,*) ('  Sweep angle (deg):')
      READ(4,*) SWP
      WRITE(6,*) ('  Max wing thickness (% chord):')
      READ(4,*) TC
      WRITE(6,*) ('  Leading edge radius (% chord):')
      READ(4,*) RLE
      WRITE(6,*) ('  Body cross-section area (ft^2):')
      READ(4,*)  SB
      WRITE(6,*) ('  Body width (ft):')
      READ(4,*) BD
```

```
WRITE(6,*) ('  Starting Mach number (5 min):')
READ(5,*) MS
WRITE(6,*) ('  Ending mach number (1Ø max):')
READ(5,*) ME
WRITE(6,*) ('  Step size (.1 multiples):')
READ(5,*) MST

WRITE(6,*) ('  Starting altitude (Øft min):')
READ(5,*) ALS
WRITE(6,*) ('  Ending altitude (1ØØØØØft max):')
READ(5,*) ALE
WRITE(6,*) ('  Step size (5ØØft multiples):')
READ(5,*) ALST

WRITE(6,*) ('  Starting angle of attack:')
READ(5,*) APS
WRITE(6,*) ('  Ending angle of attack:')
READ(5,*) APE
WRITE(6,*) ('  Step size:')
READ(5,*) APST

WRITE(6,*) ('  Max drag:')
READ(5,*) MAXD

WRITE(6,*) ('  Max lift:')
READ(5,*) MAXL

WRITE(6,*) ('  Min lift:')
READ(5,*) MINL

DO 1ØØ MACH=MS,ME,MST
   DO 11Ø ALT=ALS,ALE,ALST
      DO 12Ø ALPHAD=APS,APE,APST

         ALTSUB = ALT/5ØØ+1
         MSUB = MACH/.1+1
         ALPHA = ALPHAD*(PI/18Ø)
         MU = .317E-1Ø*(T(ALTSUB)**1.5*(734.7/(T(ALTSUB)+216)))

         CL1 = 2*(ALPHA/TC)*2/(MACH*TC)
         CL2 = 2*(ALPHA/TC)*(2.4/6*MACH*TC)*(4+(ALPHA/TC)**2)
         CL = (CL1+CL2)*TC**2

         CD1 = 4/(MACH*TC)*(4/3+(ALPHA/TC)**2)
         CD2 = 2.4/3*MACH*TC*((ALPHA/TC)**4+8*(ALPHA/TC)**2+16/5)
         CD = (CD1+CD2)*TC**3

         REB = (RHO(ALTSUB)*BL*MACH*SQRT(GAM*R*T(ALTSUB)))/MU
         CF = .455/(LOG1Ø(REB))**2.58
         CFCCFI = 1/(1+.144*MACH**2)**.65
         CDFB = CFCCFI*CF*SWETB/SE
         REW = (RHO(ALTSUB)*WL*MACH*SQRT(GAM*R*T(ALTSUB)))/MU
```

```
              CDFW = CFCCFI*CF*SWETW/SE
              CD = CD+CDFW+CDFB

              LIFT = Q(ALTSUB,MSUB)*CL*SE
              DRAG = Q(ALTSUB,MSUB)*CD*SE
              LD = CL/CD

              IF((LIFT.GT.MINL).AND.(LIFT.LT.MAXL).AND.
     *(DRAG.LT.MAXD)) THEN
                 WRITE(1,205) MACH, ALT, ALPHAD
205              FORMAT(1X,' MACH:',F7.3,'  ALT:',F12.4,
     *'  ALPHA:',F7.3)
                 WRITE(1,200) LIFT, DRAG
200              FORMAT(1X,' LIFT=',F12.5,'  DRAG=',F12.5)
                 WRITE(1,210) CL, CD
210              FORMAT(1X,' CL=',F7.4,'  CD=',F7.4)
                 WRITE(1,215) Q(ALTSUB,MSUB), LD
215              FORMAT(1X,' Q=',F12.6,' L/D:',F7.4)

                 WRITE(2,*) CL
                 WRITE(3,*) CD
                 WRITE(7,*) MACH
                 WRITE(8,*) ALT
                 WRITE(9,*) LD
                 WRITE(10,*) DRAG
                 WRITE(11,*) LIFT
                 WRITE(12,*) ALPHAD
              ENDIF

120        CONTINUE
110     CONTINUE
100  CONTINUE

     STOP
     END
```

Appendix D

Inlet Analysis Program

Input

```
      8              ;nose angle
      1              ;num of cases
      1              ;number of outside ramps
     26              ;first inlet ramp
      Ø              ;number of inside ramps
    38Ø              ;Required Mass flow rate
  5ØØØØ              ;altitude
     2.Ø             ;Mach No.
     4.Ø             ;alpha(angle of attack)
     1.4             ;gamma
```

```
   program inlet
   dimension pr(8),rh(8),te(8),pØ(8),rd(8),areas(8),betas(8)
   dimension vs(8),thetas(8)
   real mach,m1,m2,m1n,m2n
   integer stop
   common gam,theta,beta,m1,m1n,m2n,prat,pØr,rrat,trat,m2

   open(1,file=' ')
   open(2,file=' ')
   pi = 4.Ø*atan(1.Ø)
   read(1,*)thet1
   read(1,*)numcases
   write(2,45Ø)
   do 9ØØ k=1,numcases
     read(1,*)nout
     do 1Ø i=1,nout
      read(1,*)thetas(i+1)
1Ø    continue
      read(1,*)nin
      do 12 i=1,nin
         read(1,*)thetas(i+nout+1)
12    continue
      thetas(nin+nout+2)=Ø.Ø
      read(1,*)w1r
      read(1,*)alt
      read(1,*)mach
      read(1,*)alpha
      read(1,*)gamma
      gam = gamma
      thetas(1) = alpha+thet1
```

```
      theta = thetas(1)
      m1 = mach
      call oblique
      betas(1)=beta
      pØ(1) = pØr
      pr(1) = prat
      rh(1) = rrat
      te(1) = trat
      vs(1) = m2
      do 2Ø j=1,nout
        m1 = m2
        theta = thetas(j+1)
        call oblique
        betas(j+1) = beta
        vs(j+1) = m2
        pØ(j+1) = pØ(j)*pØr
        pr(j+1) = pr(j)*prat
        rh(j+1) = rh(j)*rrat
        te(j+1) = te(j)*trat
2Ø    continue
      stop=Ø
      do 22 j=1,nin
        m1 = m2
        theta = thetas(j+nout+1)
        call oblique
        if (m2.lt.1.Ø) then
          betas(j+nout+1) = Ø.Ø
          m2 = vs(j+nout)
          vs(j+nout+1) = vs(j+nout)
          pØ(j+nout+1) = pØ(j+nout)
          pr(j+nout+1) = pr(j+nout)
          rh(j+nout+1) = rh(j+nout)
          te(j+nout+1) = te(j+nout)
          stop=j
          go to 23
        endif
        betas(j+nout+1) = beta
        vs(j+nout+1) = m2
        pØ(j+nout+1) = pØ(j+nout)*pØr
        pr(j+nout+1) = pr(j+nout)*prat
        rh(j+nout+1) = rh(j+nout)*rrat
        te(j+nout+1) = te(j+nout)*trat
22    continue
23    m1 = m2
      call normal
      betas(nout+nin+2) = 9Ø.
      vs(nin+nout+2) = m2
      pØ(nin+nout+2) = pØ(j+nout)*pØr
      pr(nin+nout+2) = pr(j+nout)*prat
      rh(nin+nout+2) = rh(j+nout)*rrat
      te(nin+nout+2) = te(j+nout)*trat
      call cond(alt,pres,temp,dens)
```

```
      p1 = pr(nin+nout+2)*pres
      t1 = te(nin+nout+2)*temp
      r1 = rh(nin+nout+2)*dens
      u1 = vs(nin+nout+2)*sqrt(gamma*1716*t1)
      a1 = w1r*(p1/t1)*(518.69/2116.2)/r1/u1/32.2
      areas(nin+nout+2) = a1
      sbmt =sin(pi*(betas(j+nout)-thetas(j+nout))/18Ø.)
      areas(j+nout) = a1/sbmt
      do 3Ø i=1,j-2
        spb = sin(pi-pi*betas(nout+j-i+1)/18Ø.)
        sbmt=sin(pi*(betas(nout+j-i)-thetas(j+nout-i))/18Ø.)
        areas(nout+j-i)=spb*areas(j+nout-i+1)/sbmt
        sbb = sin(pi*(betas(j+nout-i+1)-betas(j+nout-i)
     $             +thetas(j+nout-i))/18Ø)
 3Ø     rd(nout+j-i)=sbb*areas(j+nout-i+1)/sbmt
      sb = sin(pi*betas(nout+2)/18Ø.)
      sbmt = sin(pi*(betas(nout+1)-thetas(nout+1))/18Ø.)
      areas(nout+1)=sb*areas(nout+2)/sbmt
      spb = sin(pi-pi*(1.+betas(nout+2)+betas(nout+1)-
     $     thetas(nout+1))/18Ø.)
      rd(nout+1)=spb*areas(nout+2)/sbmt
      do 32 i=1,nout-1
        spb = sin(pi-pi*(betas(nout-i+2))/18Ø.)
        sbmt=sin(pi*(betas(nout-i+1)-thetas(nout-i+1))/18Ø.)
        areas(nout-i+1)=spb*areas(nout-i+2)/sbmt
        sbb = sin(pi*(betas(nout-i+2)-betas(nout-i+1)+
     $             thetas(nout-i+1))/18Ø.)
 32     rd(nout-i+1)=sbb*areas(nout-i+2)/sbmt
      sb = sin(betas(2)*pi/18Ø.)
      areas(1) = areas(2)*sb
      ac = areas(1)
      print *,'Capture area = ',ac,'  nr = ',pØ(nin+nout+2)
      write(2,498) alt, mach, alpha,gamma
      write(2,5ØØ) '     M = ',(vs(j),j=1,nin+nout+2)
      write(2,5ØØ) 'P/Pinf = ',(pr(j),j=1,nin+nout+2)
      write(2,5ØØ) 'R/Rinf = ',(rh(j),j=1,nin+nout+2)
      write(2,5ØØ) 'T/Tinf = ',(te(j),j=1,nin+nout+2)
      write(2,5ØØ) 'Thetas = ',(thetas(j),j=1,nin+nout+2)
      write(2,5ØØ) 'Betas  = ',(betas(j),j=1,nin+nout+2)
      write(2,5ØØ) 'areas  = ',(areas(j),j=1,nin+nout+2)
      write(2,5ØØ) 'length = ',(rd(j),j=1,nin+nout+2)
      write(2,5Ø2) ac,pØ(nin+nout+2)
9ØØ continue
45Ø format(2Øx,'Mach Ø-6 Inlet analysis')
498 format(/,'Altitude = ',f7.Ø,' ft.   Mach No. = ',
   $       f6.2,'   Alpha = ',f6.2,' degrees  Gamma = ',f5.3)
5ØØ format(1x,a9,8f11.4)
5Ø2 format(5x,'Capture Area = ',f8.4,'  Pr. ratio(nr) = ',f1Ø.6)
    stop
    end
```

```
      subroutine oblique
      real thetbm,m1,m1n,m2n,m2
      common gam,theta,beta,m1,m1n,m2n,prat,pØr,rrat,trat,m2
      pi = 4.Ø*atan(1.Ø)
      beta = thetbm(gam,theta,m1)
      m1n = m1*sin(beta*pi/18Ø.Ø)
      rrat = ((gam+1)*m1n**2)/((gam-1)*m1n**2+2)
      prat = 1 + 2*gam*(m1n**2-1)/(gam+1)
      trat = prat/rrat
      m2n = sqrt((m1n**2 + 2.Ø/(gam-1))/(2*gam*m1n**2/(gam-1) -1))
      m2 = m2n/sin((beta-theta)*pi/18Ø.Ø)
      rat=(1.Ø+(gam-1.Ø)*m2n**2/2.Ø)/(1.Ø+(gam-1.Ø)*m1n**2/2.Ø)
      pØr=prat*(rat)**(gam/(gam-1.Ø))
      print *,'oblique =',m1,m1n,rrat,prat,trat,m2n,m2,pØr
      return
      end



      subroutine normal
      real m1,m1n,m2n,m2
      common gam,theta,beta,m1,m1n,m2n,prat,pØr,rrat,trat,m2
      m2 = sqrt((1+(gam-1)*m1**2/2)/(gam*m1**2-(gam-1)/2))
      rrat = (gam+1)*m1**2/(2.Ø+(gam-1)*m1**2)
      prat = 1 + 2.Ø*gam*(m1**2-1)/(gam+1)
      trat = prat/rrat
      powg = gam/(gam-1.Ø)
      rat=(1.+(gam-1.)*m2**2/2.)**powg/(1.+(gam-1.)*m1**2/2.)**powg
      pØr=prat*(rat)
      print *,'normal =',m1,m2,rrat,prat,trat,pØr
      return
      end



      function thetbm(gam,th,m1)
      real m1
      ffn(be)=(m1*sin(be))**2 - 1.Ø
      ff(be)=2*(ffn(be)/(m1**2*(gam+cos(2.Ø*be))+2.Ø))*cotan(be)
      pi = 4.Ø*atan(1.Ø)
      tth = tan(th*pi/18Ø.Ø)
      b1 = 1.Ø
    1 tth1 = ff(b1)
      if(abs(tth1-tth).lt.Ø.ØØØØØ1) go to 999
      if(tth1.gt.1.Ø) then
        b1 = (pi/4.Ø+b1/2.Ø)
        go to 1
      endif
      b2 = b1*Ø.8
    2 tth2 = ff(b2)
      if(abs(tth2-tth).lt.Ø.ØØØØØ1) then
        b1 = b2
```

```
      go to 999
    endif
    if(tth2.gt.1.Ø) then
      b2 = (b1+b2)/2.Ø
      go to 2
    endif
  3 bnew = b1-(b1-b2)*(tth1-tth)/(tth1-tth2)
    if(bnew.gt.(pi/2.Ø)) then
      b1 = -1.Ø
      go to 999
    endif
    tthnew = ff(bnew)
    if(abs(tthnew-tth).lt.Ø.ØØØØØ1) then
      b1 = bnew
      go to 999
    endif
    b1 = b2
    tth1 = tth2
    b2 = bnew
    tth2 = tthnew
    go to 3
999 thetbm = b1*18Ø/pi
    print *,'thetbm = ',gam,th,m1,'->',b1*19Ø/pi
    return
    end



    subroutine cond(alt,pres,temp,dens)
    if(alt.gt.155349.5)then
      temp = 5Ø8.79
      pres = 2.4566*exp(-32.2/1716/5Ø8.79*(alt-156ØØØ.Ø))
    elseif(alt.gt.82345.Ø) then
      temp = 389.99+Ø.ØØ1631*(alt-82345.Ø)
      pres = 51.592 * (temp/39Ø.24)**(-32.2/Ø.ØØ1631/1716)
    elseif(alt.gt.36152.Ø)then
      temp = 389.99
      pres = 464.86*exp(-32.2/1716/389.99*(alt-365ØØ.Ø))
    else
      temp = 518.69-Ø.ØØ356*alt
      pres = 2116.2*(temp/518.69)**(32.2/Ø.ØØ356/1716)
    endif
    dens = pres/1716/temp
    print *,'cond =',alt,pres,temp,dens
    return
    end
```